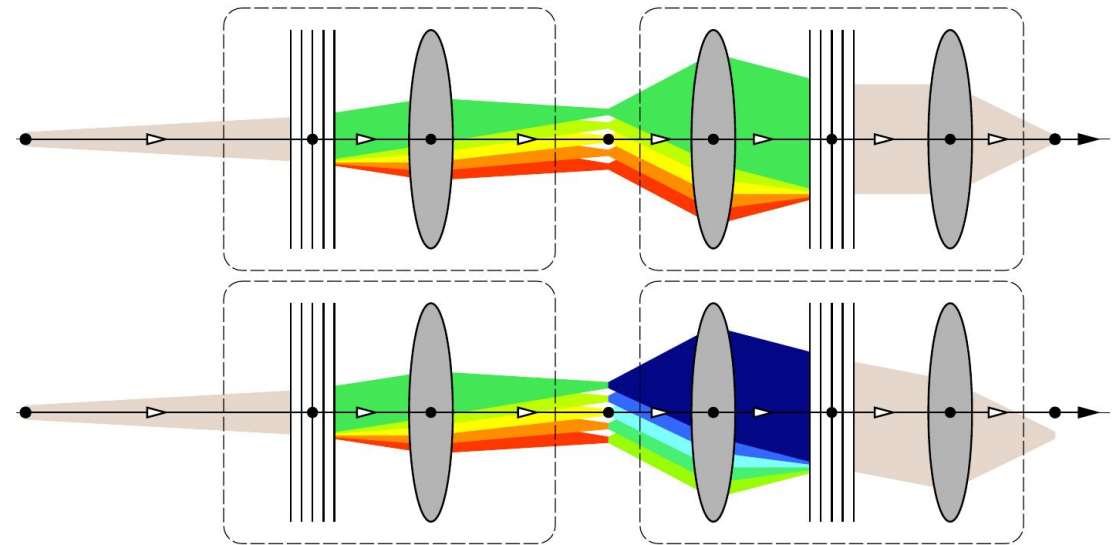


X-ray Echo Spectroscopy

Yuri Shvyd'ko



Acknowledgments

Stephen Streiffer (APS)

Di-Jing Huang (NSRRC)

Becky Sikes (APS)

Conni Vanni (APS)

Kelly Cunningham (APS)

Brian Robinson (APS)

Colleen Trattner (APS)

Deana Kinzler (APS)

Christine McGhee (APS)

Yong Cai (BNL)

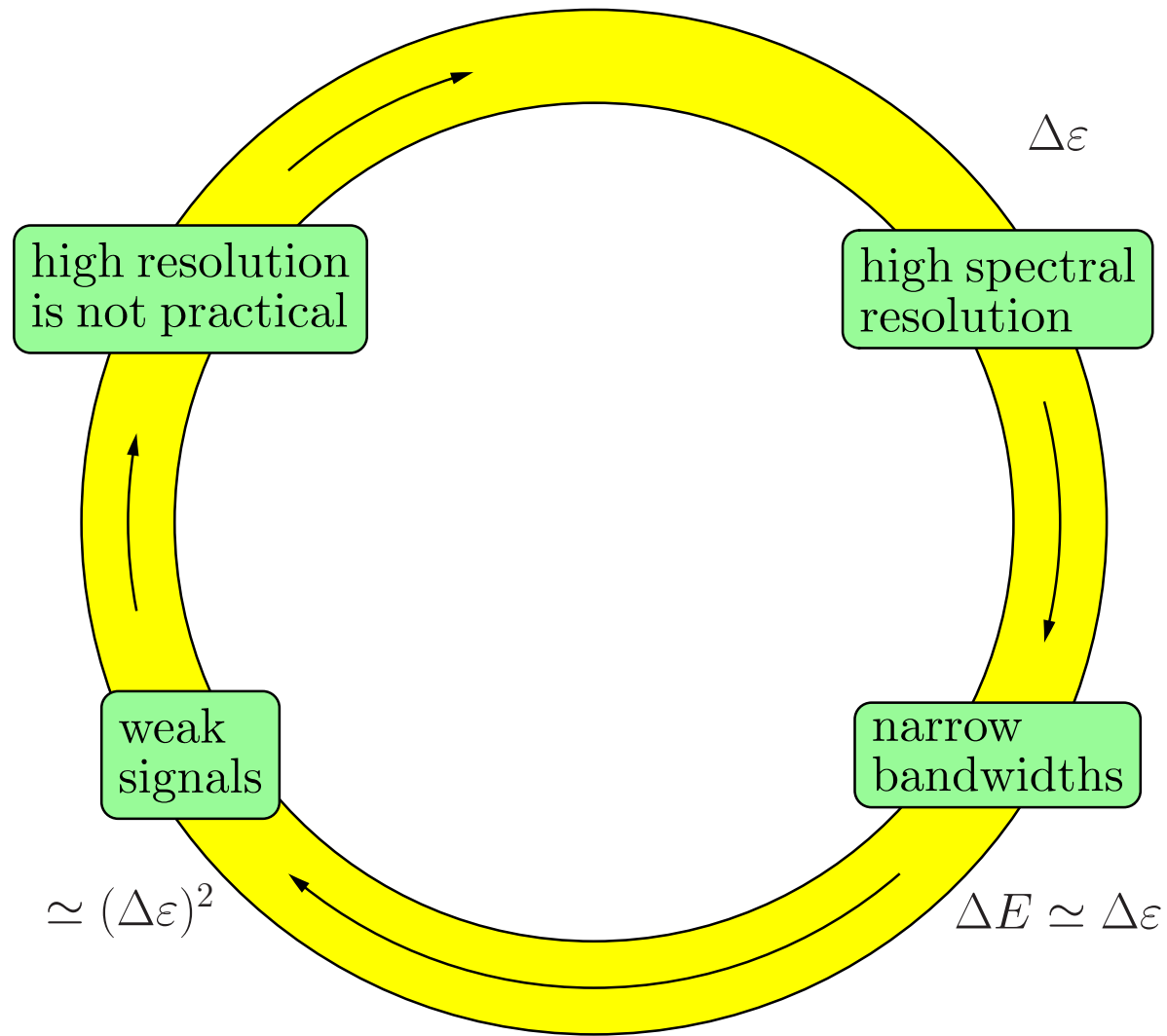


Inelastic X-ray Scattering (IXS) requires improvements in:

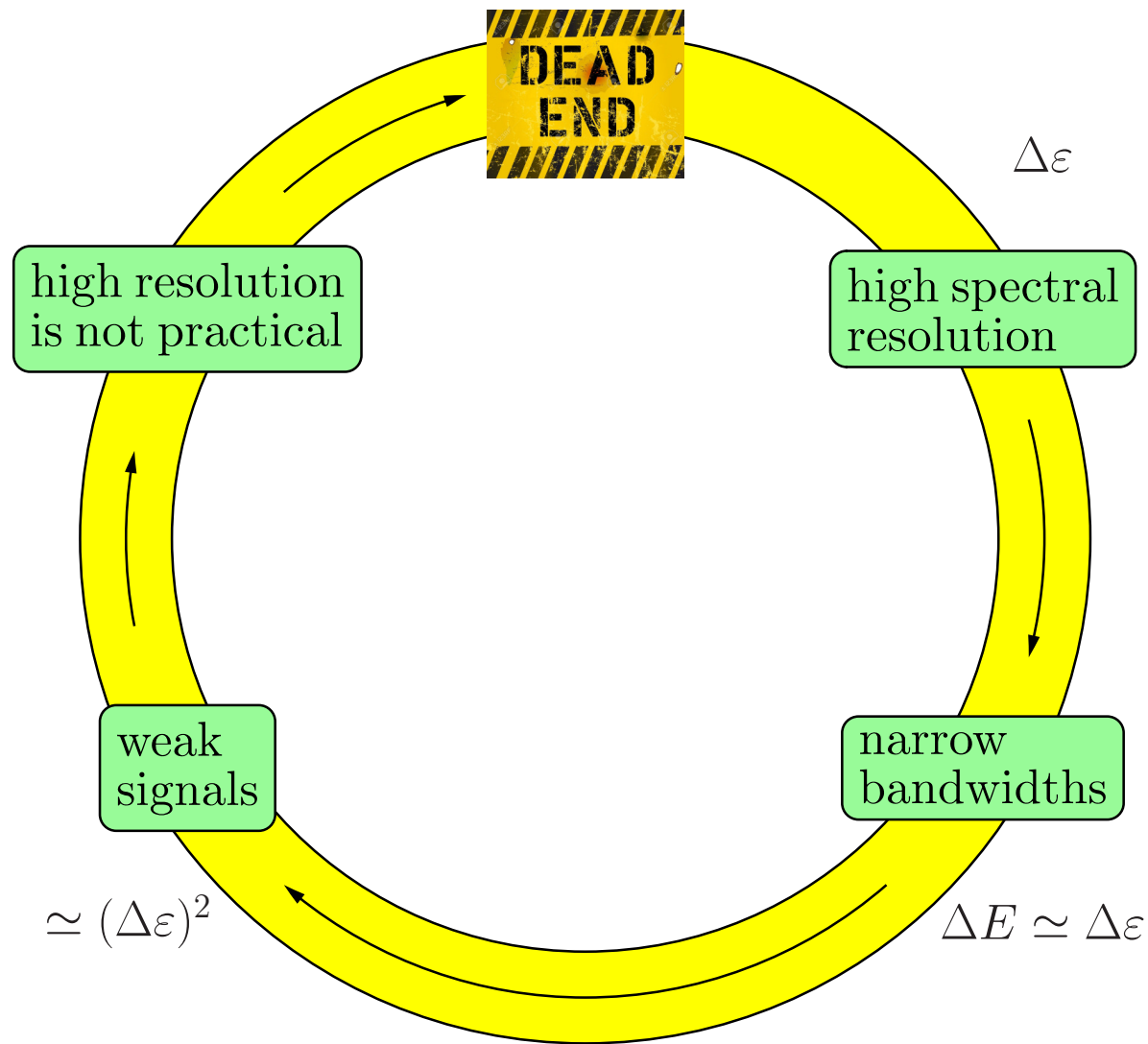
- Spectral resolution $\Delta\varepsilon$.
- Momentum-transfer resolution ΔQ .
- IXS signal strength.



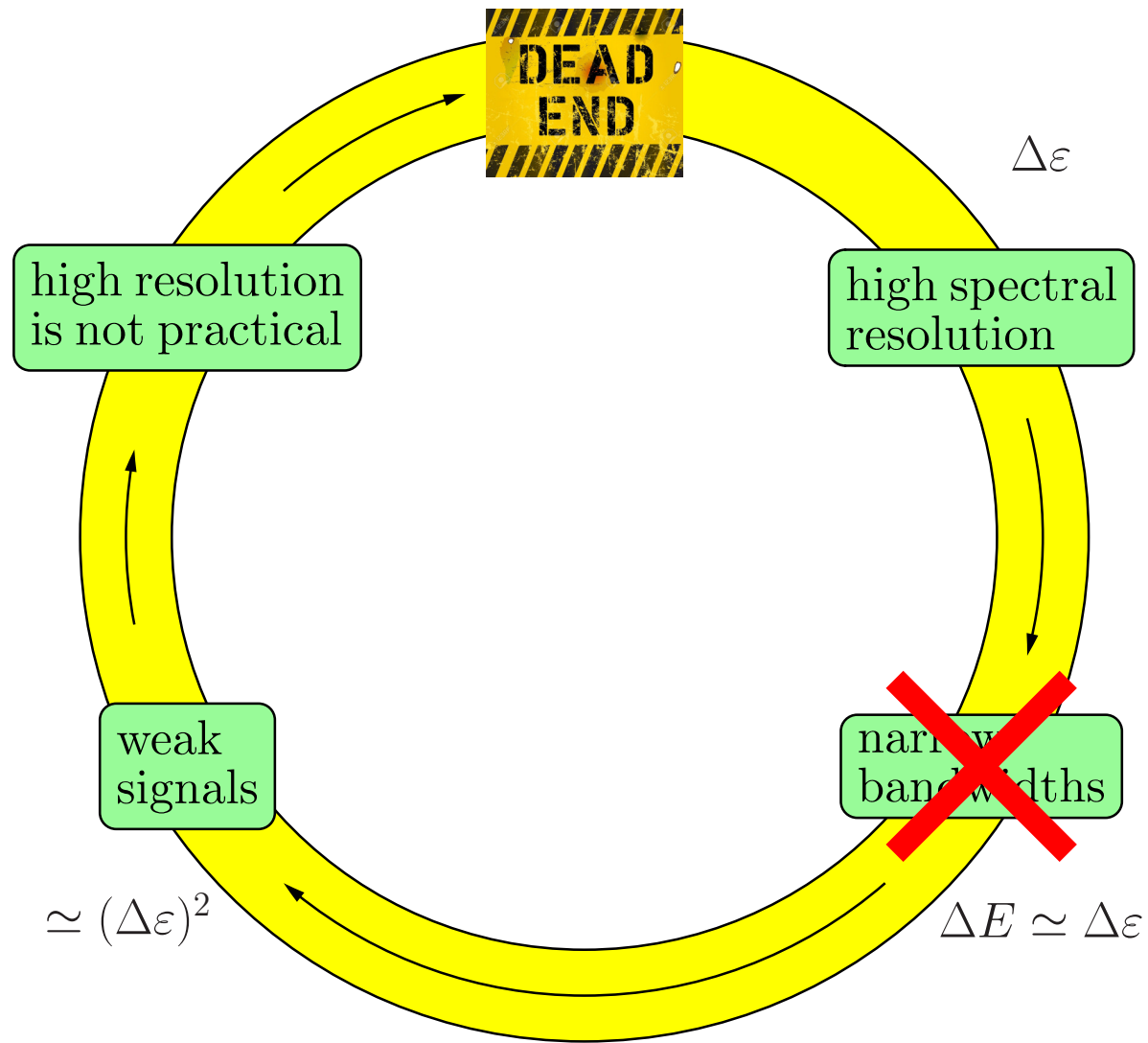
IXS is at an Impasse over Spectral Resolution



IXS is at an Impasse over Spectral Resolution

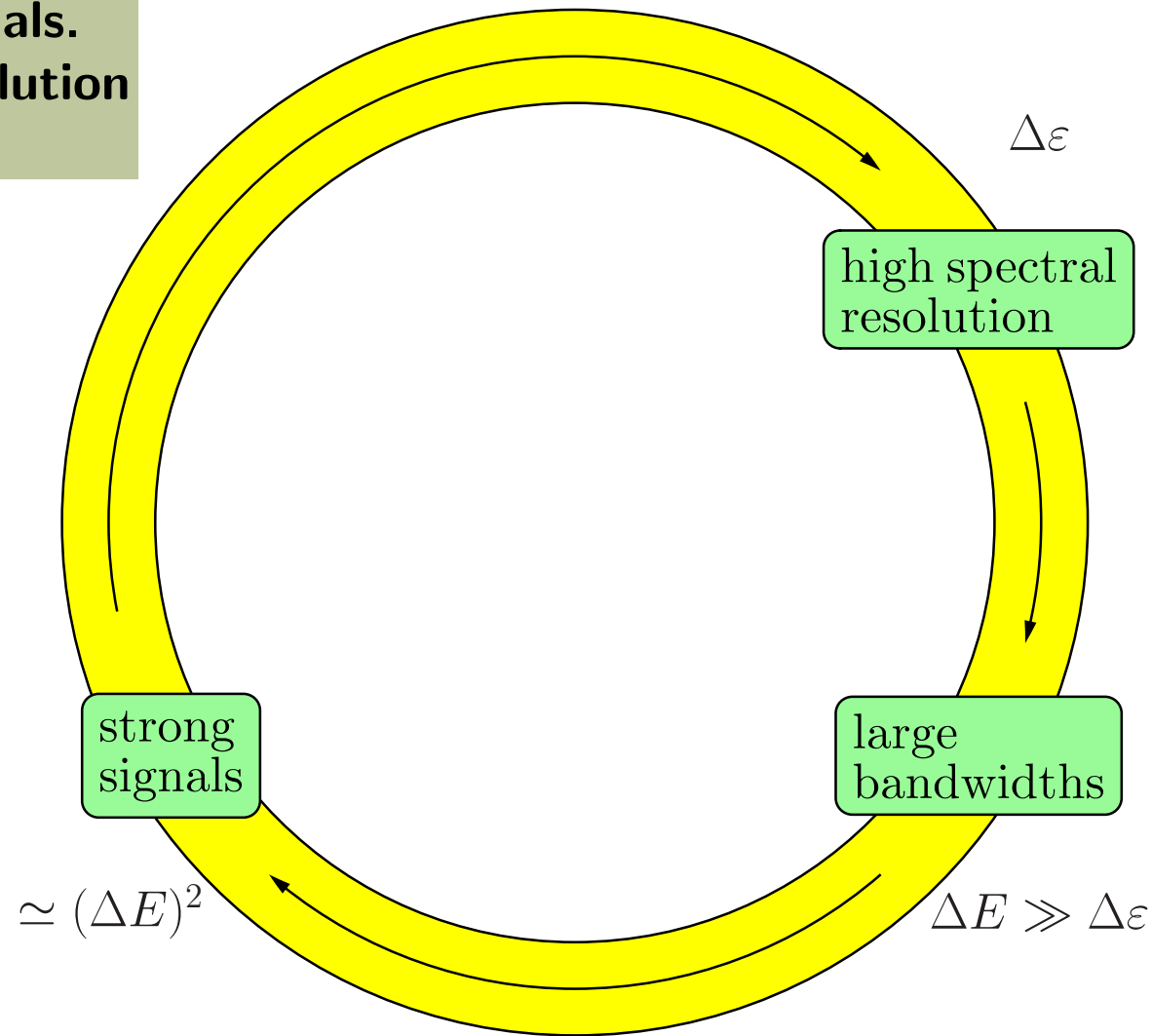


IXS is at an Impasse. How to Overcome?



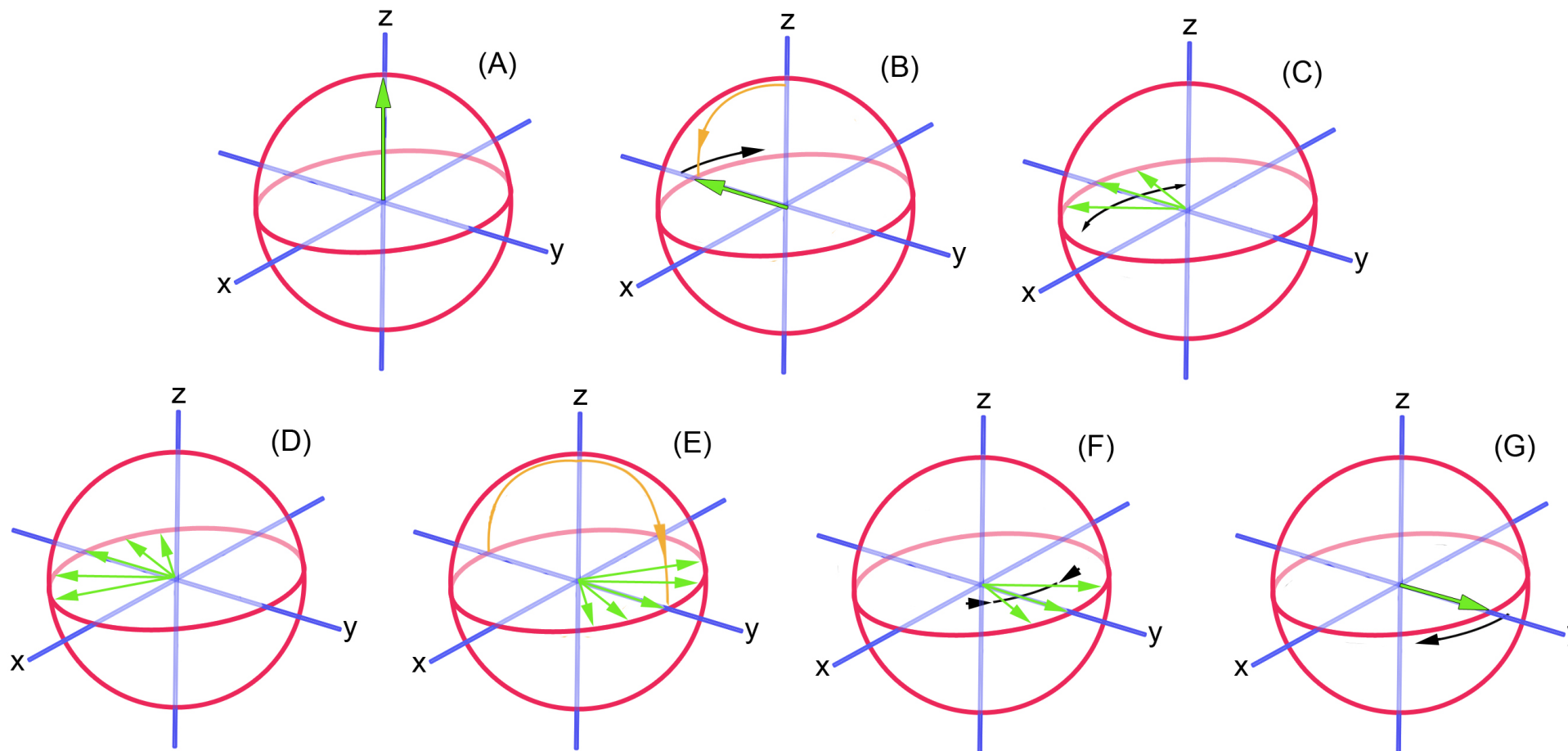
Decoupling the spectral resolution from the bandwidth of the x-rays

- ⇒ Stronger IXS signals.
- ⇒ High spectral resolution is practical.



Spin Echo

Spin echo is the refocusing in the time domain of the defocused spin magnetization by time reversal.



E. L. Hahn, "Spin Echos", Phys. Rev. 80, 580 (1950)

F. Mezei, "Neutron Spin Echo", vol. 128 of Lecture Notes in Physics (Springer, Berlin) (1980)

Soft X-Ray RIXS - Energy-Compensation

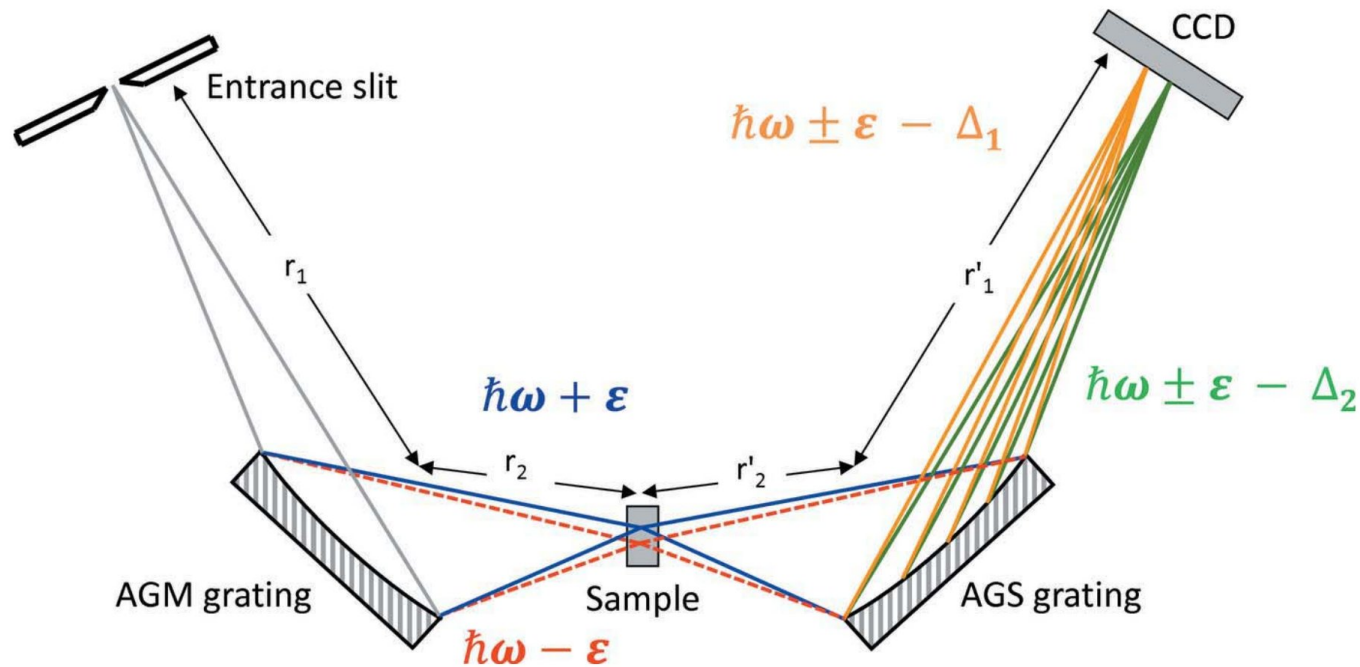


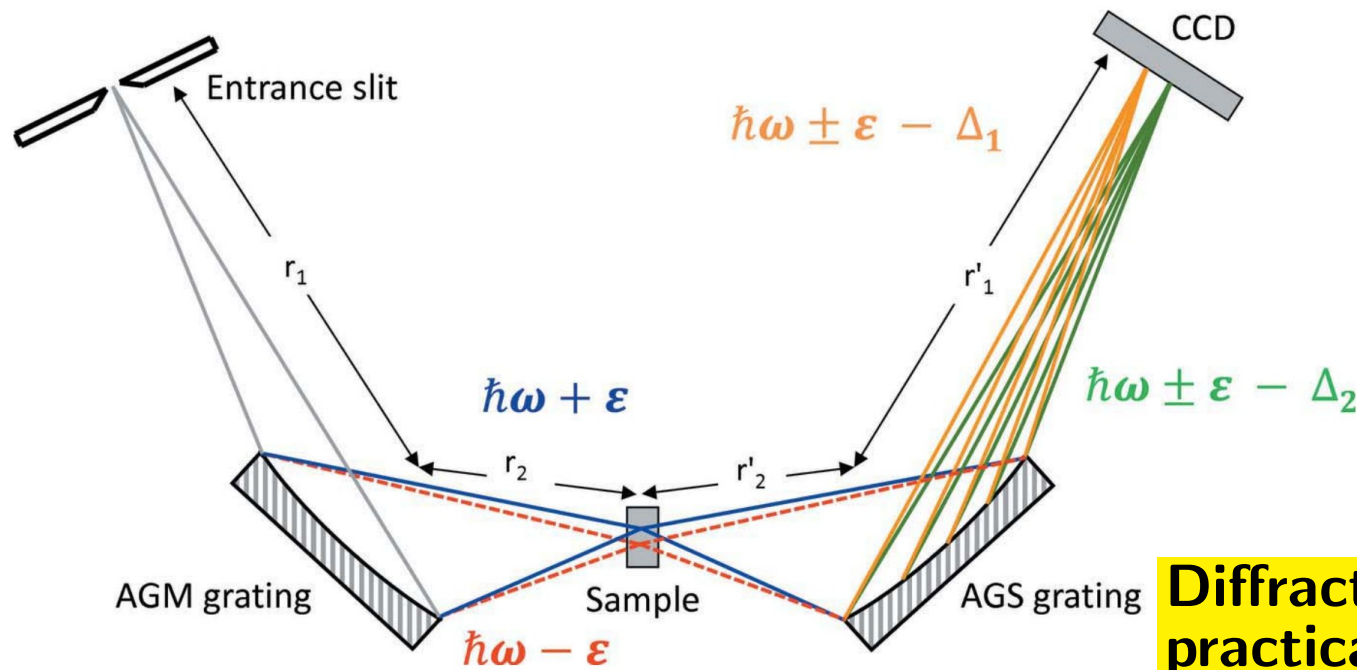
Figure 2

Illustration of the energy-compensation principle of grating dispersion applied to a RIXS measurement. Both gratings have an identical central groove density and the same distance to the sample. After passing through the entrance slit, X-rays of varied energy $\hbar\omega \pm \varepsilon$ are dispersed onto the sample and experience inelastic scattering. Scattered X-rays of identical energy loss (Δ_1 or Δ_2) are dispersed and focused to the same point on the CCD.

H. S. Fung et al., AIP Conf.Proc. 705, 655 (2004).

C. H. Lai, ..., D.J. Huang, J. Synchrotron Radiat. 21, 325 (2014)

Soft X-Ray RIXS - Energy-Compensation



Diffraction gratings are not practical in hard x-ray regime

Figure 2

Illustration of the energy-compensation principle of grating dispersion applied to a RIXS measurement. Both gratings have an identical central groove density and the same distance to the sample. After passing through the entrance slit, X-rays of varied energy $\hbar\omega \pm \epsilon$ are dispersed onto the sample and experience inelastic scattering. Scattered X-rays of identical energy loss (Δ_1 or Δ_2) are dispersed and focused to the same point on the CCD.

H. S. Fung et al., AIP Conf.Proc. 705, 655 (2004).

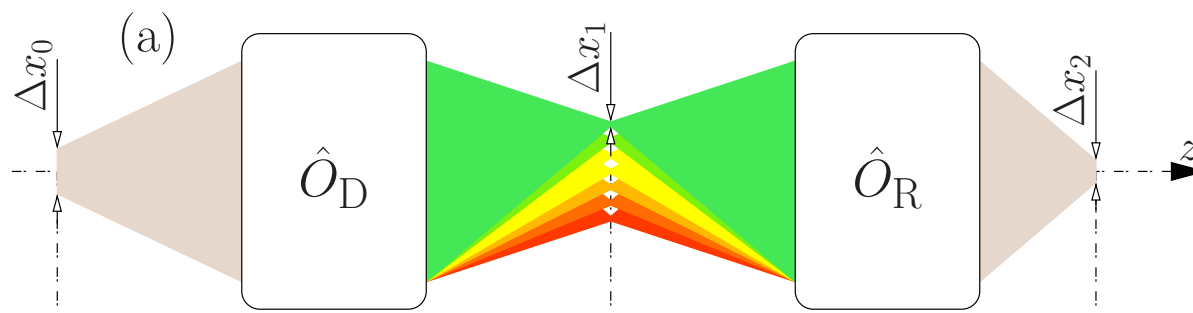
C. H. Lai, ..., D.J. Huang, J. Synchrotron Radiat. 21, 325 (2014)

Content

- X-ray echo spectroscopy principles.
- X-ray echo spectrometer design & performance.
- Comparison with HERIX.
- Feasibility.
- Conclusions and outlook.

X-Ray Echo - Generic Scheme

- X-ray echo spectroscopy, is a space-domain analog of the spin echo spectroscopy.
- An image of an x-ray source is defocused by a focusing-dispersing system \hat{O}_D .
- The defocused image is refocused in a time-reversal focusing-dispersing system \hat{O}_R (echo).

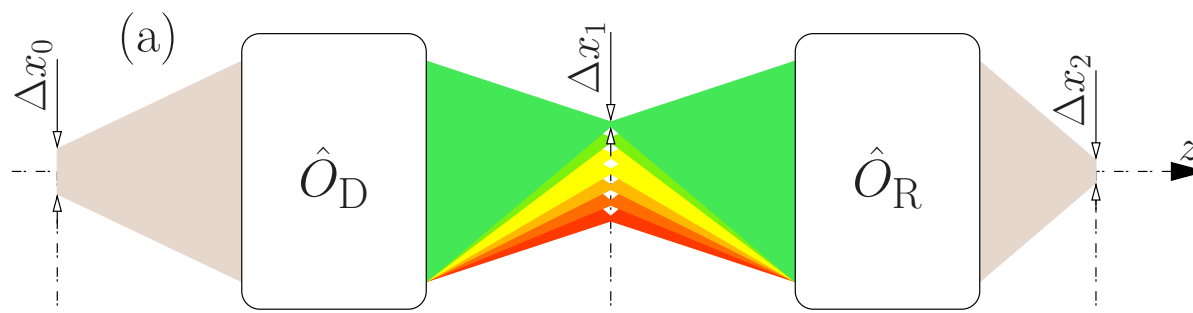


X-Ray Echo - Generic Scheme

- X-ray echo spectroscopy, is a space-domain analog of the spin echo spectroscopy.
- An image of an x-ray source is defocused by a focusing-dispersing system \hat{O}_D .
- The defocused image is refocused in a time-reversal focusing-dispersing system \hat{O}_R (echo).

Refocusing (echo) takes place if the linear dispersion G_D in \hat{O}_D is compensated (time-reversed) by linear dispersion G_D in \hat{O}_D :

$$G_D + G_R/A_R = 0$$



X-Ray Echo - Generic Scheme

- X-ray echo spectroscopy, is a space-domain analog of the spin echo spectroscopy.
- An image of an x-ray source is defocused by a focusing-dispersing system \hat{O}_D .
- The defocused image is refocused in a time-reversal focusing-dispersing system \hat{O}_R (echo).

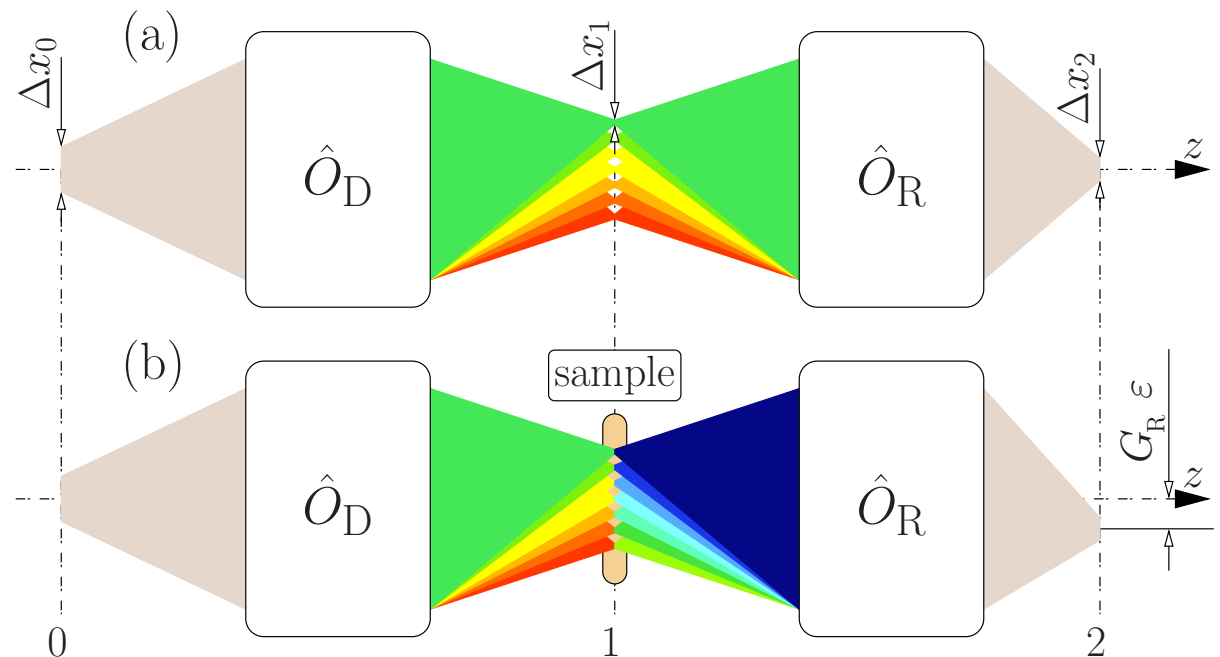
• If the defocused beam is inelastically scattered from a sample with an energy transfer ε , the echo signal acquires a lateral shift $G_R \varepsilon$.

• An inelastic scattering spectrum is measured by mapping ε on the pixel detector.

• Spectral resolution:

$$\Delta\varepsilon = \frac{\Delta x_2}{G_R}$$

does not rely on the monochromaticity of x-rays!



X-Ray Echo - Generic Scheme

- X-ray echo spectroscopy, is a space-domain analog of the spin echo spectroscopy.
- An image of an x-ray source is defocused by a focusing-dispersing system \hat{O}_D .
- The defocused image is refocused in a time-reversal focusing-dispersing system \hat{O}_R (echo).

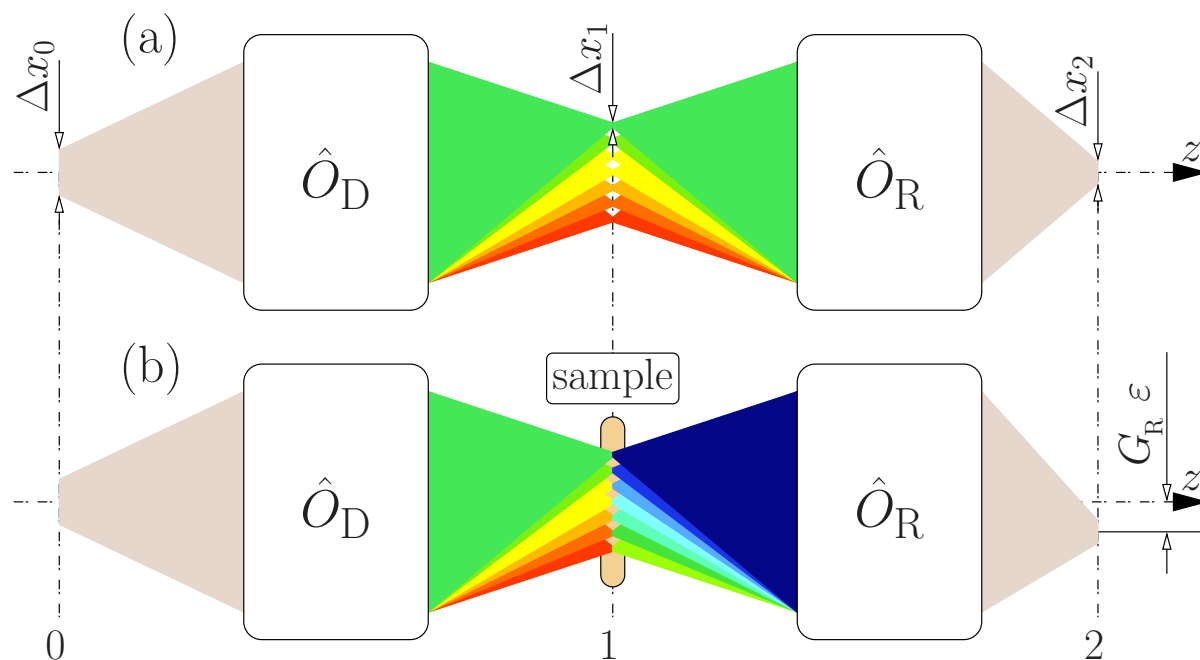
• If the defocused beam is inelastically scattered from a sample with an energy transfer ε , the echo signal acquires a lateral shift $G_R \varepsilon$.

• An inelastic scattering spectrum is measured by mapping ε on the pixel detector.

• Spectral resolution:

$$\Delta\varepsilon = \frac{\Delta x_1 A_R}{G_R}$$

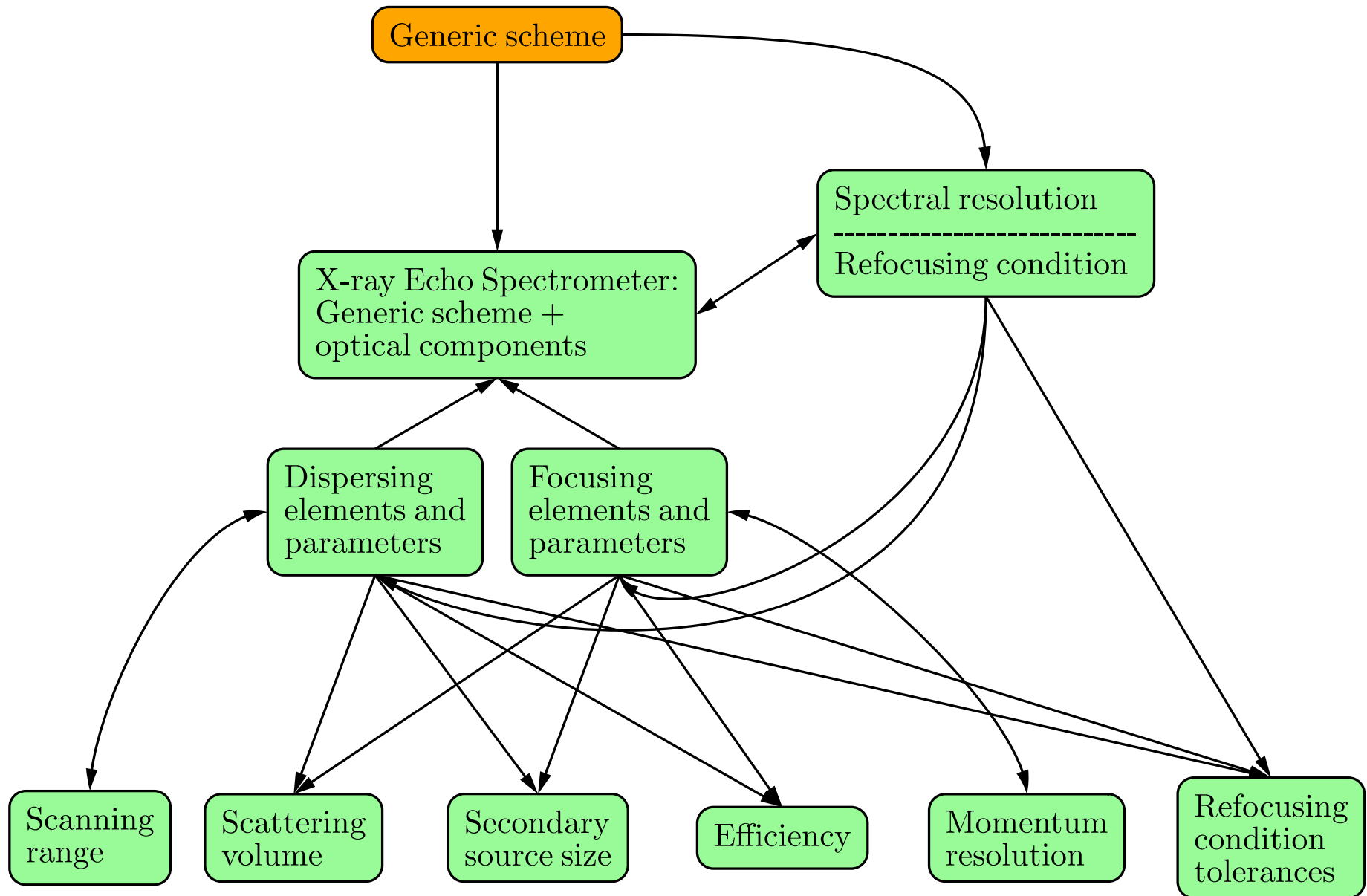
does not rely on the monochromaticity of x-rays!



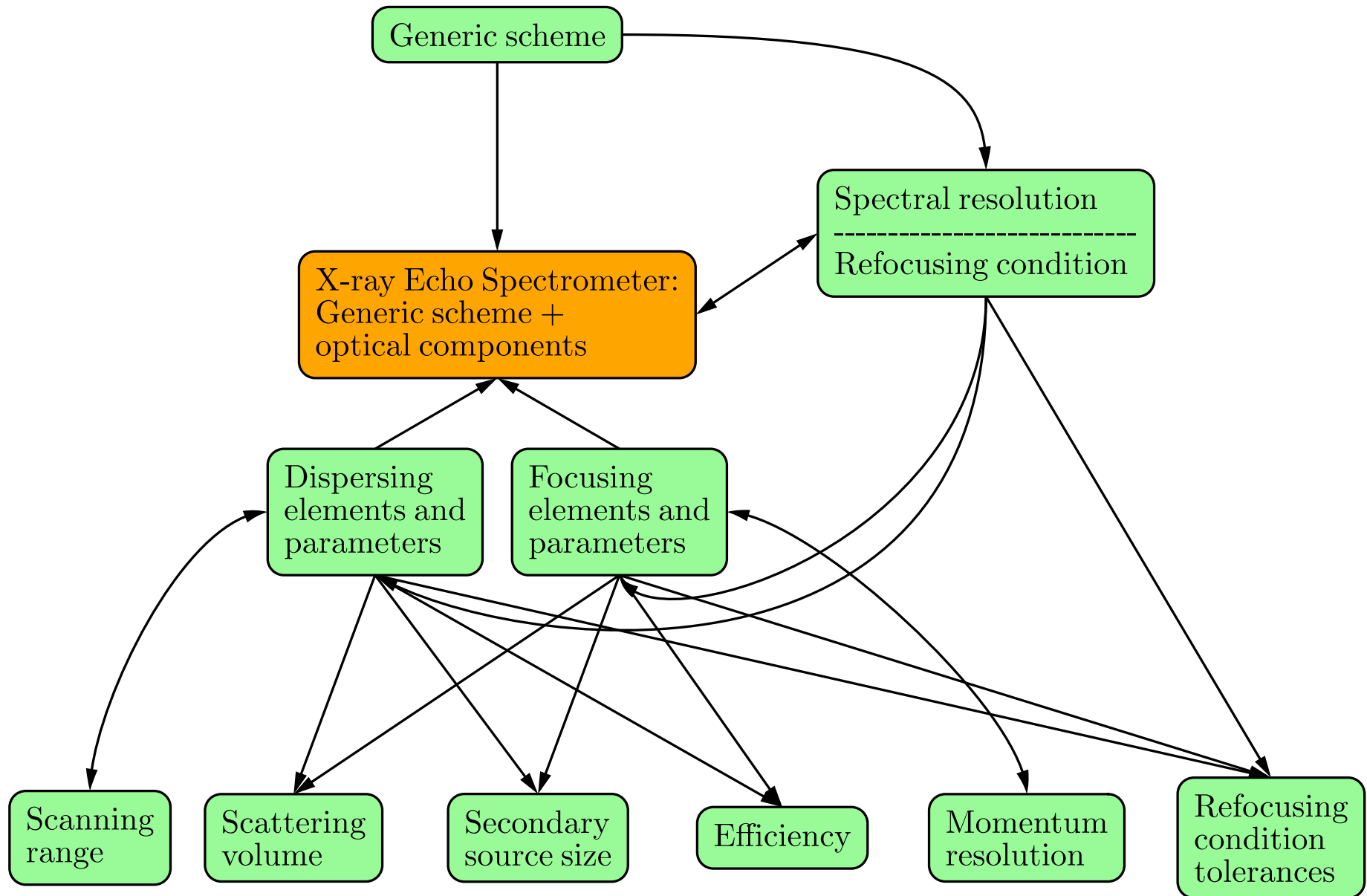
Content

- X-ray echo spectroscopy principles.
- **X-ray echo spectrometer design & performance.**
- Comparison with HERIX.
- Feasibility.
- Conclusions and outlook.

X-ray echo spectrometer design & performance



X-ray echo spectrometer design & performance



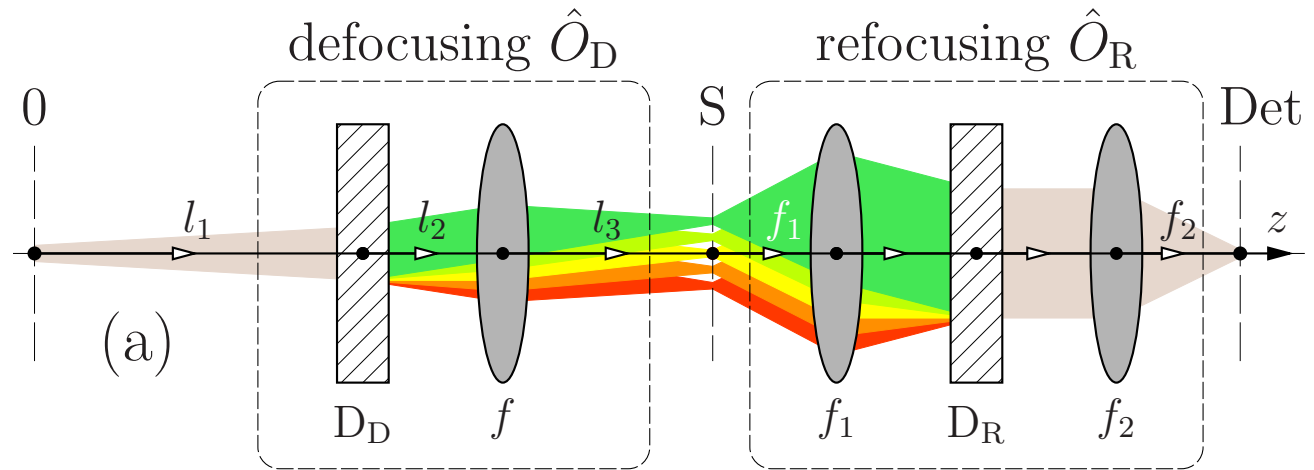
X-ray Echo Spectrometer - Elastic Scattering

Defocusing dispersing system \hat{O}_D is a broadband device with a bandwidth $\Delta E_{UD} \gg \Delta \epsilon$.

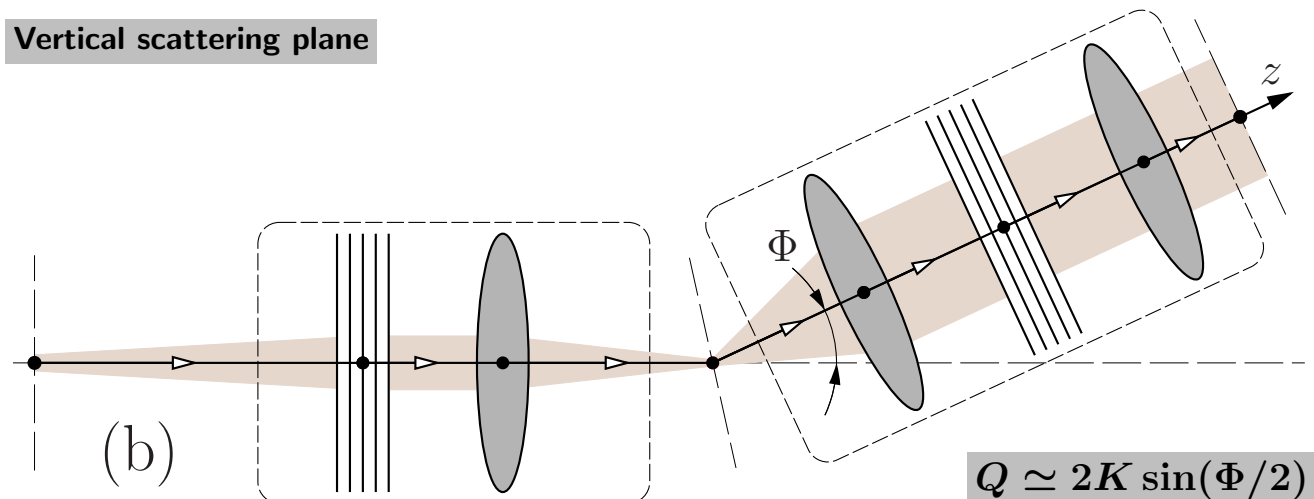
Refocusing dispersing system \hat{O}_R is a broadband spectrograph with a bandwidth $\Delta E_{UR} \gg \Delta \epsilon$

Refocusing (echo) takes place if the linear dispersion G_D in \hat{O}_D is compensated (time-reversed) by linear dispersion G_D in \hat{O}_D :

$$G_D + G_R/A_R = 0$$



Vertical scattering plane



Horizontal scattering plane

$$Q \simeq 2K \sin(\Phi/2)$$

X-ray Echo Spectrometer - Inelastic Scattering

Defocusing dispersing system \hat{O}_D is a broadband device with a bandwidth $\Delta E_{UD} \gg \Delta \epsilon$.

Refocusing dispersing system \hat{O}_R is a broadband spectrograph with a bandwidth $\Delta E_{UR} \gg \Delta \epsilon$

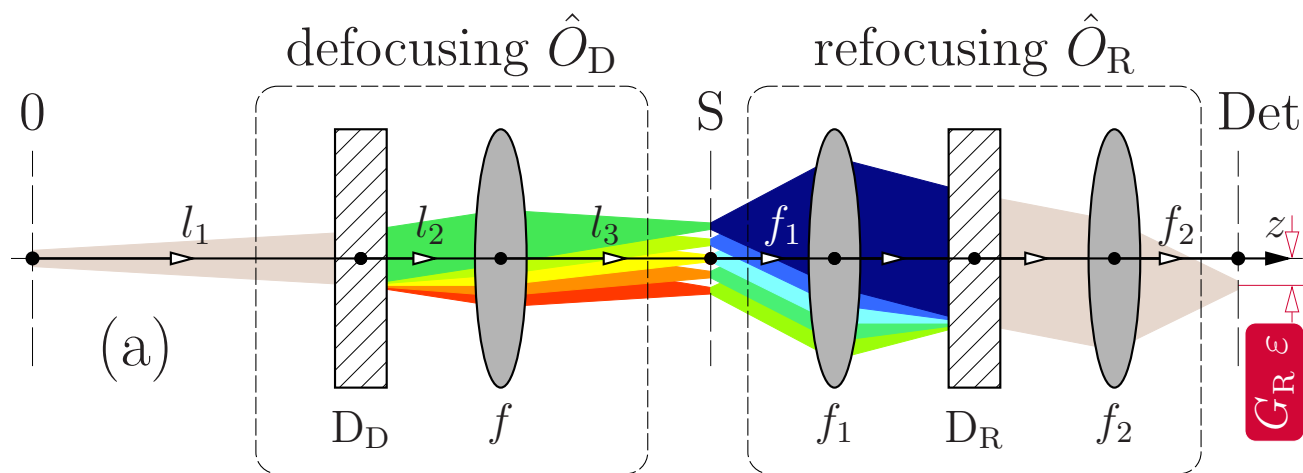
Refocusing (echo) takes place if the linear dispersion G_D in \hat{O}_D is compensated (time-reversed) by linear dispersion G_D in \hat{O}_D :

$$G_D + G_R/A_R = 0$$

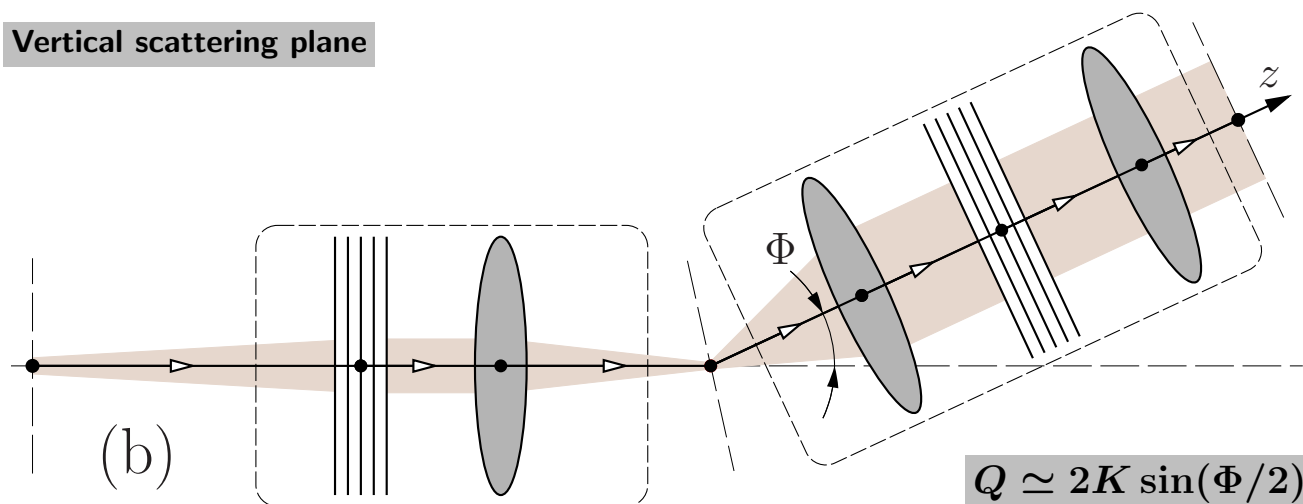
Energy transfer ϵ is measured by mapping ϵ on the pixel detector.

Energy resolution $\Delta \epsilon = \Delta x_1 A_R / G_R$

Does not rely on the monochromaticity of incident x-rays!



Vertical scattering plane



Horizontal scattering plane



X-ray Echo Spectrometer - Inelastic Scattering

Defocusing dispersing system \hat{O}_D is a broadband device with a bandwidth $\Delta E_{UD} \gg \Delta \epsilon$.

Refocusing dispersing system \hat{O}_R is a broadband spectrograph with a bandwidth $\Delta E_{UR} \gg \Delta \epsilon$

Refocusing (echo) takes place if the linear dispersion G_D in \hat{O}_D is compensated (time-reversed) by linear dispersion G_D in \hat{O}_D :

$$G_D + G_R/A_R = 0$$

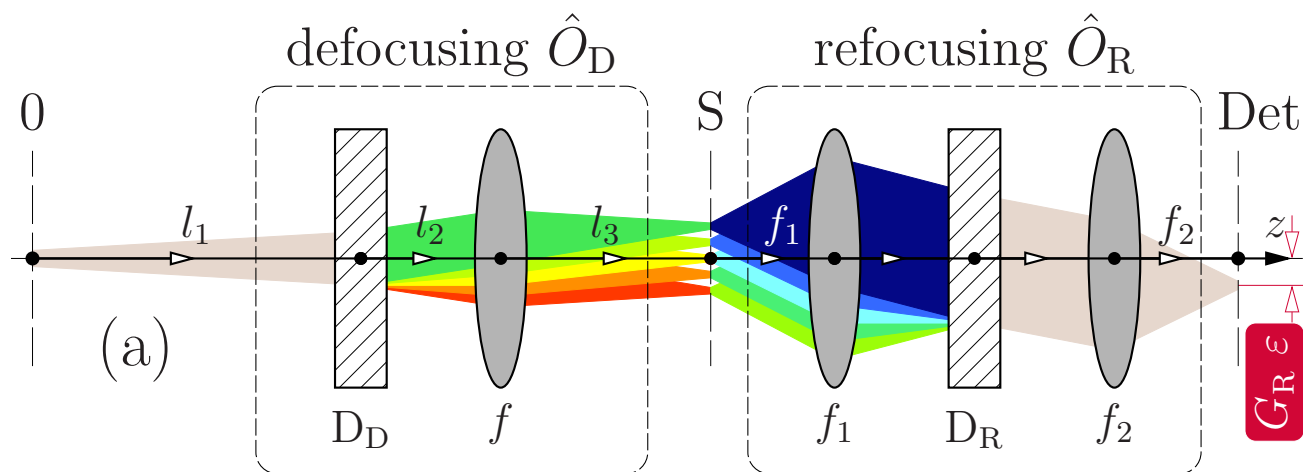
Energy transfer ϵ is measured by mapping ϵ on the pixel detector.

Energy resolution $\Delta \epsilon = \Delta x_1 A_R / G_R$

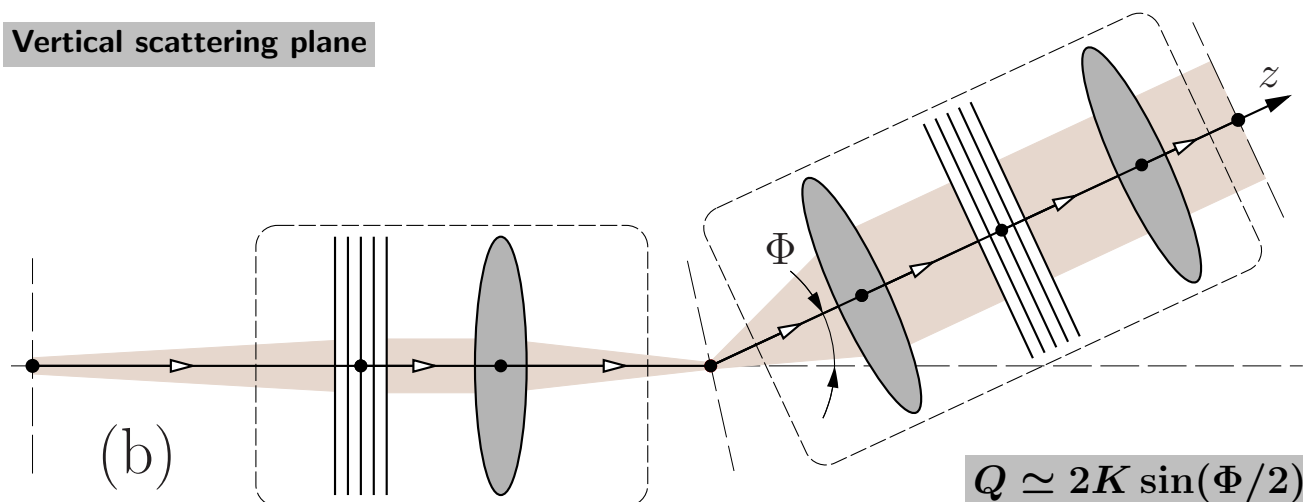
Does not rely on the monochromaticity of incident x-rays!

Signal strength:

$$S_{\text{echo}} \propto \Delta E_{UD} \times \Delta E_{UR}$$



Vertical scattering plane



Horizontal scattering plane

$$Q \simeq 2K \sin(\Phi/2)$$



X-ray Echo Spectrometer - Inelastic Scattering

Defocusing dispersing system \hat{O}_D is a broadband device with a bandwidth $\Delta E_{UD} \gg \Delta \epsilon$.

Refocusing dispersing system \hat{O}_R is a broadband spectrograph with a bandwidth $\Delta E_{UR} \gg \Delta \epsilon$

Refocusing (echo) takes place if the linear dispersion G_D in \hat{O}_D is compensated (time-reversed) by linear dispersion G_D in \hat{O}_D :

$$G_D + G_R/A_R = 0$$

Energy transfer ϵ is measured by mapping ϵ on the pixel detector.

Energy resolution $\Delta \epsilon = \Delta x_1 A_R / G_R$

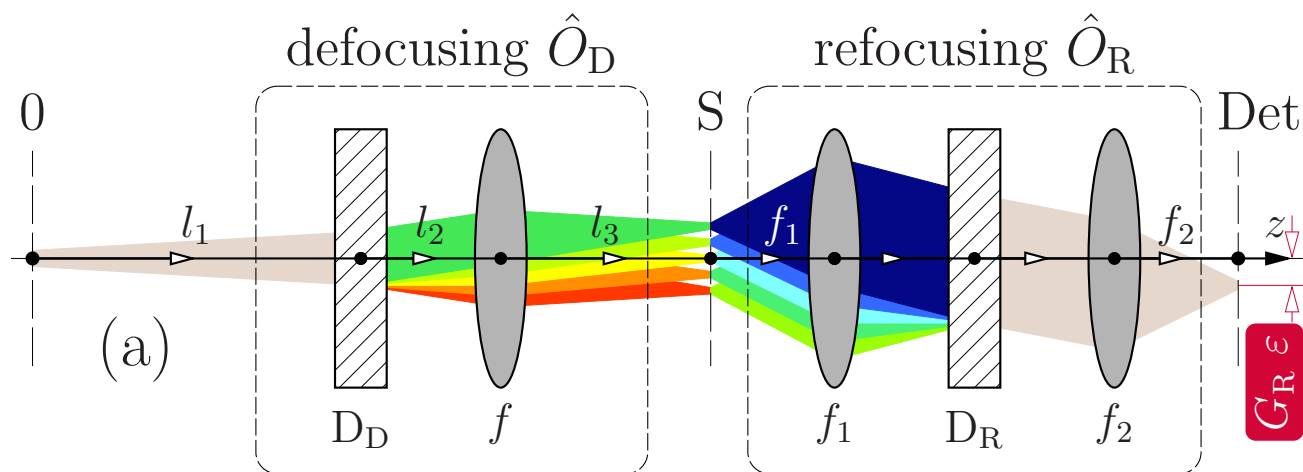
Does not rely on the monochromaticity of incident x-rays!

Signal strength:

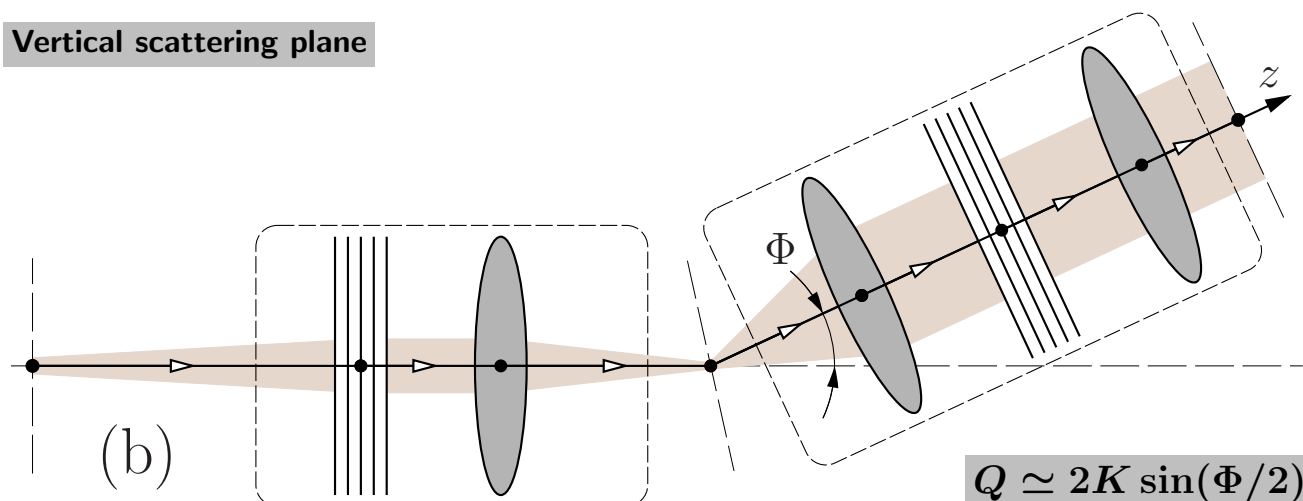
$$S_{\text{echo}} \propto \Delta E_{UD} \times \Delta E_{UR}$$

Signal enhancement:

$$\frac{S_{\text{echo}}}{S_{\text{scanning}}} = \frac{\Delta E_{UD} \times \Delta E_{UR}}{(\Delta \epsilon)^2} > 10^2 - 10^4$$



Vertical scattering plane

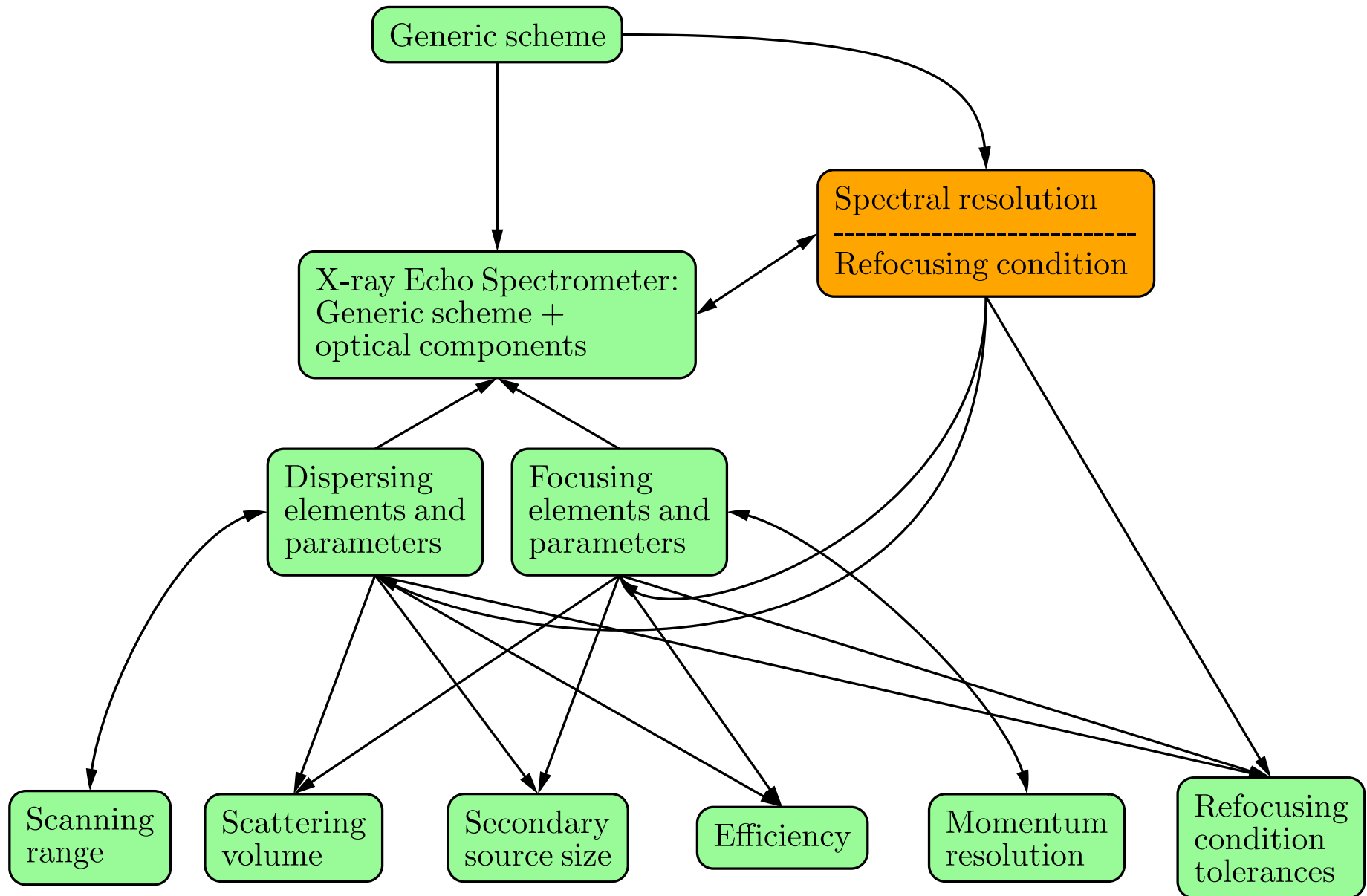


Horizontal scattering plane

$$Q \simeq 2K \sin(\Phi/2)$$



X-ray echo spectrometer design & performance



X-ray Echo Spectrometer - Spectral Resolution

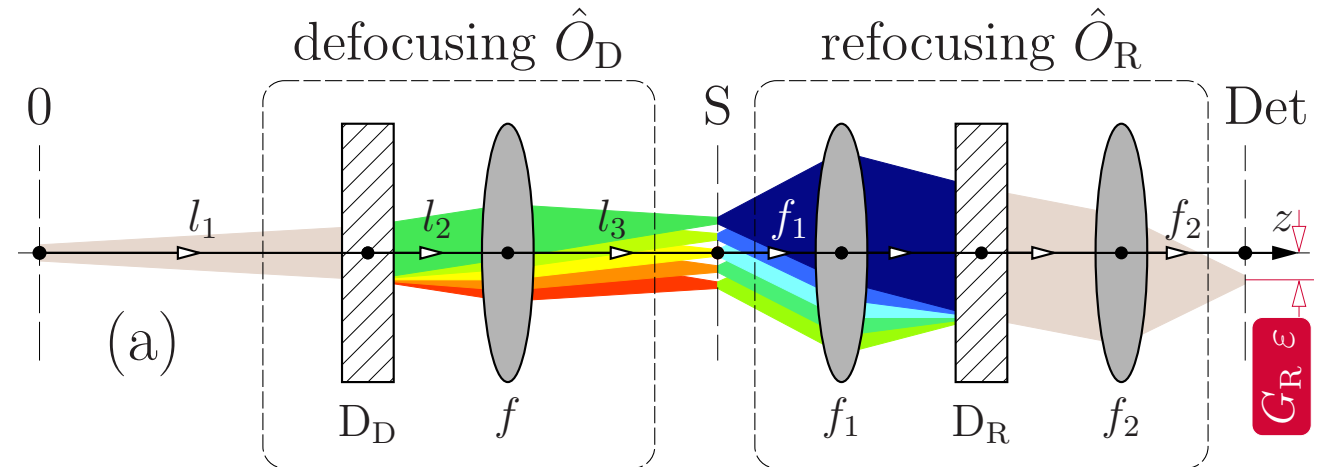
$$\Delta\varepsilon = \frac{\Delta x_2}{G_R}$$

⇓

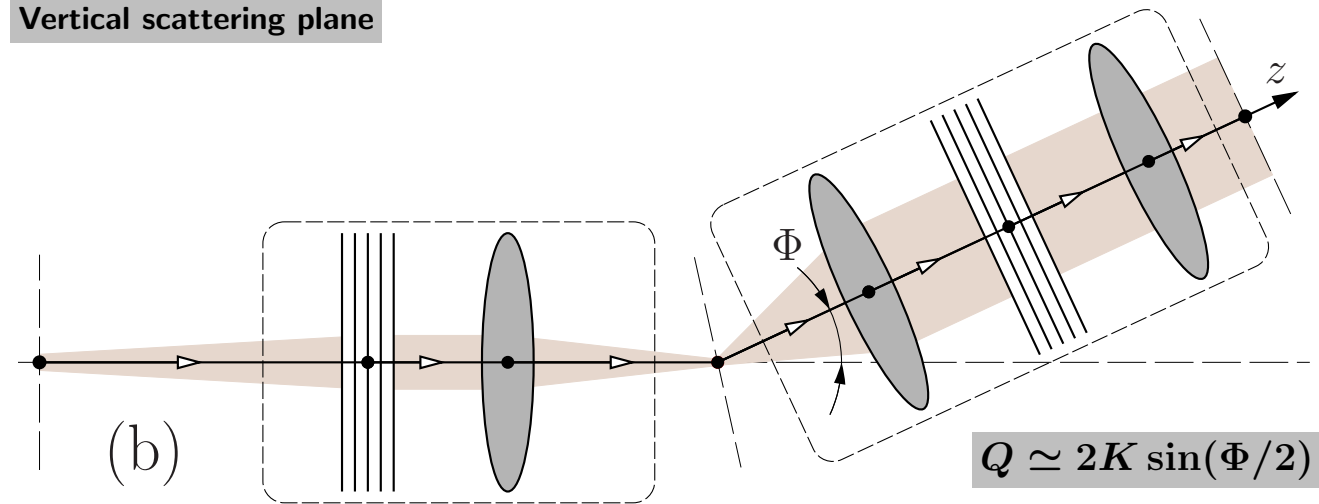
$$\Delta\varepsilon = \frac{\Delta x_1 A_R}{G_R}$$

⇓

$$\Delta\varepsilon = \frac{\Delta x_1}{f_1} \frac{b_{UR}}{D_{UR}}$$



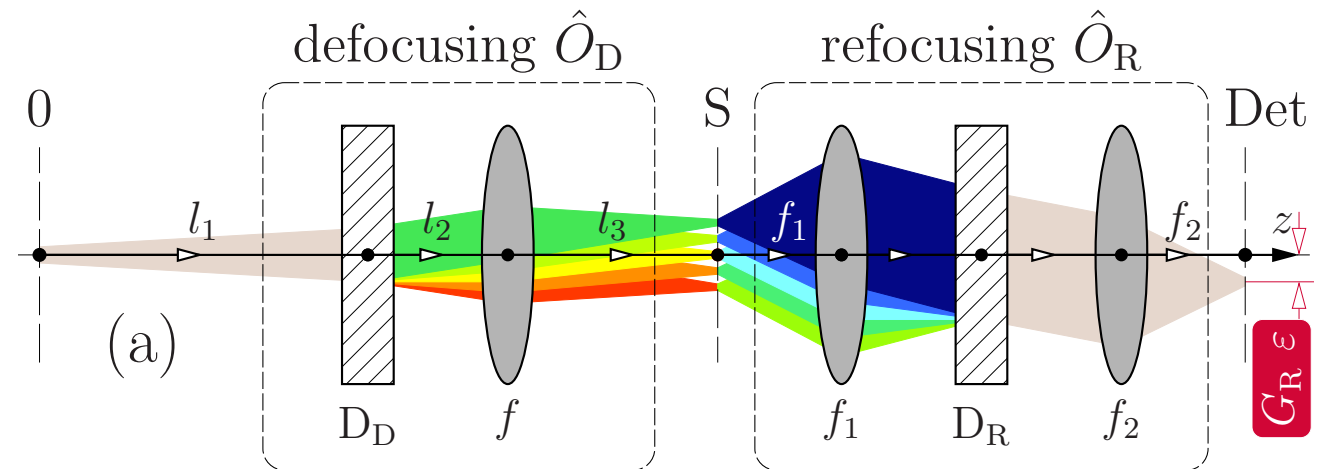
Vertical scattering plane



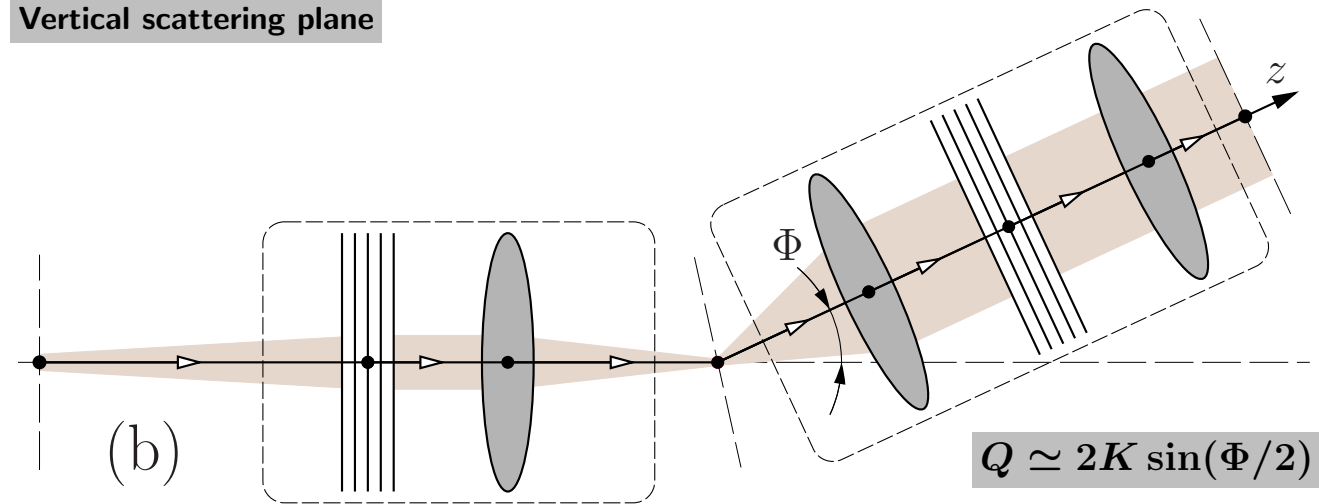
Horizontal scattering plane

X-ray Echo Spectrometer - Spectral Resolution

$$\Delta\varepsilon = \frac{\Delta x_1}{f_1} \frac{b_{UR}}{\mathcal{D}_{UR}}$$



Vertical scattering plane



Horizontal scattering plane

$$Q \simeq 2K \sin(\Phi/2)$$

Δx_1 – monochromatic secondary source size (on the sample)
 f_1 – focal lengths of the collimating optic
 \mathcal{D}_{UR} – cumulative angular dispersion rate of the dispersing element D_R
 b_{UR} – cumulative asymmetry factor of the dispersing element D_R

X-ray Echo Spectrometer - Spectral Resolution

$$\Delta\varepsilon = \frac{\Delta x_1}{f_1} \frac{b_{UR}}{\mathcal{D}_{UR}}$$

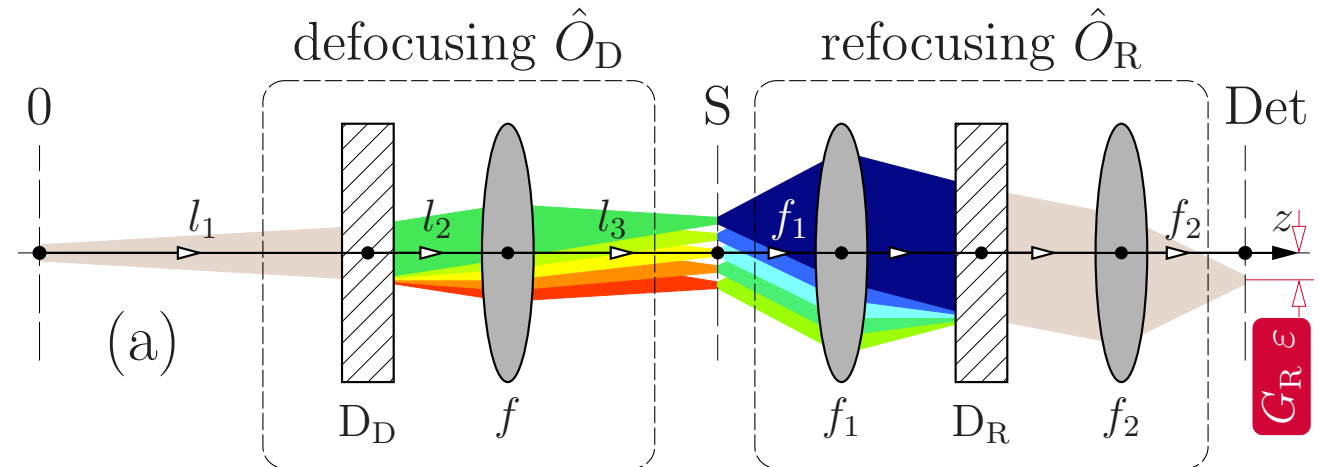
$$\Delta\varepsilon = 0.1 \text{ meV}$$

$$\Delta x_1 = 5 \text{ }\mu\text{m}$$

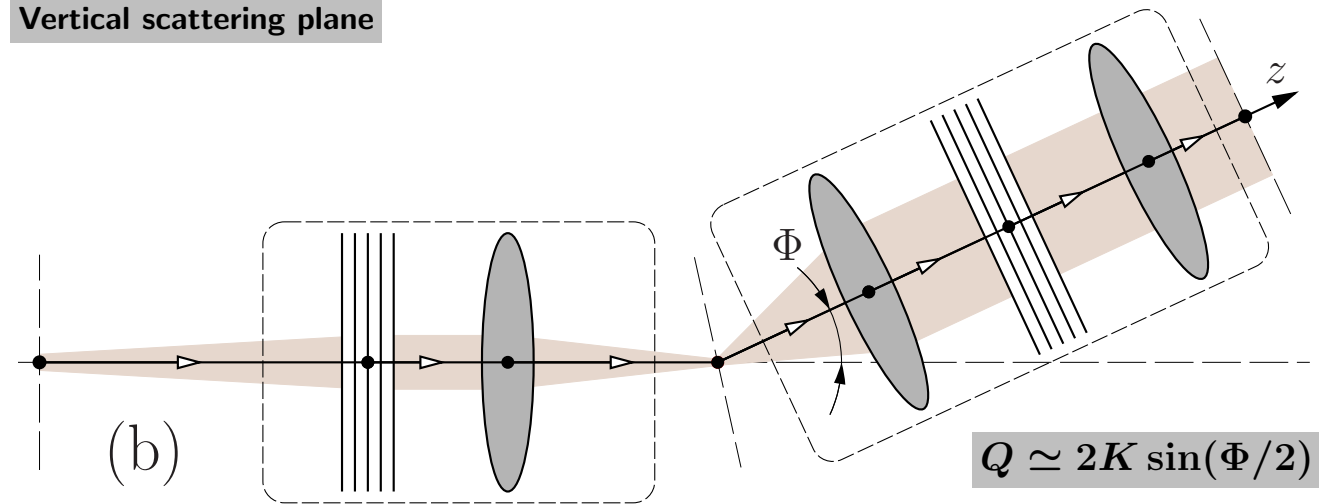
$$f_1 = 0.4 \text{ m}$$



$$\frac{\mathcal{D}_{UR}}{b_{UR}} = 125 \text{ }\mu\text{rad/meV}$$



Vertical scattering plane



Horizontal scattering plane

$$Q \simeq 2K \sin(\Phi/2)$$

Δx_1 – monochromatic secondary source size (on the sample)

f_1 – focal lengths of the collimating optic

\mathcal{D}_{UR} – cumulative angular dispersion rate of the dispersing element D_R

b_{UR} – cumulative asymmetry factor of the dispersing element D_R

X-ray Echo Spectrometer - Spectral Resolution

$$\Delta\varepsilon = \frac{\Delta x_1}{f_1} \frac{b_{UR}}{\mathcal{D}_{UR}}$$

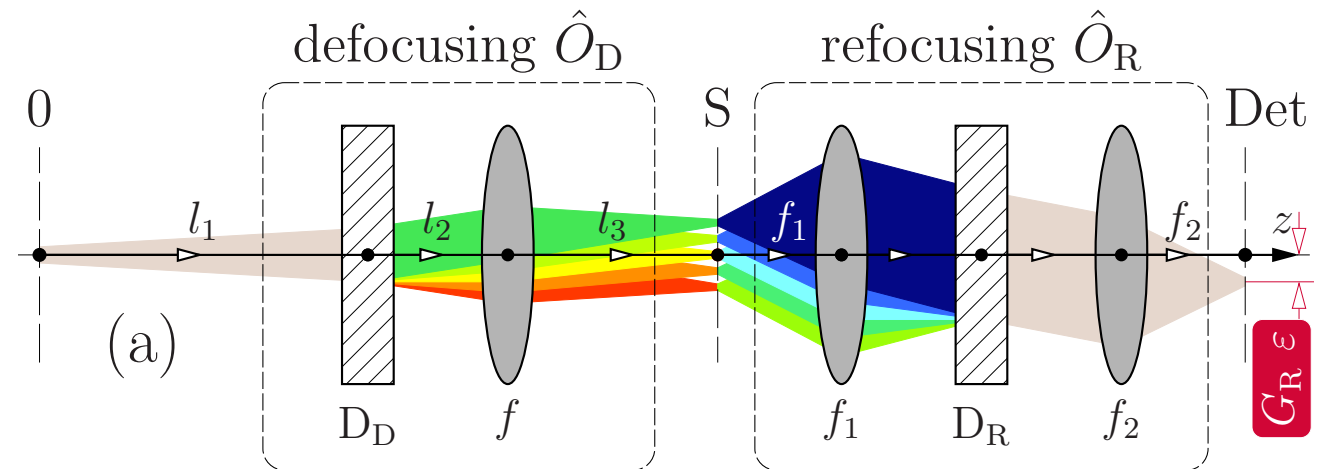
$$\Delta\varepsilon = 1 \text{ meV}$$

$$\Delta x_1 = 5 \text{ }\mu\text{m}$$

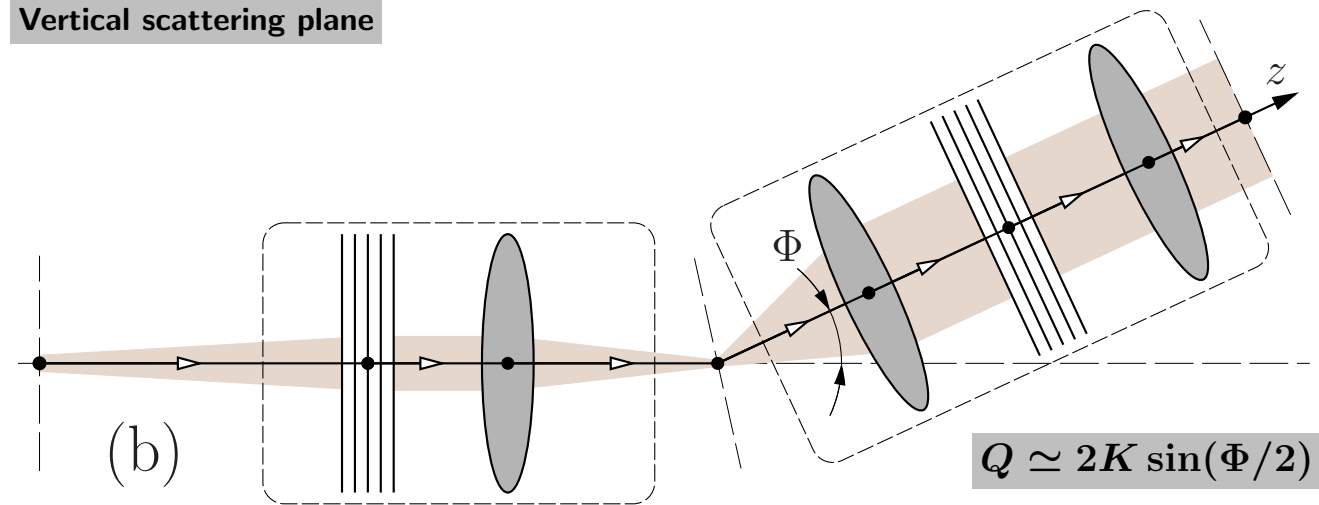
$$f_1 = 0.2 \text{ m}$$



$$\frac{\mathcal{D}_{UR}}{b_{UR}} = 25 \text{ }\mu\text{rad/meV}$$



Vertical scattering plane



Horizontal scattering plane

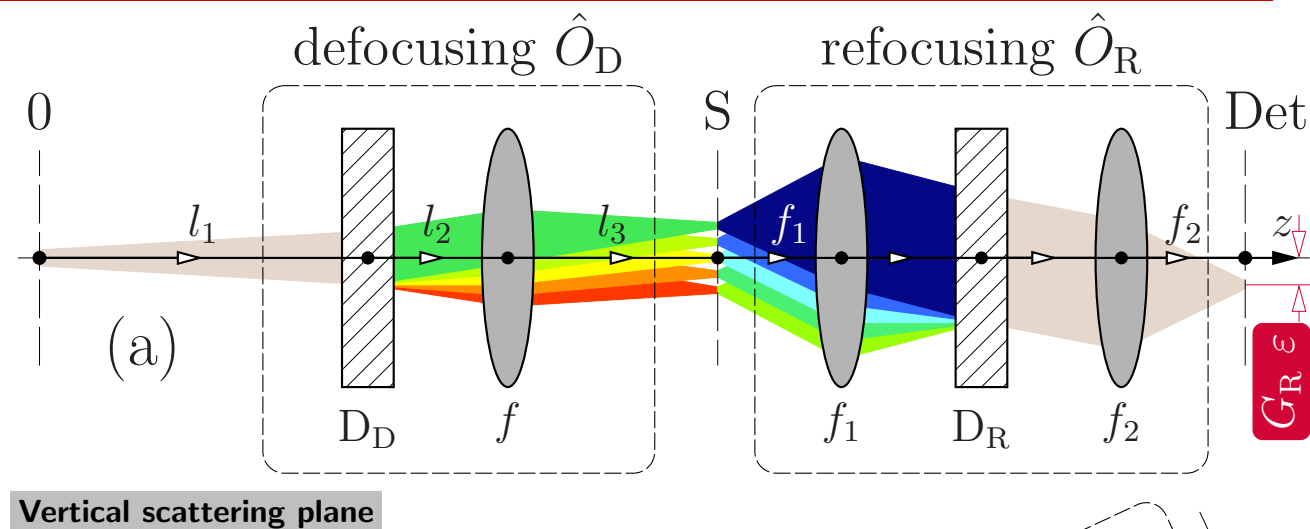
Δx_1 – monochromatic secondary source size (on the sample)
 f_1 – focal lengths of the collimating optic
 \mathcal{D}_{UR} – cumulative angular dispersion rate of the dispersing element D_R
 b_{UR} – cumulative asymmetry factor of the dispersing element D_R

X-ray Echo Spectrometer - Refocusing Condition

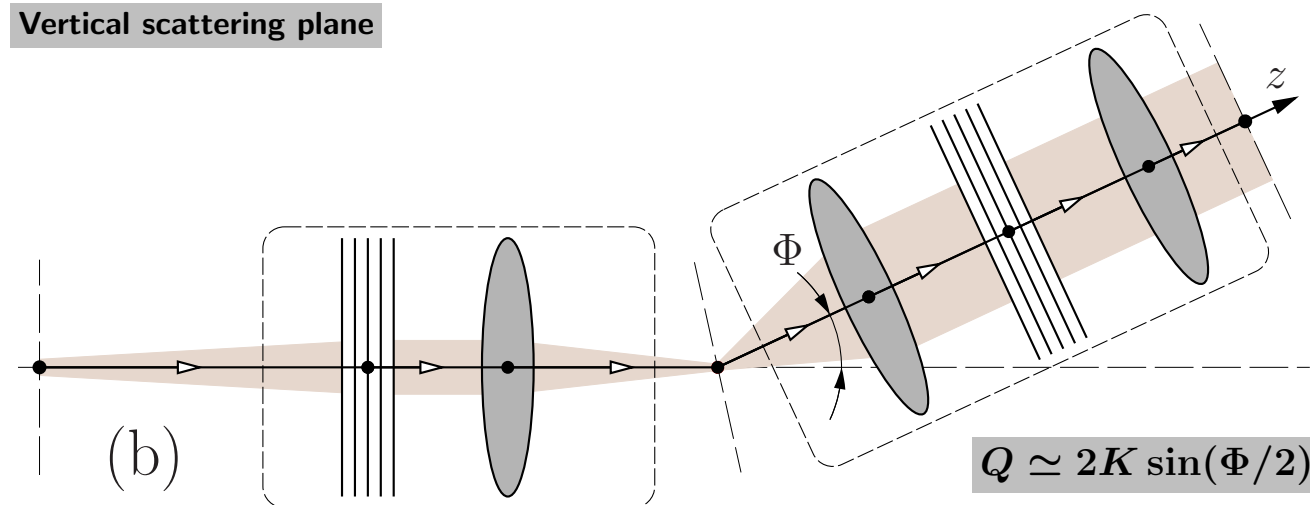
$$G_D + G_R/A_R = 0$$

⇓

$$l_3 \mathcal{D}_{U_D} \simeq f_1 \frac{\mathcal{D}_{U_R}}{b_{U_R}}$$



Vertical scattering plane



Horizontal scattering plane

l_3 – distance to the sample from the focusing optic f
 \mathcal{D}_{U_R} – cumulative angular dispersion rate of the dispersing element D_D



X-ray Echo Spectrometer - Refocusing Condition

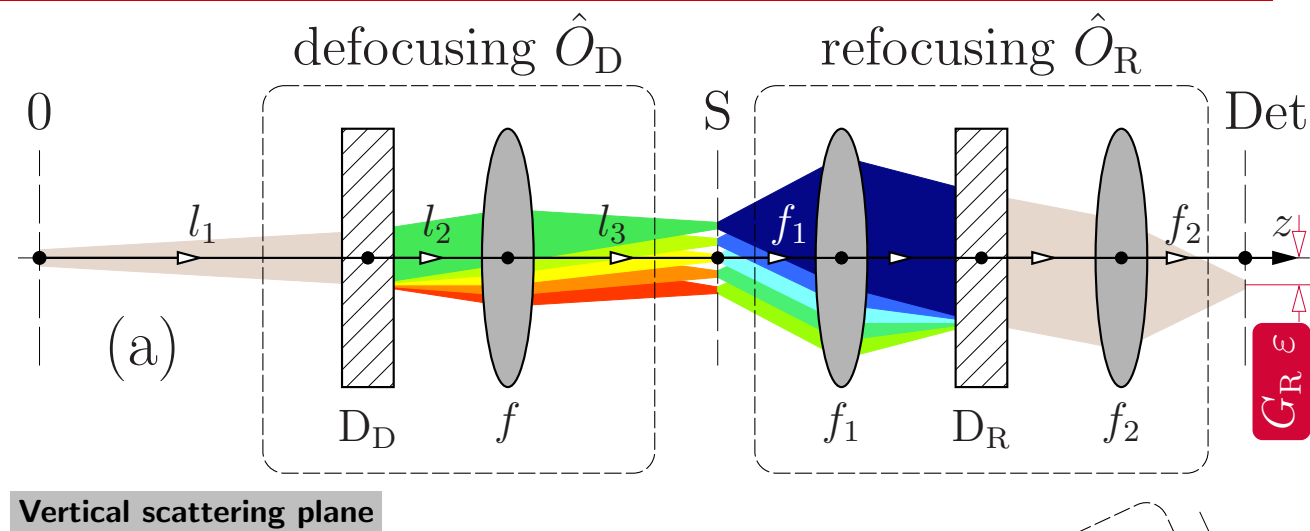
$$G_D + G_R/A_R = 0$$

⇓

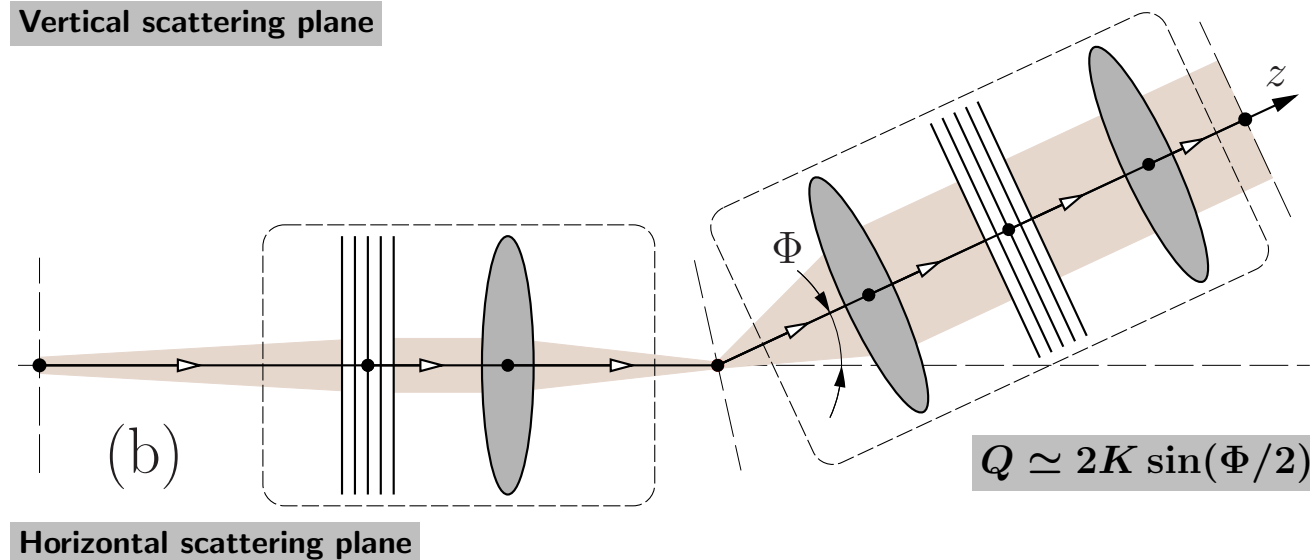
$$l_3 \mathcal{D}_{U_D} \simeq f_1 \frac{\mathcal{D}_{U_R}}{b_{U_R}}$$

⇓

Defined by the spectral resolution.



Vertical scattering plane



Horizontal scattering plane

$$Q \simeq 2K \sin(\Phi/2)$$

l_3 – distance to the sample from the focusing optic f
 \mathcal{D}_{U_R} – cumulative angular dispersion rate of the dispersing element D_D



X-ray Echo Spectrometer - Refocusing Condition

$$G_D + G_R/A_R = 0$$

⇓

$$l_3 \mathcal{D}_{U_D} \simeq f_1 \frac{\mathcal{D}_{U_R}}{b_{U_R}}$$

⇓

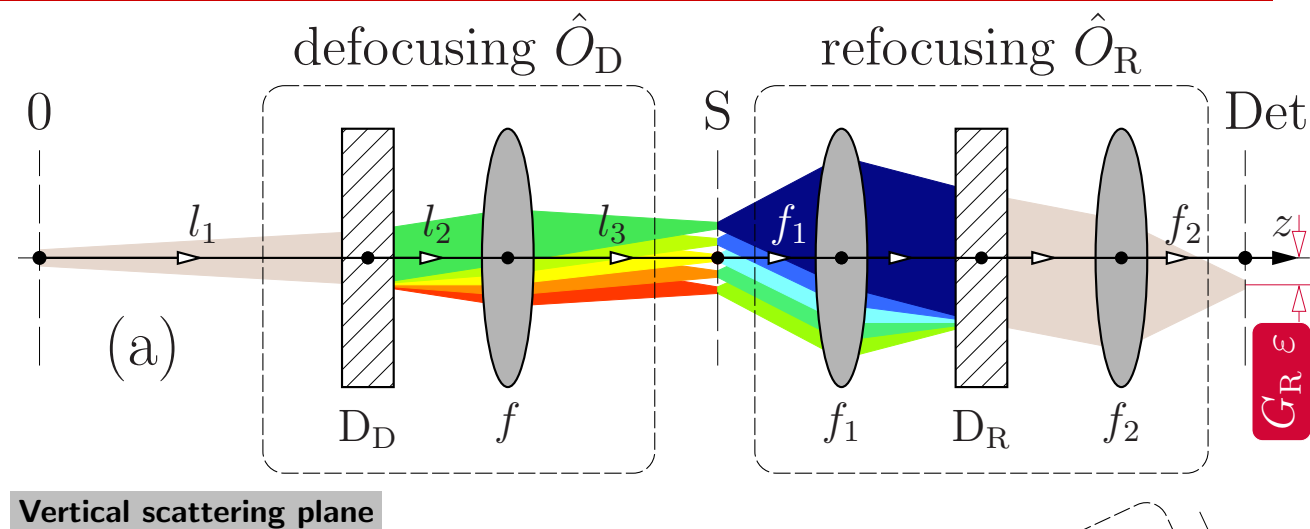
Defined by the spectral resolution.

$$\Delta \varepsilon = 0.1 \text{ meV}$$

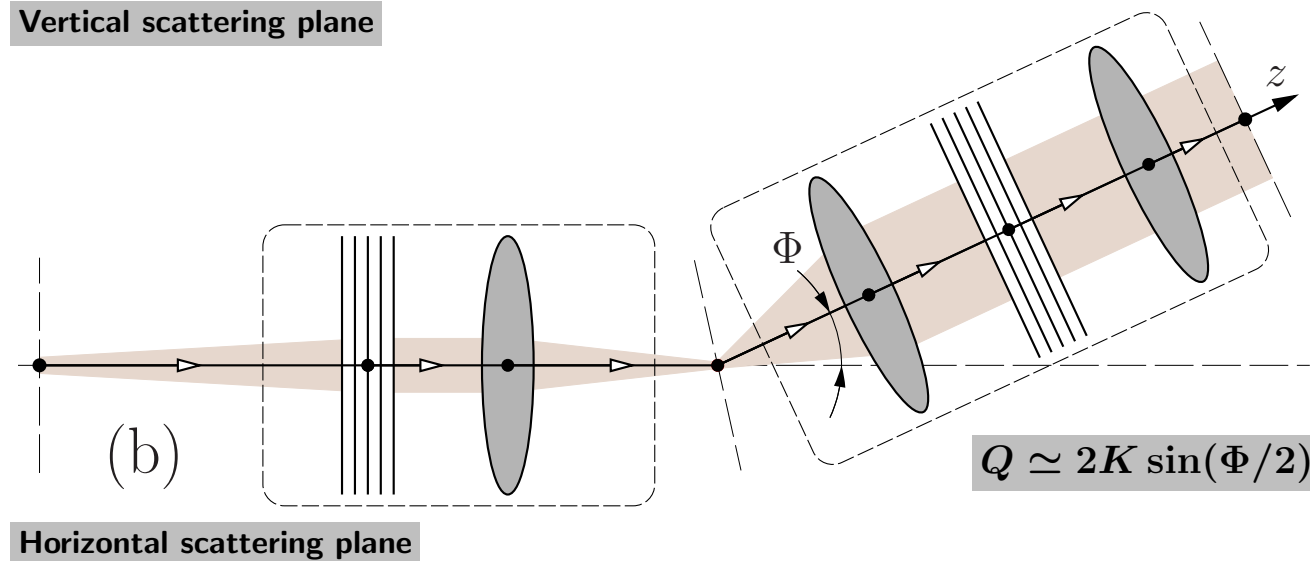
$$l_3 = 2 \text{ m}$$

⇓

$$\mathcal{D}_{U_D} = 25 \text{ } \mu\text{rad/meV}$$



Vertical scattering plane



Horizontal scattering plane

$$Q \simeq 2K \sin(\Phi/2)$$



X-ray Echo Spectrometer - Refocusing Condition

$$G_D + G_R/A_R = 0$$

⇓

$$l_3 \mathcal{D}_{U_D} \simeq f_1 \frac{\mathcal{D}_{U_R}}{b_{U_R}}$$

⇓

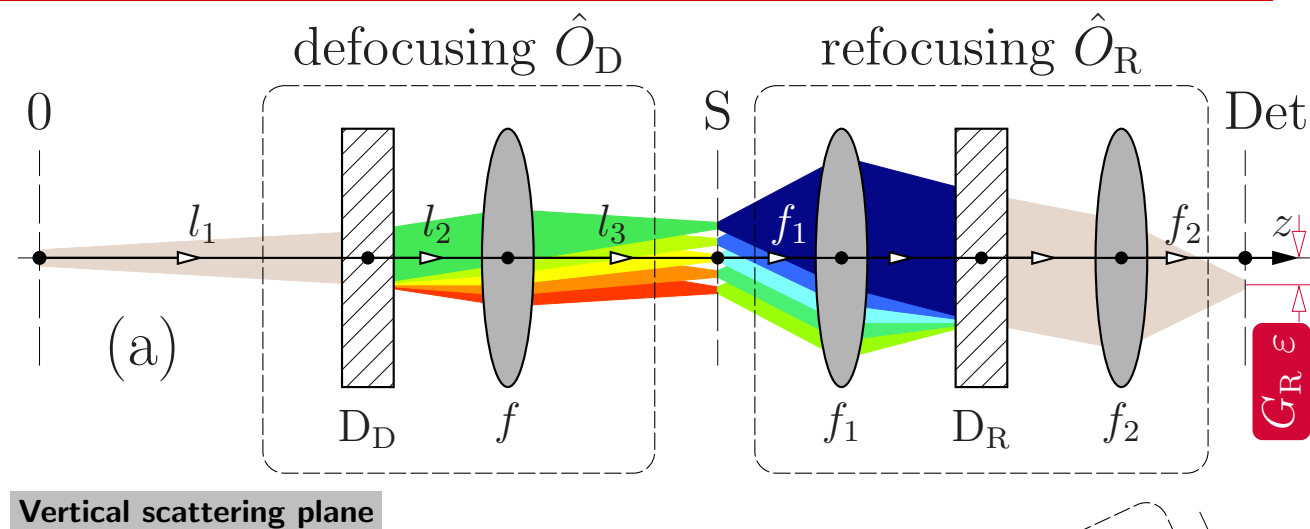
Defined by the spectral resolution.

$$\Delta \varepsilon = 1 \text{ meV}$$

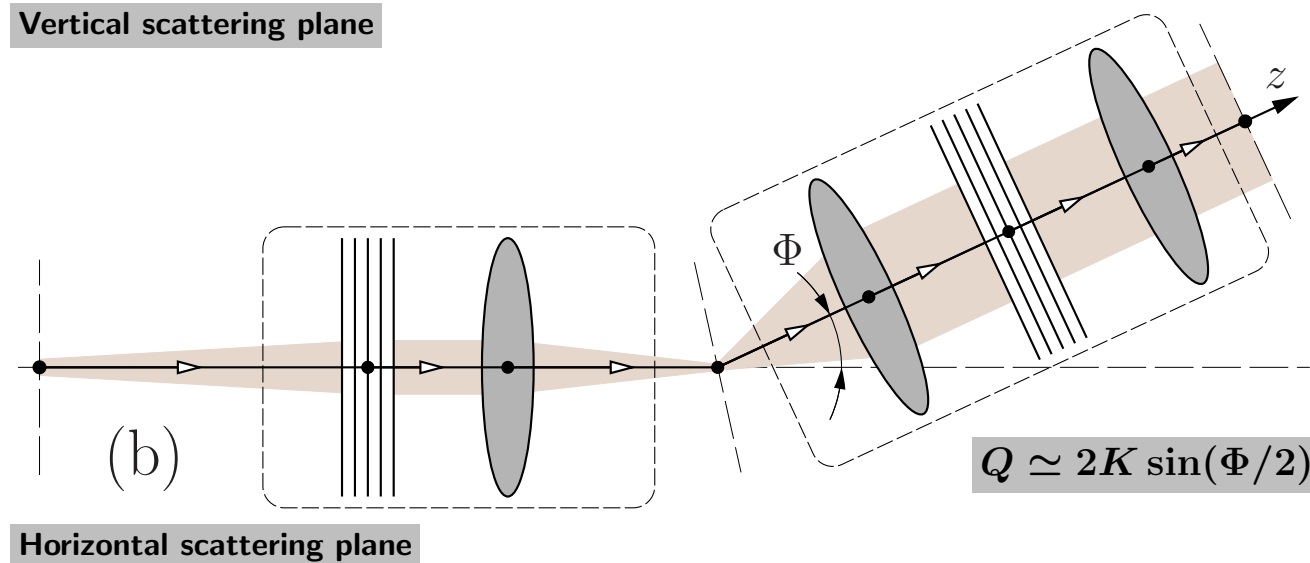
$$l_3 = 2 \text{ m}$$

⇓

$$\mathcal{D}_{U_D} = 2.5 \text{ } \mu\text{rad/meV}$$



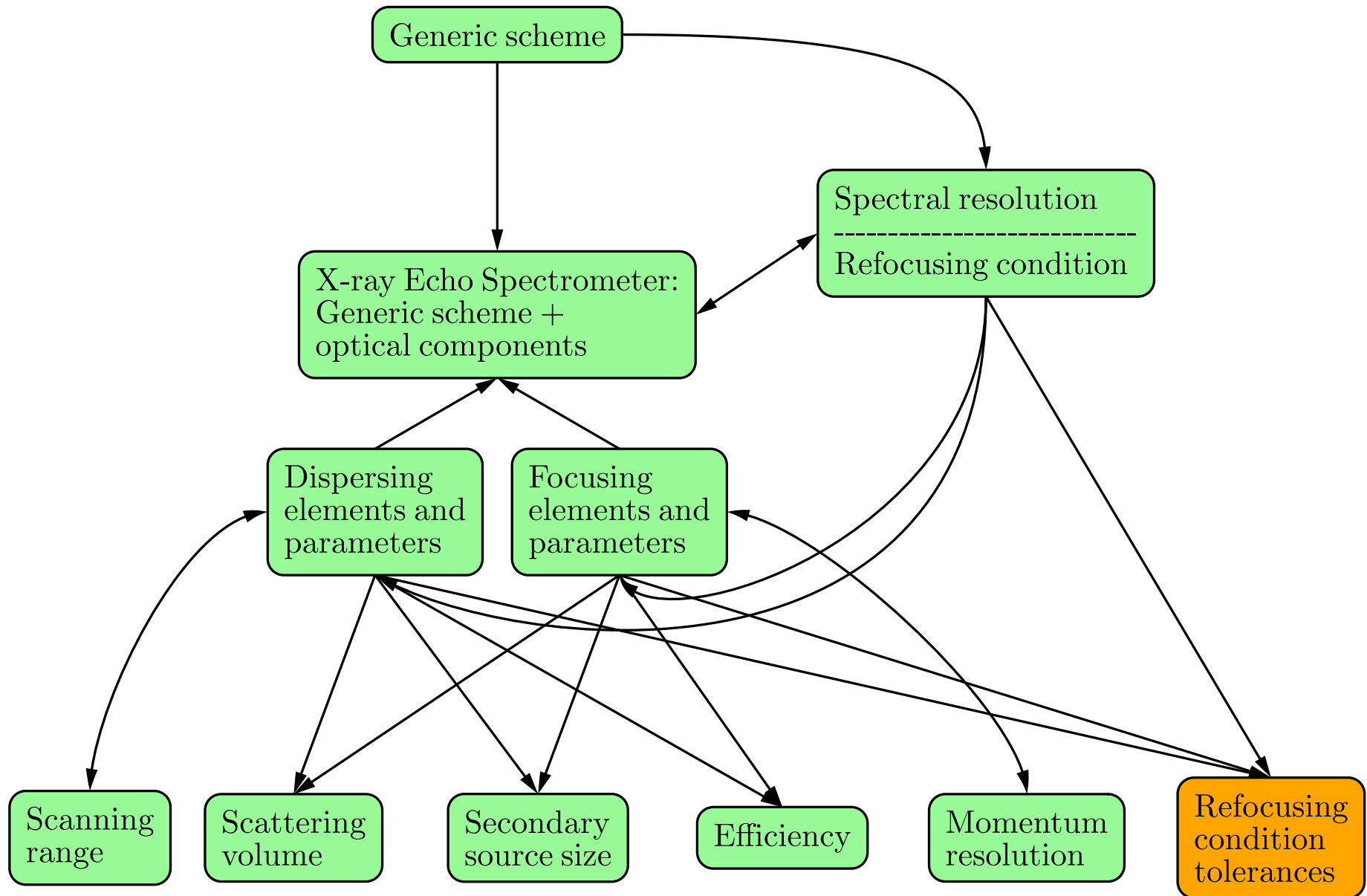
Vertical scattering plane



Horizontal scattering plane



X-ray echo spectrometer design & performance



X-ray Echo Spectrometer Tolerances

$$|G_D + G_R/A_R| \Delta E_U \ll \Delta x_1$$

⇓

$$\left| \mathcal{D}_{U_D} l_3 - \frac{\mathcal{D}_{U_R} f_1}{b_{U_R}} \right| \Delta E_U \ll \Delta x_1$$

⇓

$$|\Delta l_3| \ll \frac{\Delta x_1}{|\mathcal{D}_{U_D}| \Delta E_U} \text{ or}$$

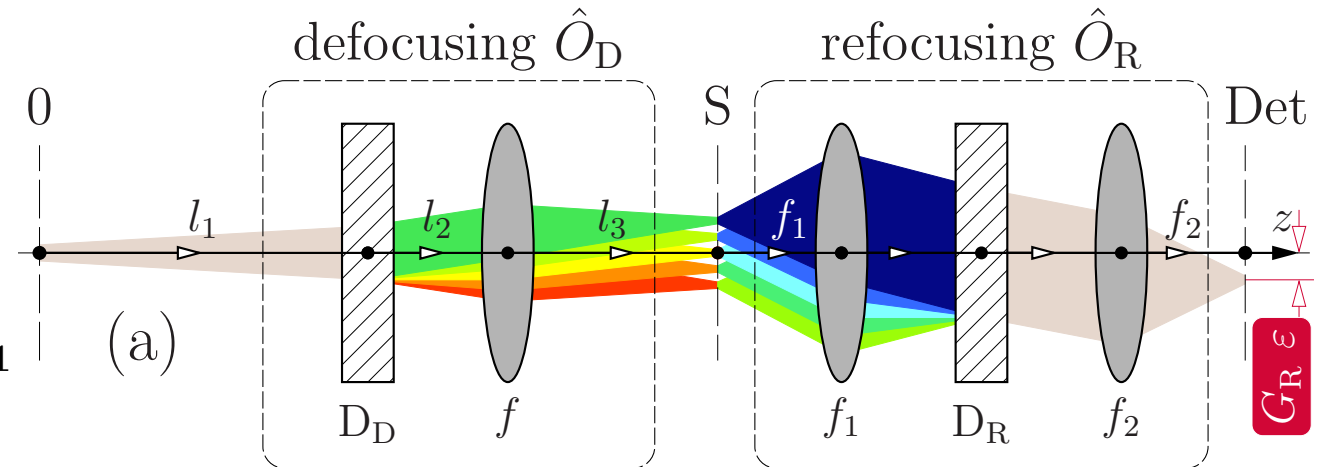
$$|\Delta f_1| \ll \frac{\Delta x_1 b_{U_R}}{|\mathcal{D}_{U_R}| \Delta E_U}$$

$$\Delta \epsilon = 0.1 \text{ meV}$$

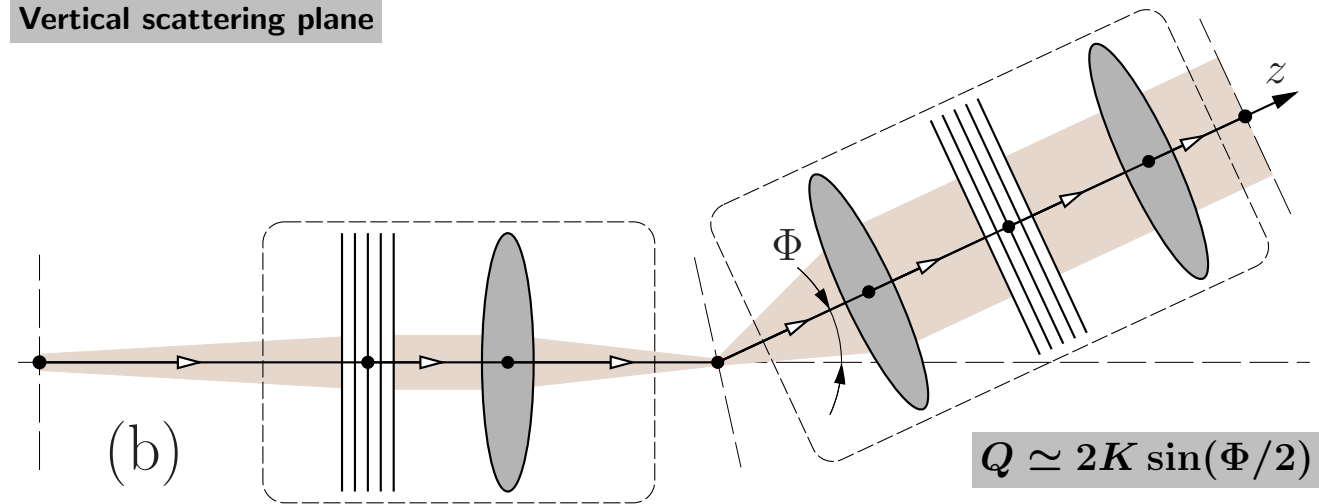
$$\Delta E_U = 5.5 \text{ meV}$$

⇓

$$|\Delta l_3| \ll 36 \text{ mm, and } |\Delta f_1| \ll 7 \text{ mm}$$



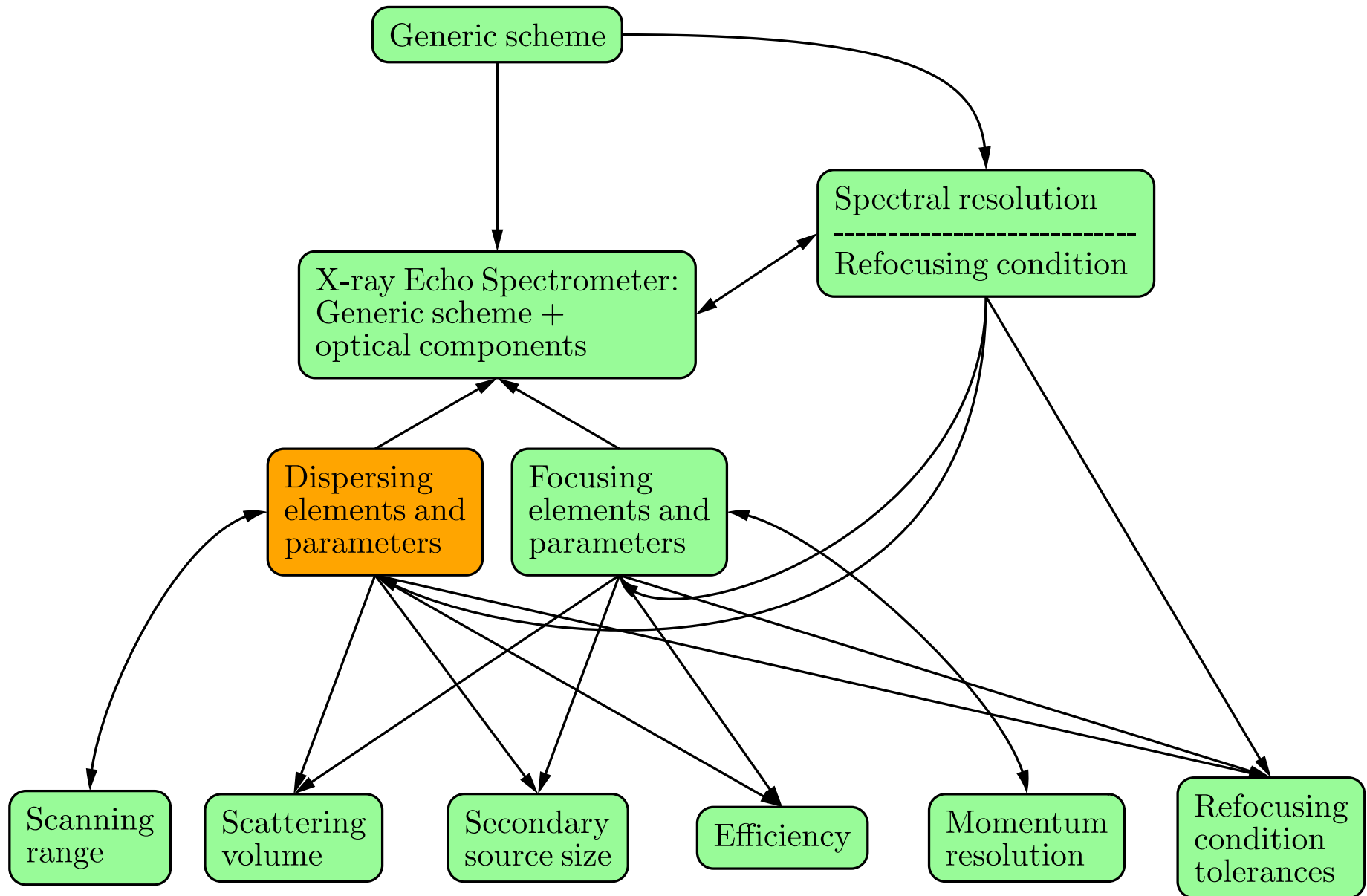
Vertical scattering plane



Horizontal scattering plane



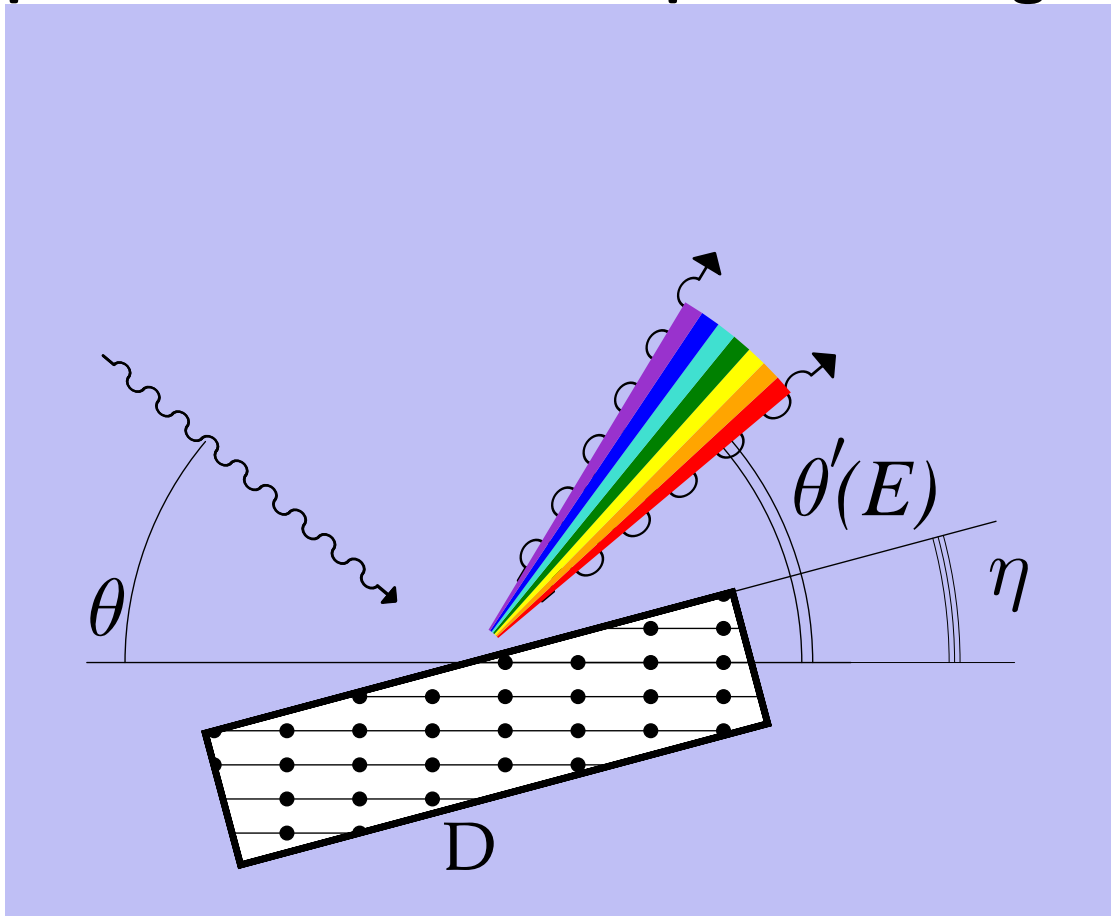
X-ray echo spectrometer design & performance



Bragg-Diffracting Crystals as Diffraction Gratings

Angular Dispersion

An asymmetrically cut crystal behaves like a diffraction grating dispersing photons with different photon energies: **effect of angular dispersion.**



$$\mathcal{D} = \delta\theta' / \delta E = \text{dispersion rate}$$

$$\mathcal{D} = \frac{2 \sin \theta \sin \eta}{E \sin(\theta - \eta)}$$

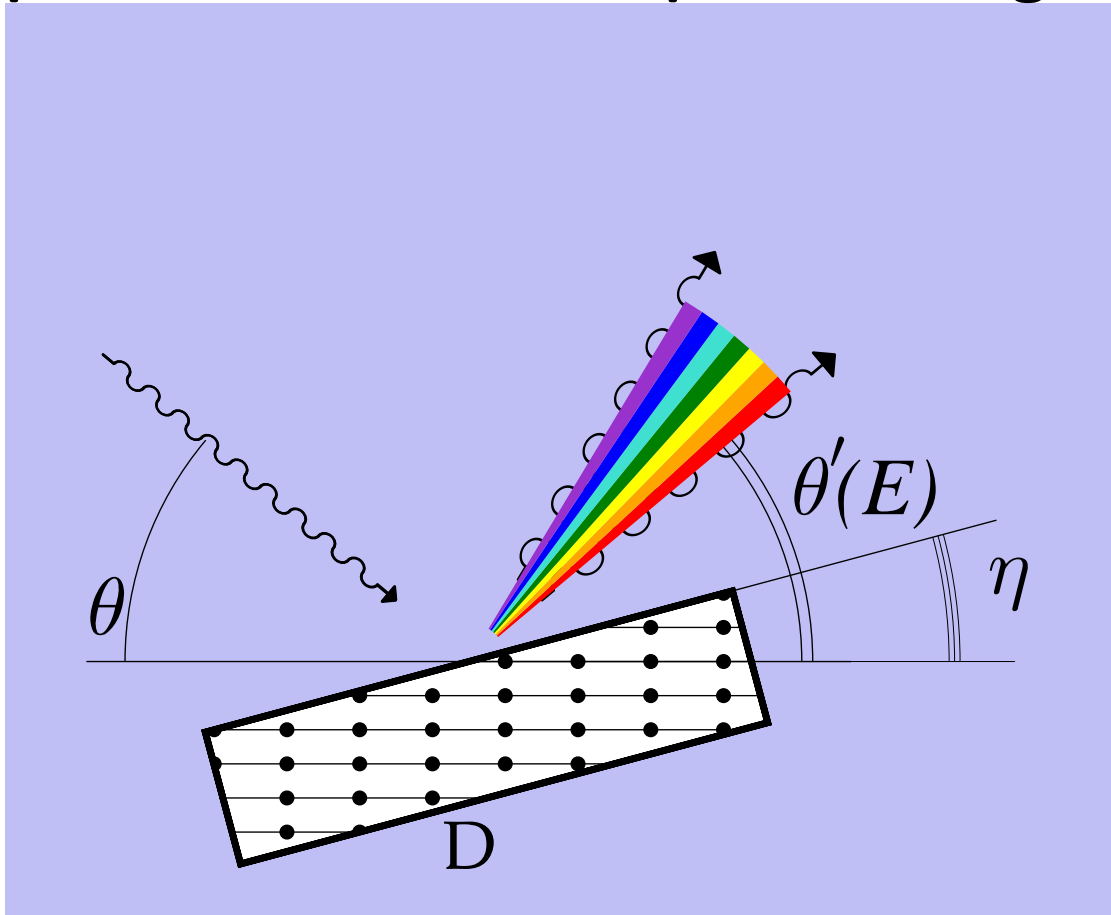
T. Matsushita and U. Kaminaga, *J. Appl. Crystallogr.*, 13 (1980) 472

Yu. Shvyd'ko *X-Ray Optics*, Springer-Verlag (2004)

Bragg-Diffracting Crystals as Diffraction Gratings

Angular Dispersion

An asymmetrically cut crystal behaves like a diffraction grating dispersing photons with different photon energies: **effect of angular dispersion.**



Angular dispersion rate \mathcal{D} is biggest for:

$$\mathcal{D} = \delta\theta' / \delta E = \text{dispersion rate}$$

$$\mathcal{D} = \frac{2 \sin \theta \sin \eta}{E \sin(\theta - \eta)} \implies \frac{2 \tan \eta}{E}$$

1. $\theta' - \eta \rightarrow 0^\circ$ and $\theta \rightarrow 90^\circ$.

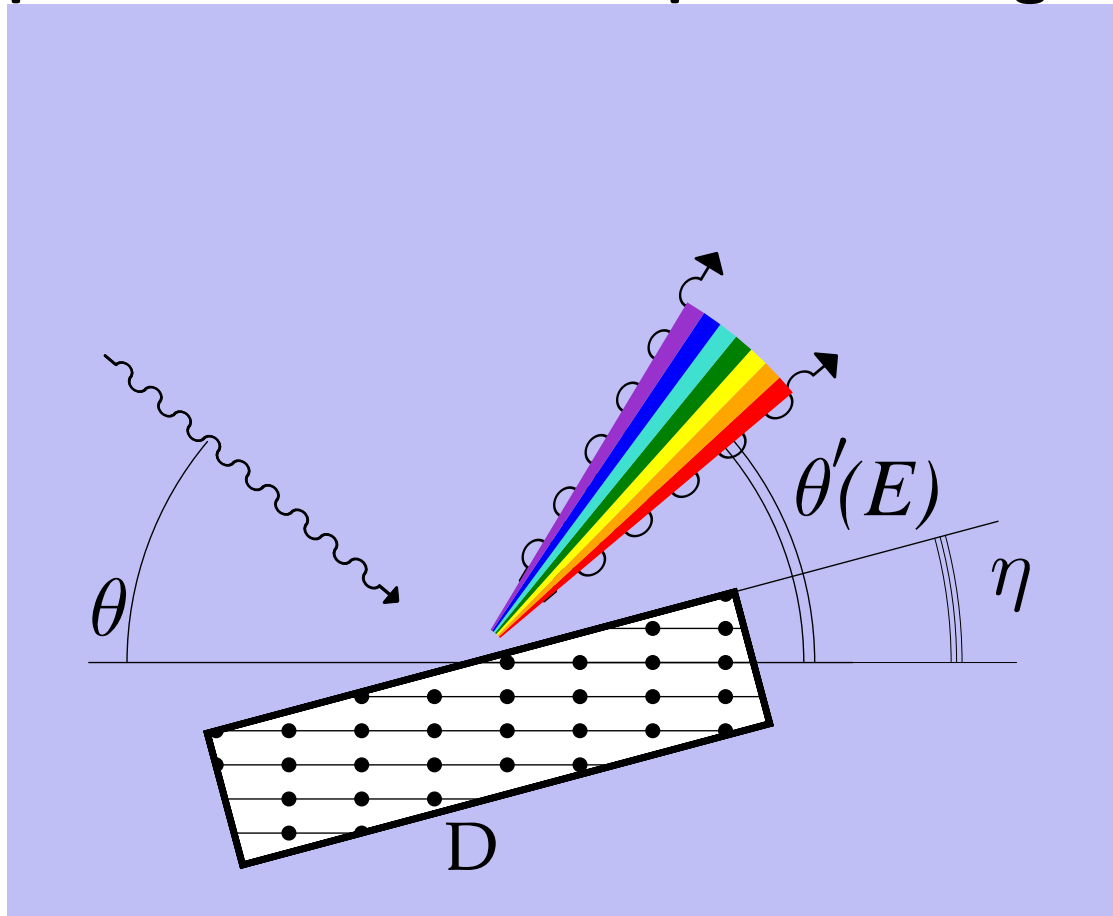
2. lower photon energies E ;

$E=9$ keV is chosen as a compromise

Bragg-Diffracting Crystals as Diffraction Gratings

Angular Dispersion

An asymmetrically cut crystal behaves like a diffraction grating dispersing photons with different photon energies: **effect of angular dispersion.**



$$\mathcal{D} = \delta\theta' / \delta E = \text{dispersion rate}$$

$$\mathcal{D} = \frac{2 \sin \theta \sin \eta}{E \sin(\theta - \eta)} \implies \frac{2 \tan \eta}{E}$$

$$\mathcal{D} \lesssim 10 \mu\text{rad}/\text{meV}$$

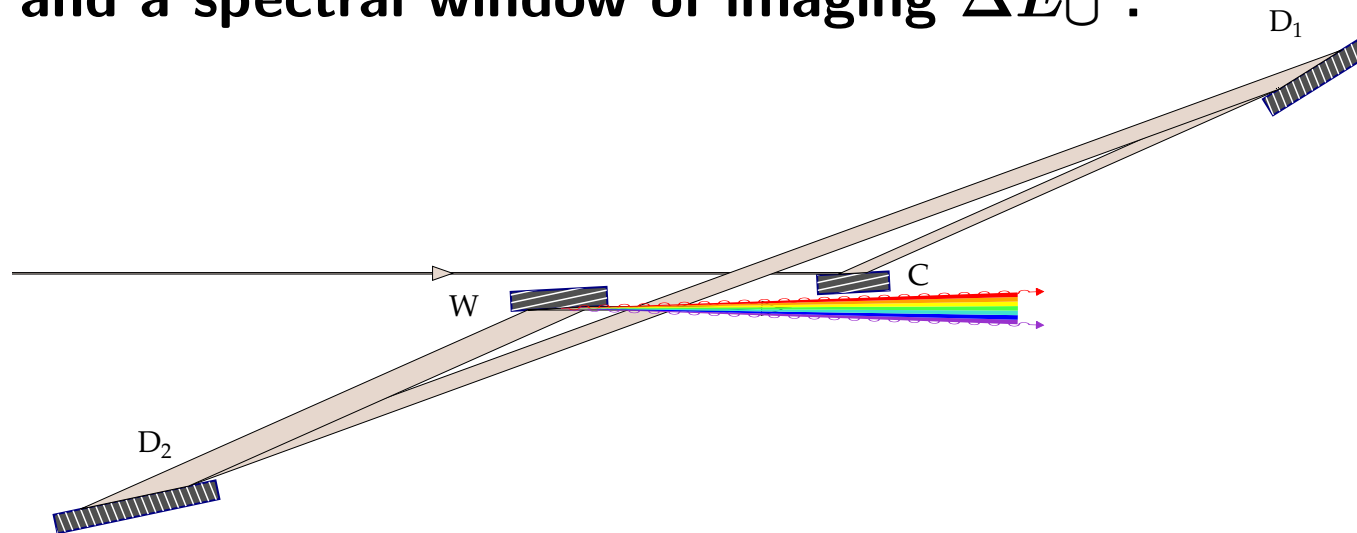
Yet often insufficient for practical applications

Multi-Crystal Optic as a Diffraction Grating with Enhanced Angular Dispersion Rate

The angular dispersion rate in a multicrystal optic can be dramatically **enhanced by almost two orders of magnitude** compared to that of a single crystal:

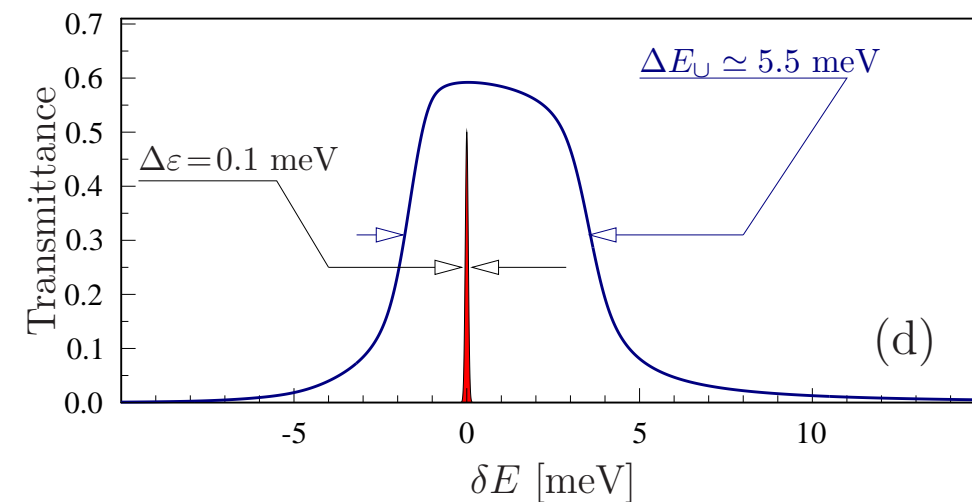
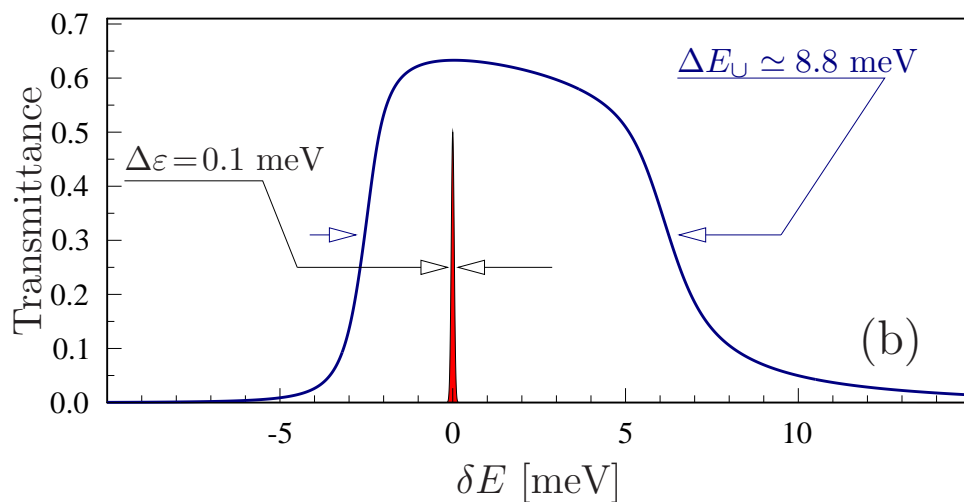
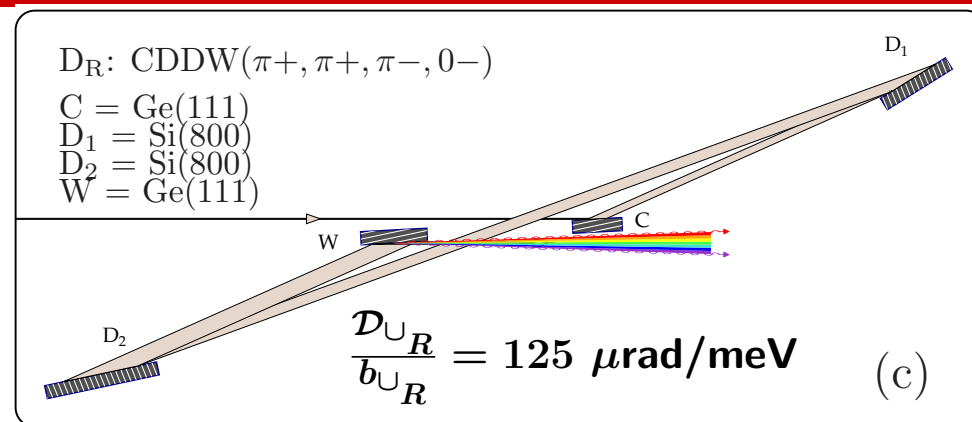
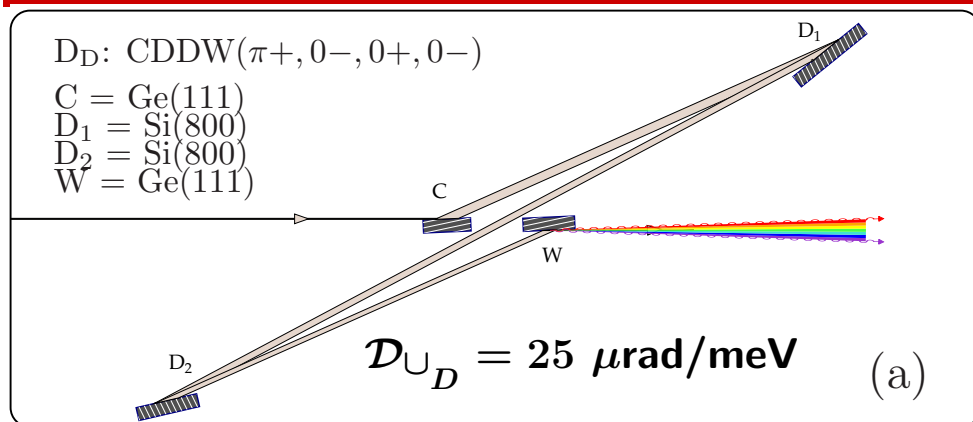
$$\mathcal{D}_{U_n} = b_n \mathcal{D}_{U_{n-1}} + \mathcal{D}_n$$

The multi-crystal dispersing element (“diffraction grating”) is characterized by a cumulative angular dispersion rate \mathcal{D}_U , a cumulative asymmetry parameter b_U , and a spectral window of imaging ΔE_U .



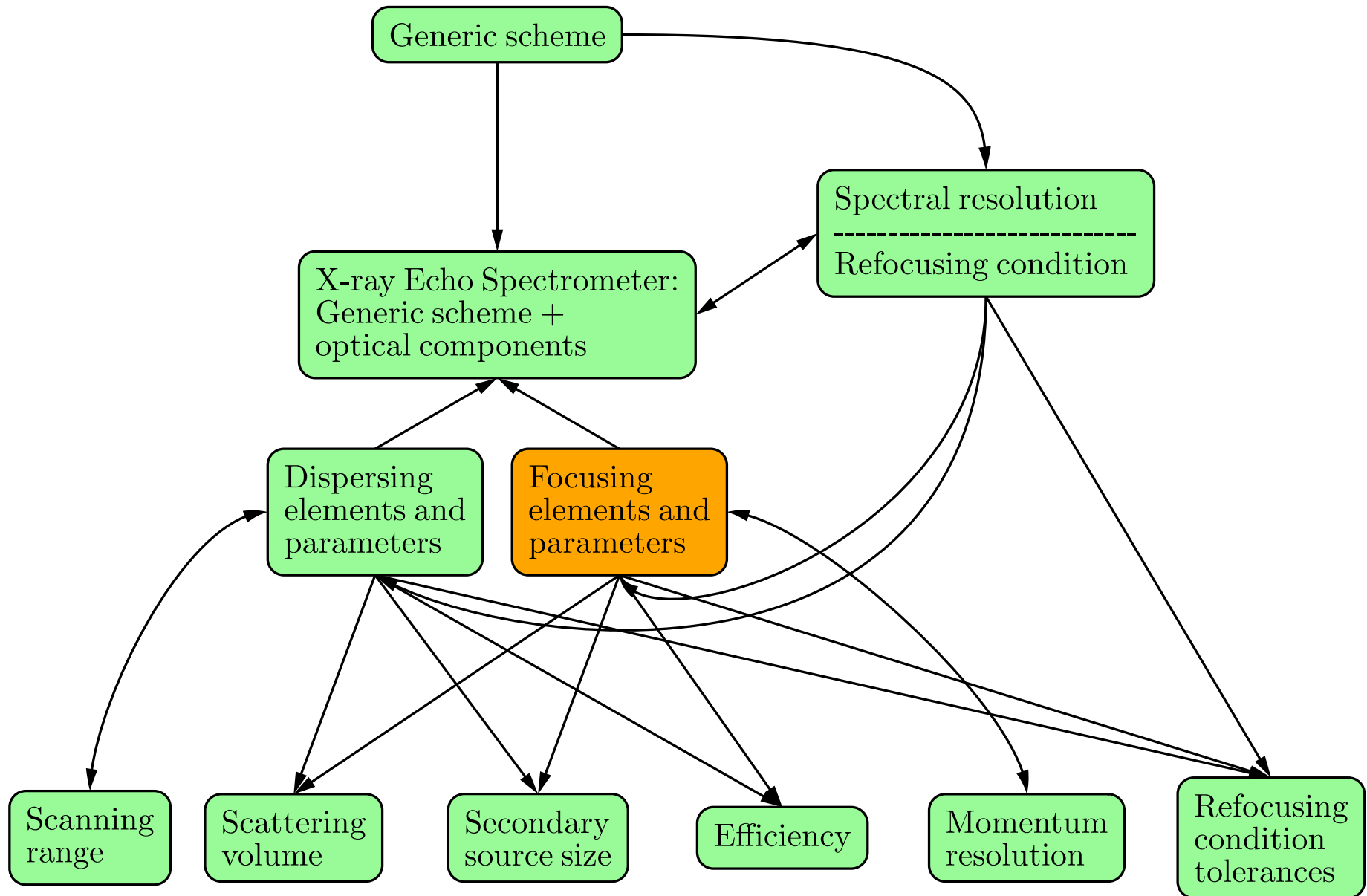
Yu.Sh., S. Stoupin, K. Mundboth, J.H. Kim, *PRA* 87 (2013) 043835

Multi-Crystal “Diffraction Gratings” for 0.1-meV-Resolution Echo Spectrometers



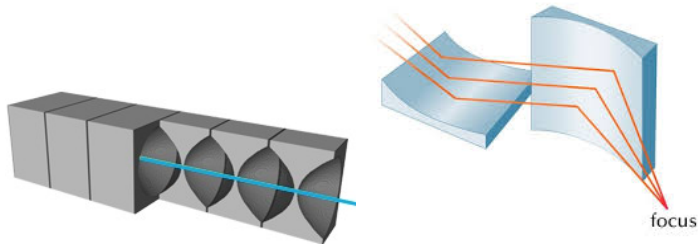
Dispersing elements D_D (a) and D_R (c) of the defocusing \hat{O}_D and the refocusing system \hat{O}_R , and their spectral transmittance function (b) and (d), respectively. The dispersing elements are examples of an in-line four-crystal CDDW-type optic, comprised of collimating (C), dispersing (D_1 , D_2), and wavelength-selecting (W) crystals ensuring large cumulative dispersion rate \mathcal{D}_U , large bandwidth ΔE_U , and large angular acceptance $\Delta \theta_U$. Different functions of D_D (a) and D_R (c) dictate their different designs.

X-ray echo spectrometer design & performance

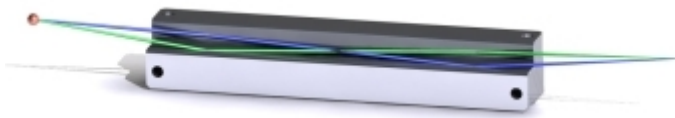


Focusing, Collimating, and Imaging Optics

2D focusing optics f : a Be CRL, or a graded multilayer KB mirror.



2D collimating optics f_1 : Montel mirror with an angular acceptance of up to 10×10 mrad²



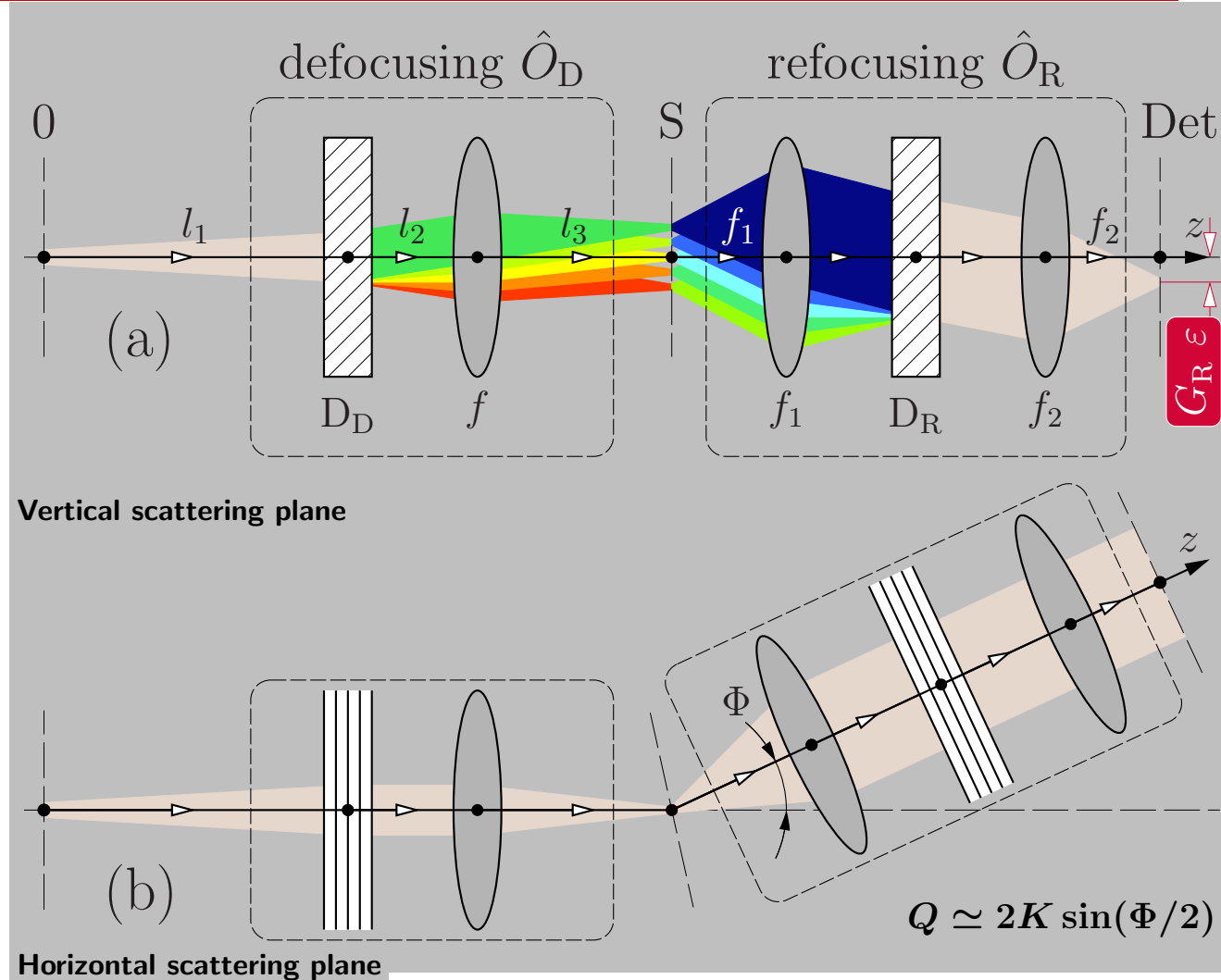
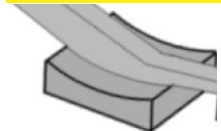
K. Mundboth, et al, *J. Synchrotron Rad.*, 21, 16-23, (2014)

Yu. Shvyd'ko, et al, *Nat. Commun.*, 5, 5219, (2014)

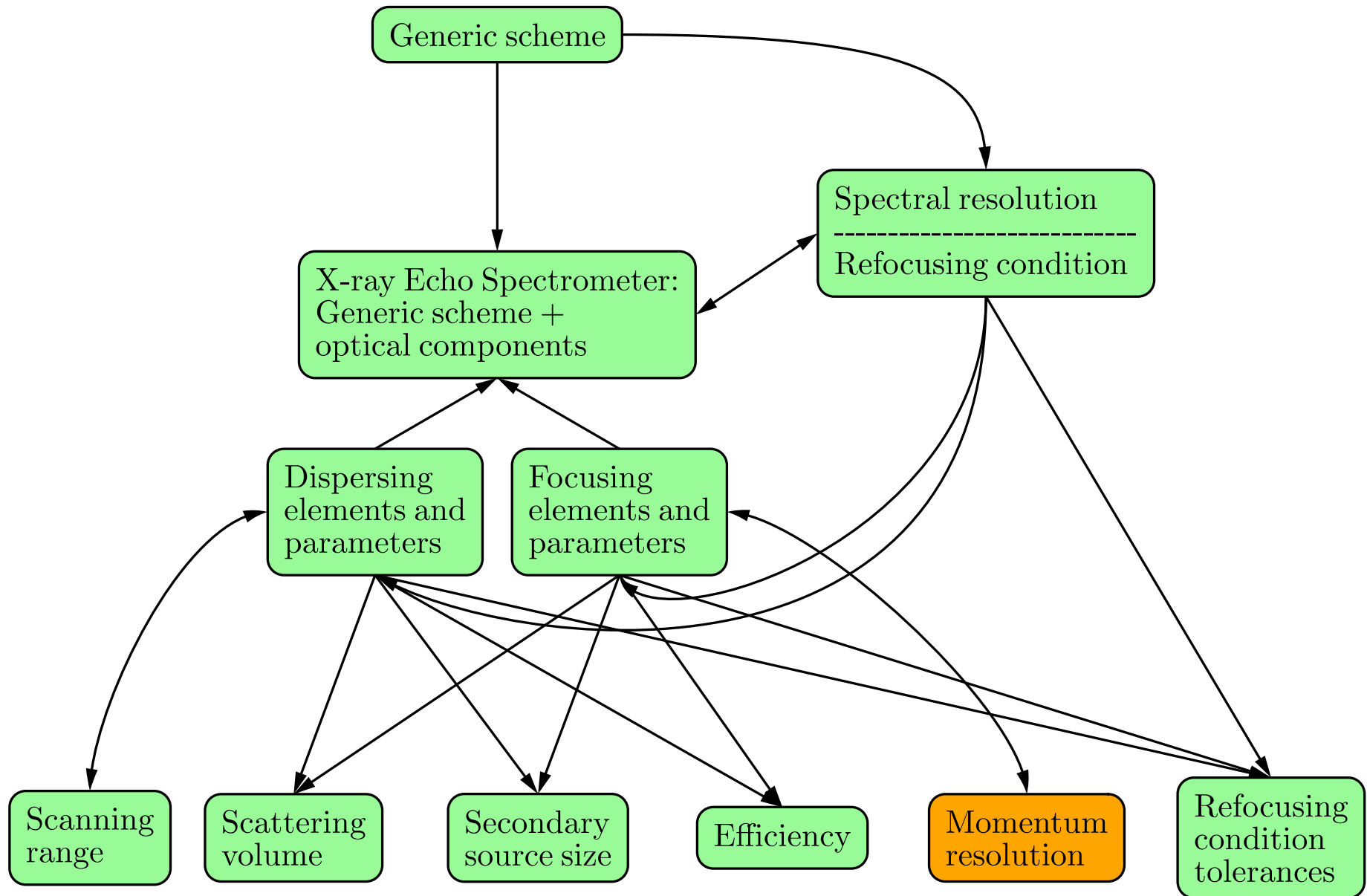
A. Suvorov, et al, *J. Synchrotron Rad.*, 21, 473478, (2014)

J.-H. Kim, et al, *J. Synchrotron Rad.*, 23, 880-886, (2016)

1D imaging optics f_2 : graded multilayer mirror



X-ray echo spectrometer design & performance

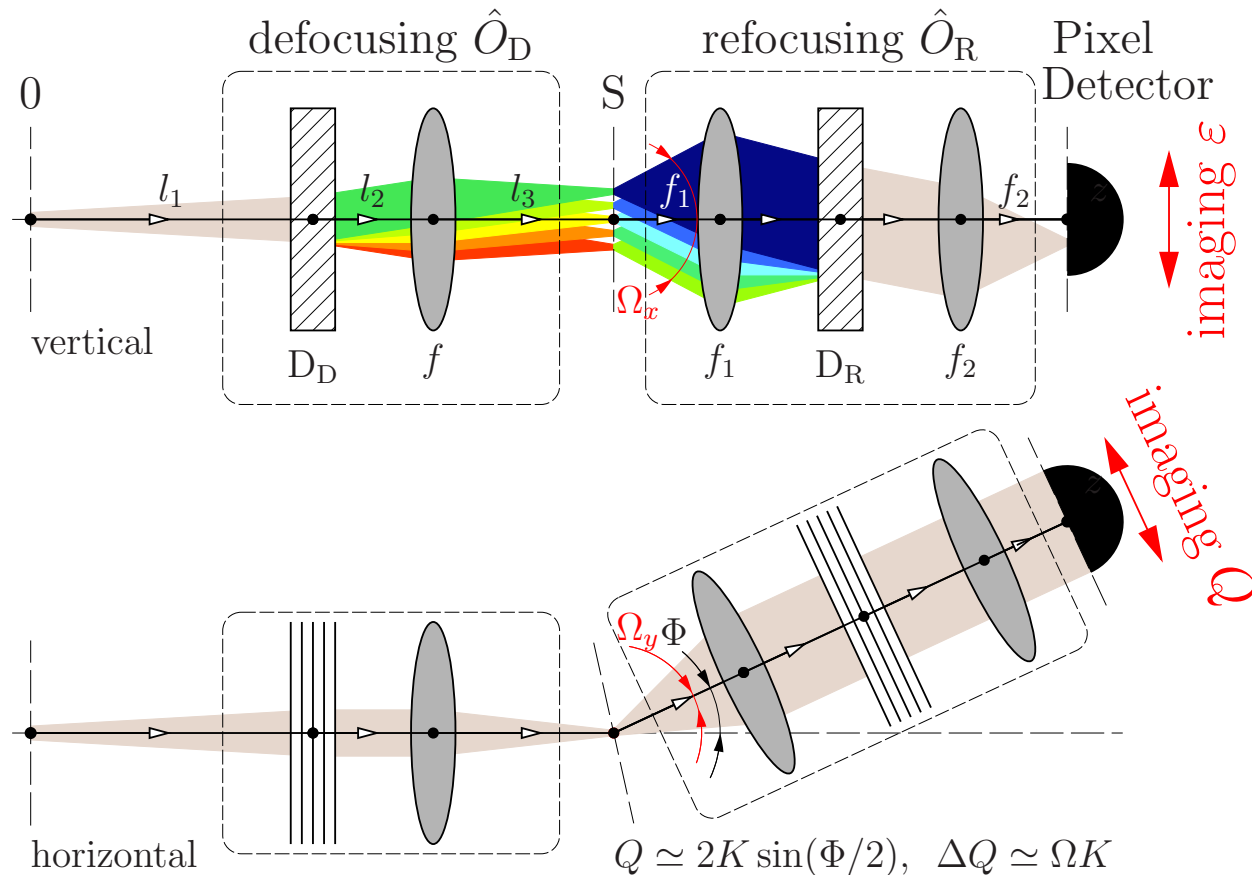


Momentum transfer resolution

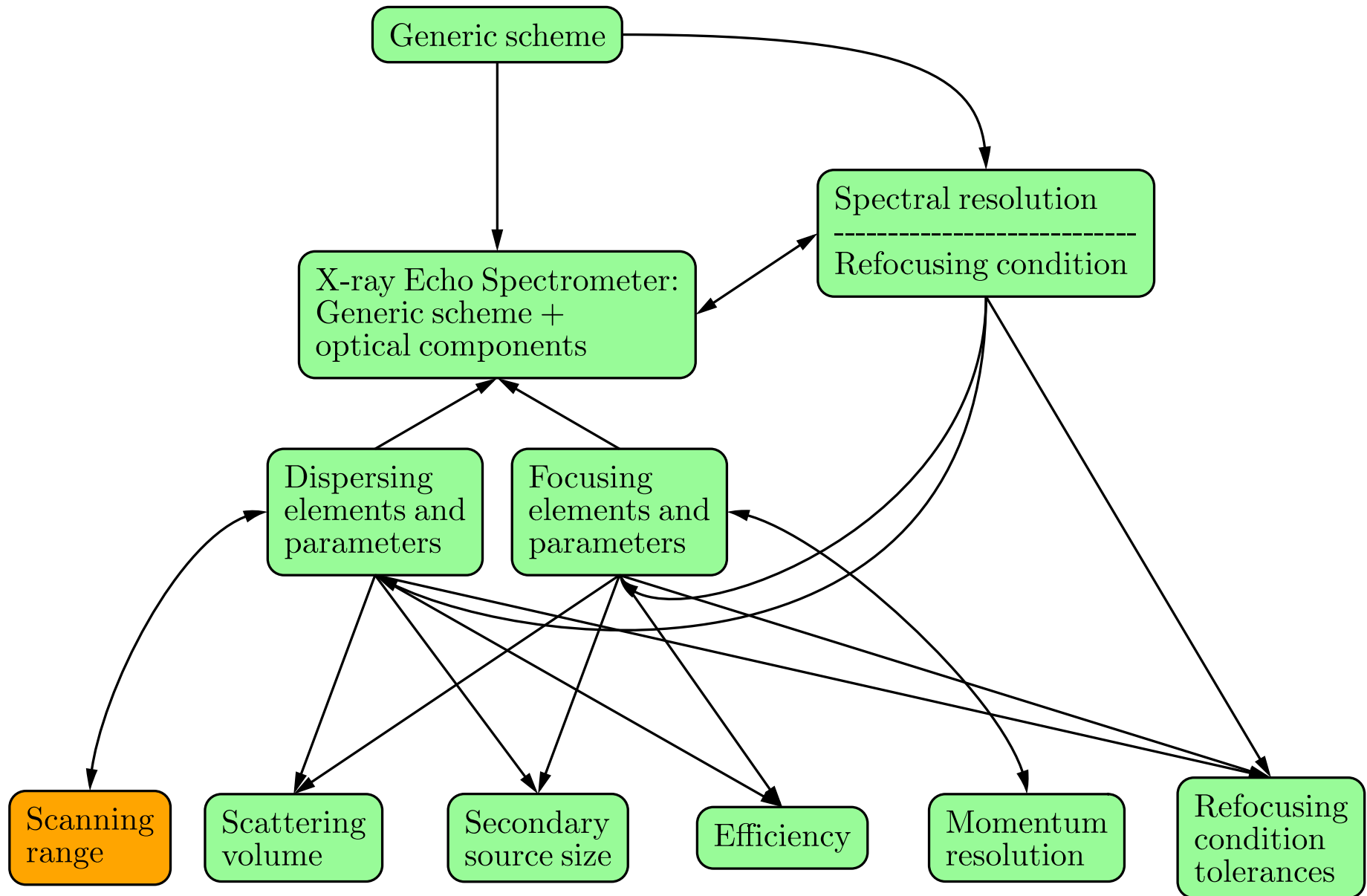
The required momentum transfer resolution ΔQ determines the needed angular acceptance $\Omega_x \times \Omega_y$ of the collimating optic f_1 : $\Delta Q \simeq \Omega K$ ($\Omega = \Omega_x \simeq \Omega_y$)

$$\Delta Q = 0.1 \text{ nm}^{-1} \Rightarrow \Omega = 2.2 \text{ mrad @9.1 keV}$$

$$\Delta Q = 0.45 \text{ nm}^{-1} \Rightarrow \Omega = 10 \text{ mrad @9.1 keV (proven Montel mirror acceptance)}$$

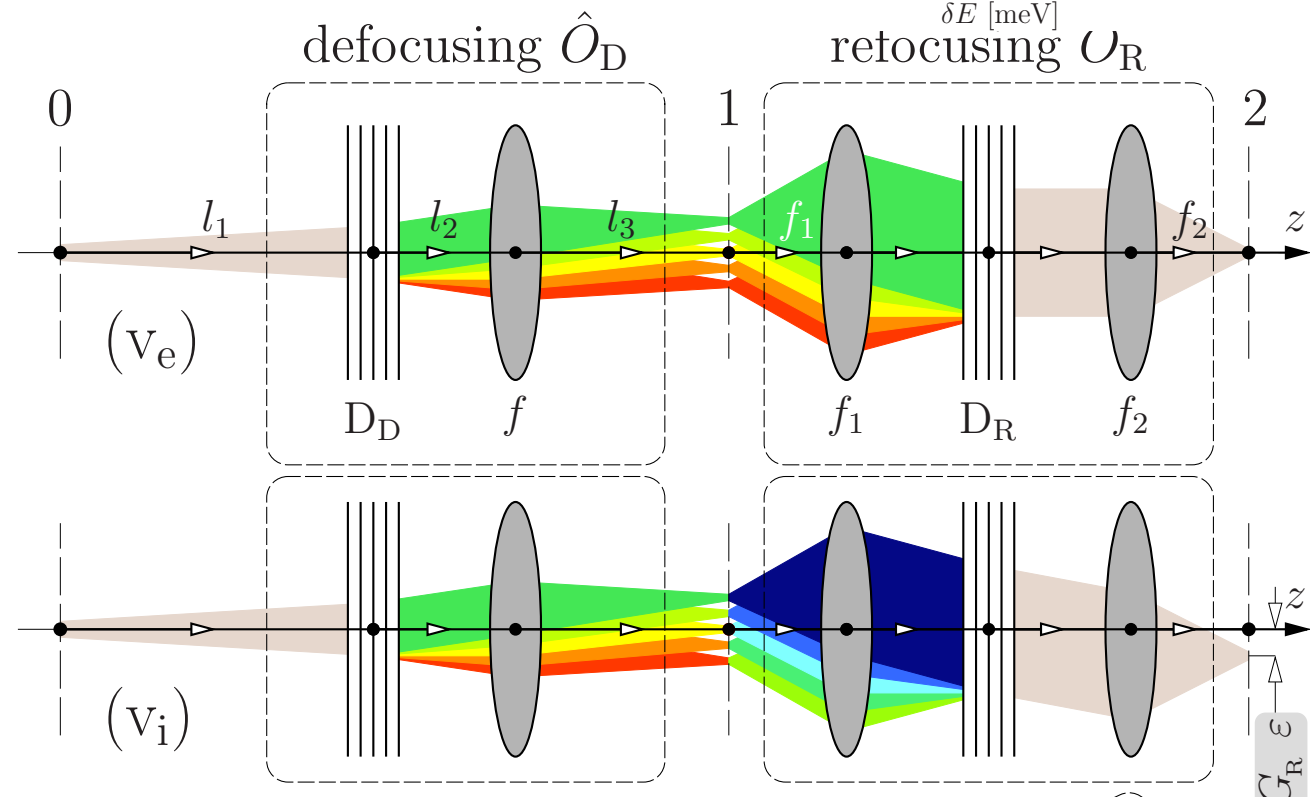
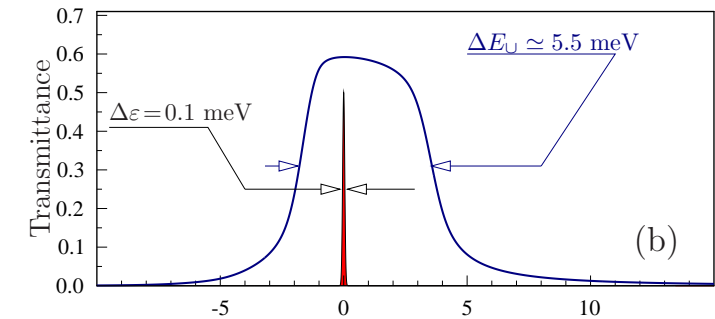
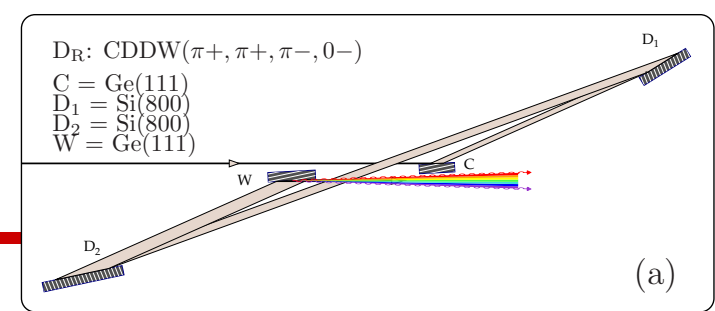


X-ray echo spectrometer design & performance



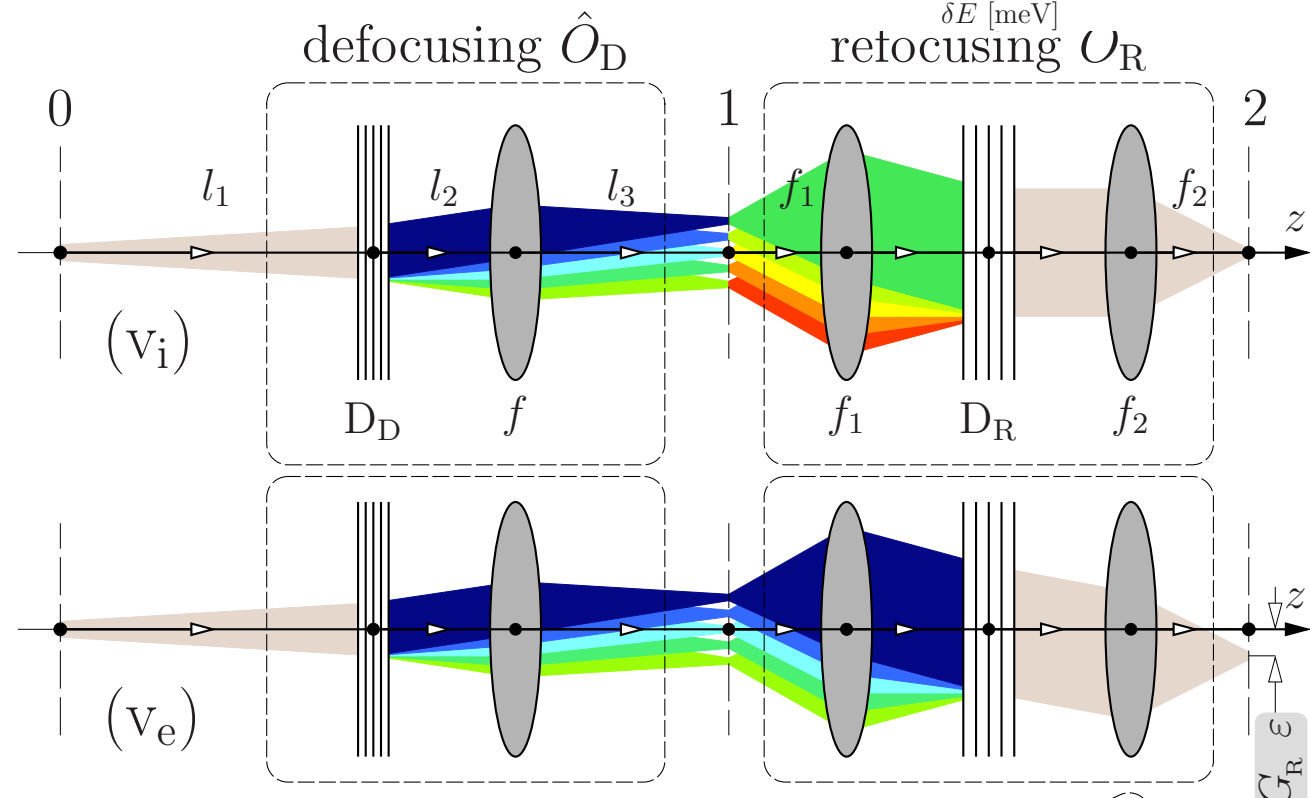
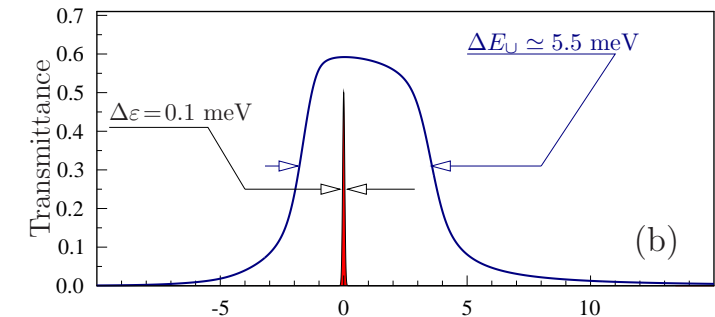
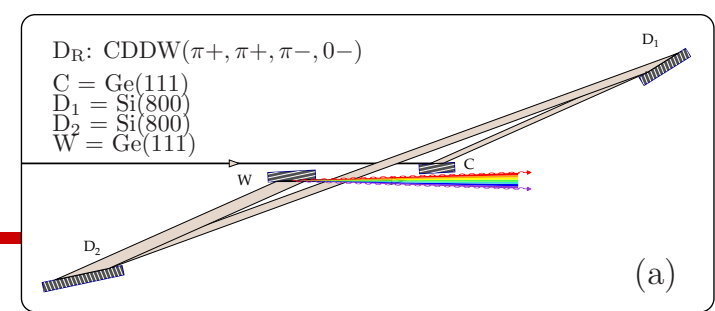
Spectral Window of Imaging & the Scanning Range

- X-ray echo spectrometers are imaging IXS spectrometers.
- The spectral window of imaging is determined by the spectral transmission bandwidth of the dispersing element of the refocusing system.
- The proposed 0.1-meV echo spectrometer can image IXS spectra in a 5.5-meV spectral window.

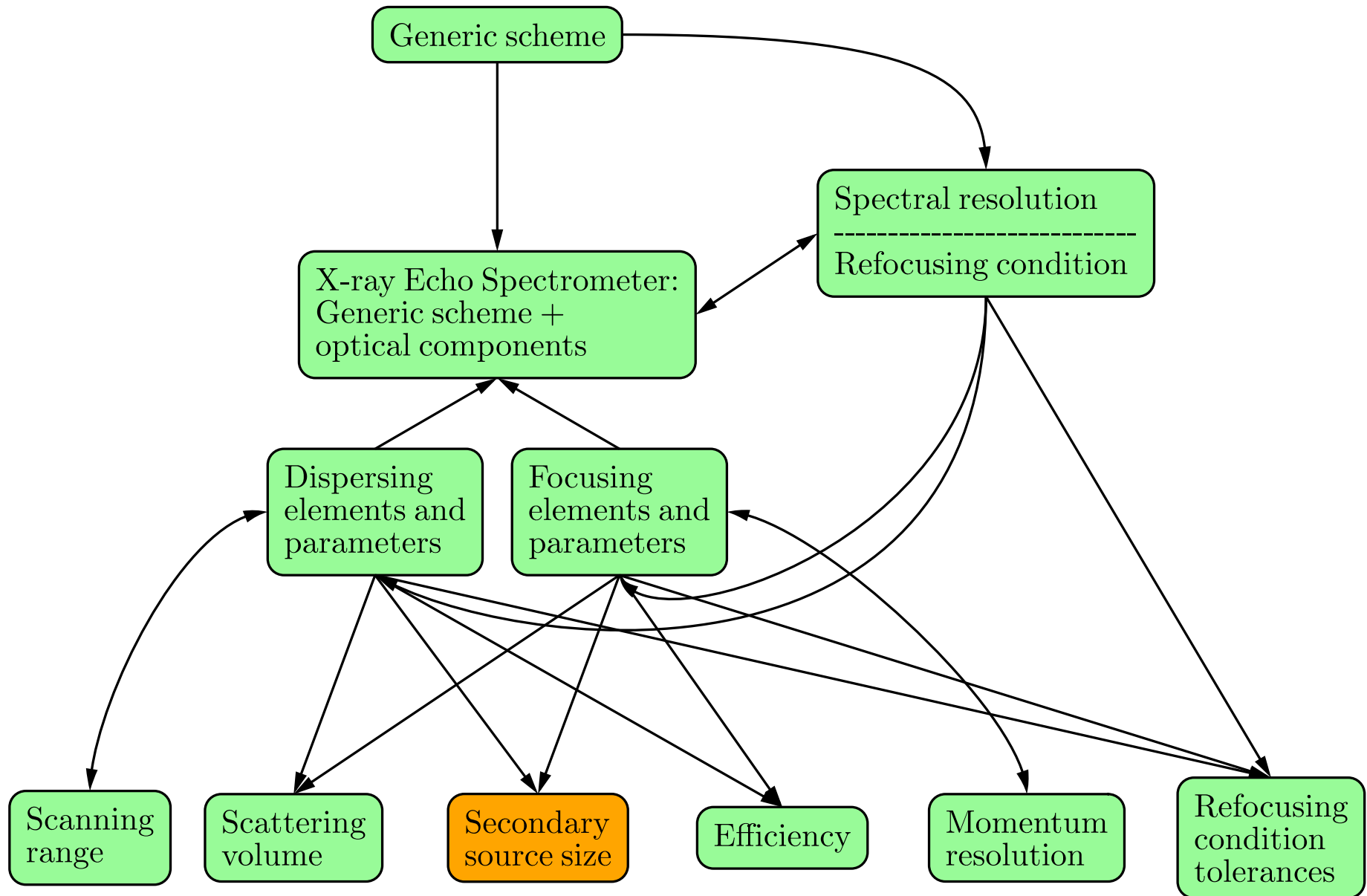


Spectral Window of Imaging & the Scanning Range

- X-ray echo spectrometers are imaging IXS spectrometers.
- The spectral window of imaging is determined by the spectral transmission bandwidth of the dispersing element of the refocusing system.
- The proposed 0.1-meV echo spectrometer can image IXS spectra in a 5.5-meV spectral window.
- The window of imaging can be shifted by changing the Bragg angles of the D-crystals of the dispersing element of the defocusing system. Nothing has to be changed in the refocusing system.
- The scanning range of the echo-type spectrometer is similar to that of the HERIX-type spectrometers.

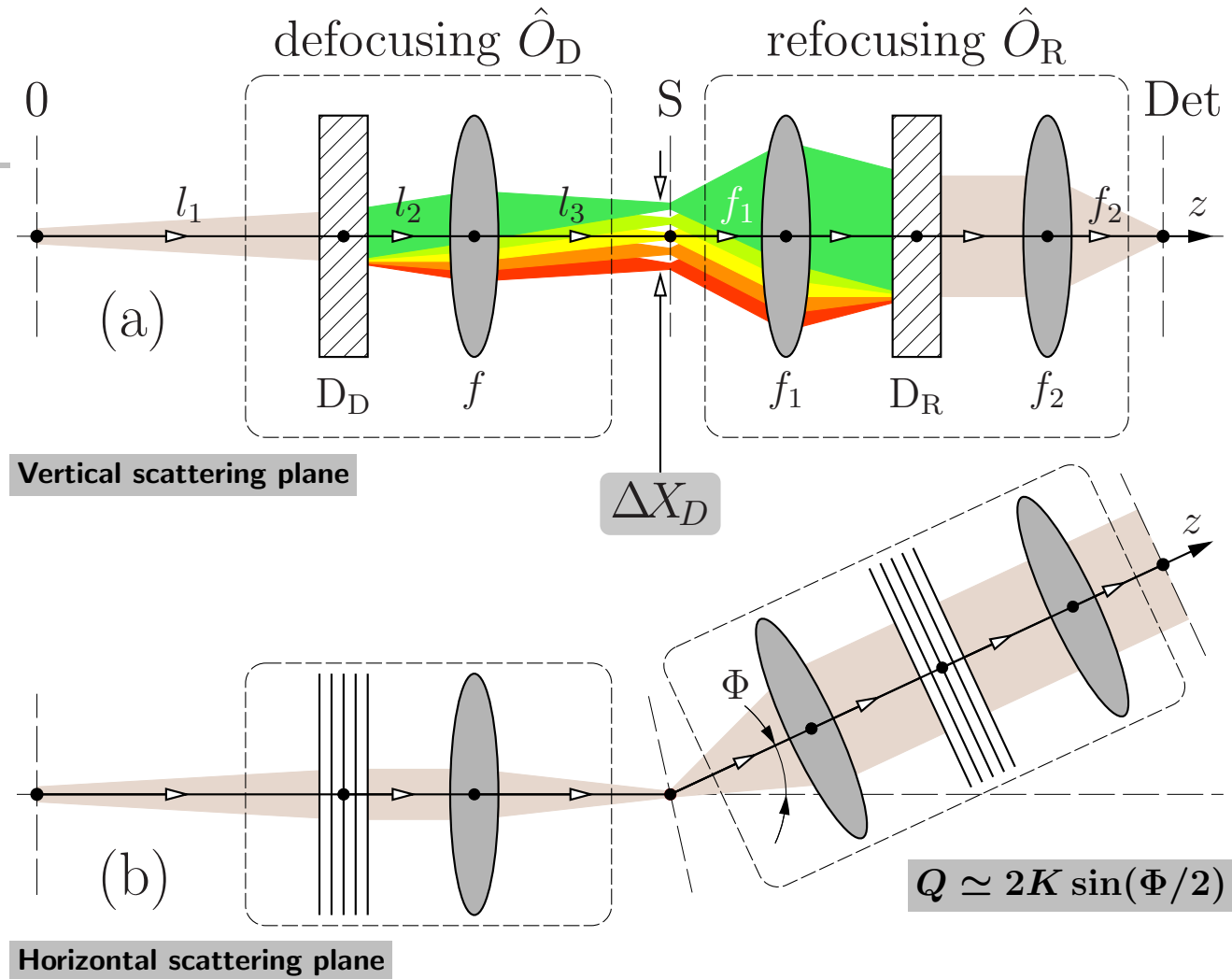


X-ray echo spectrometer design & performance



Vertical spot size on the sample ΔX_D

$$\Delta X_D = G_D \Delta E_{UD}$$



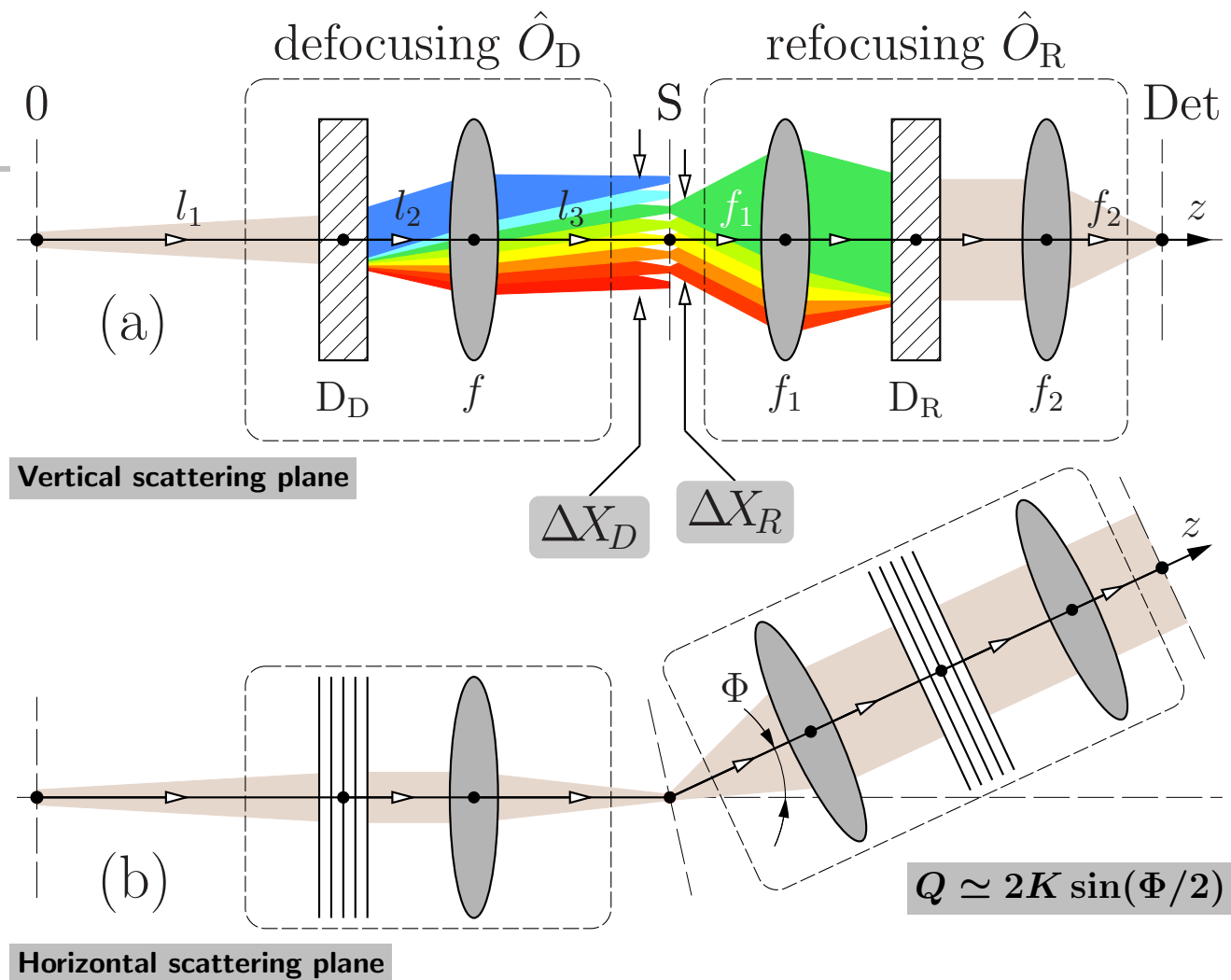
Vertical spot size on the sample

$$\Delta X_D = G_D \Delta E_{UD}$$

Typically: $\Delta E_{UD} > \Delta E_{UR}$.

Therefore, the spot size accepted by the refocusing system $\Delta X_R < \Delta X_D$:

$$\Delta X_R = G_D \Delta E_{UR}$$



Vertical spot size on the sample

$$\Delta X_D = G_D \Delta E_{UD}$$

Typically: $\Delta E_{UD} > \Delta E_{UR}$.

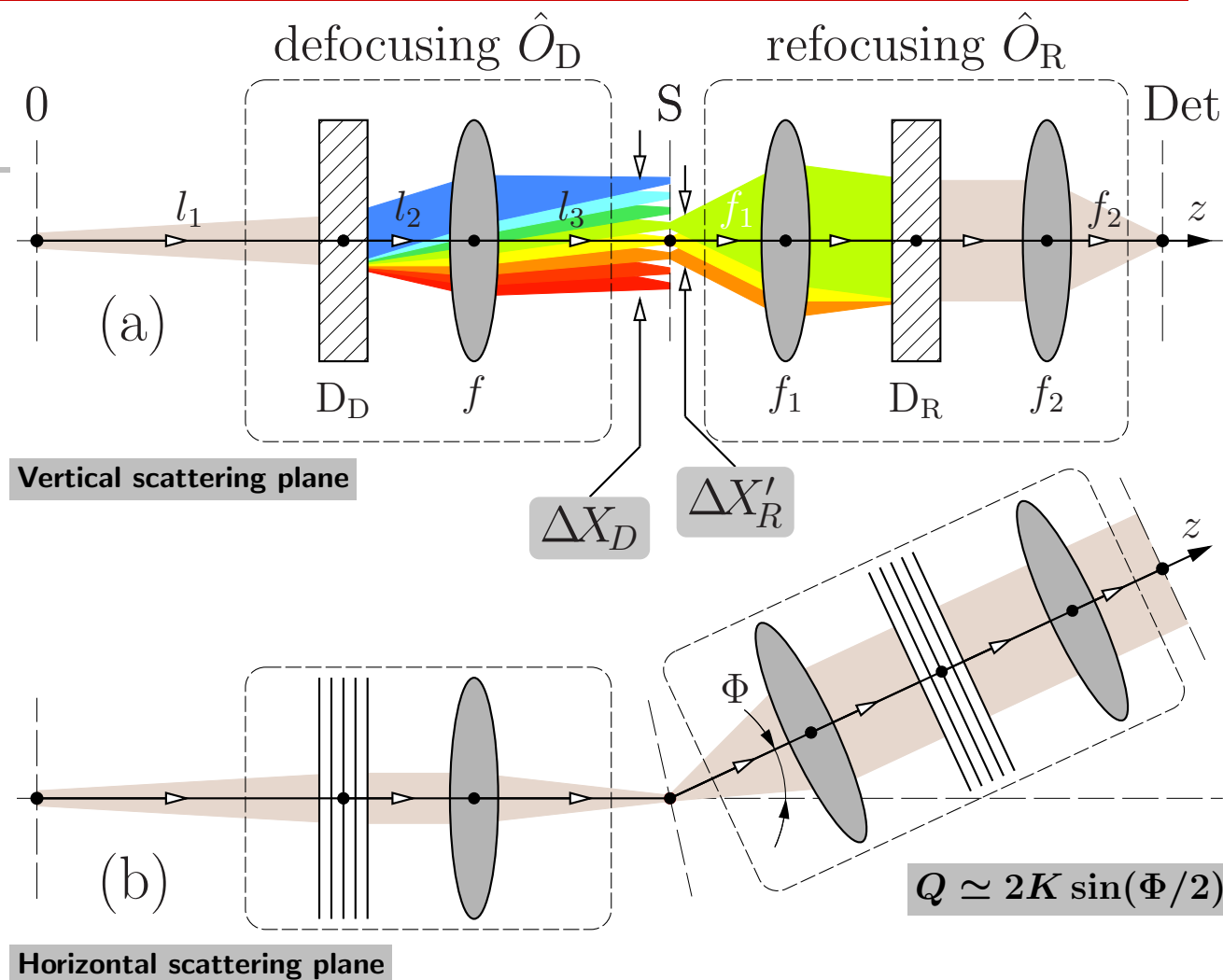
Therefore, the spot size accepted by the refocusing system $\Delta X_R < \Delta X_D$:

$$\Delta X_R = G_D \Delta E_{UR}$$

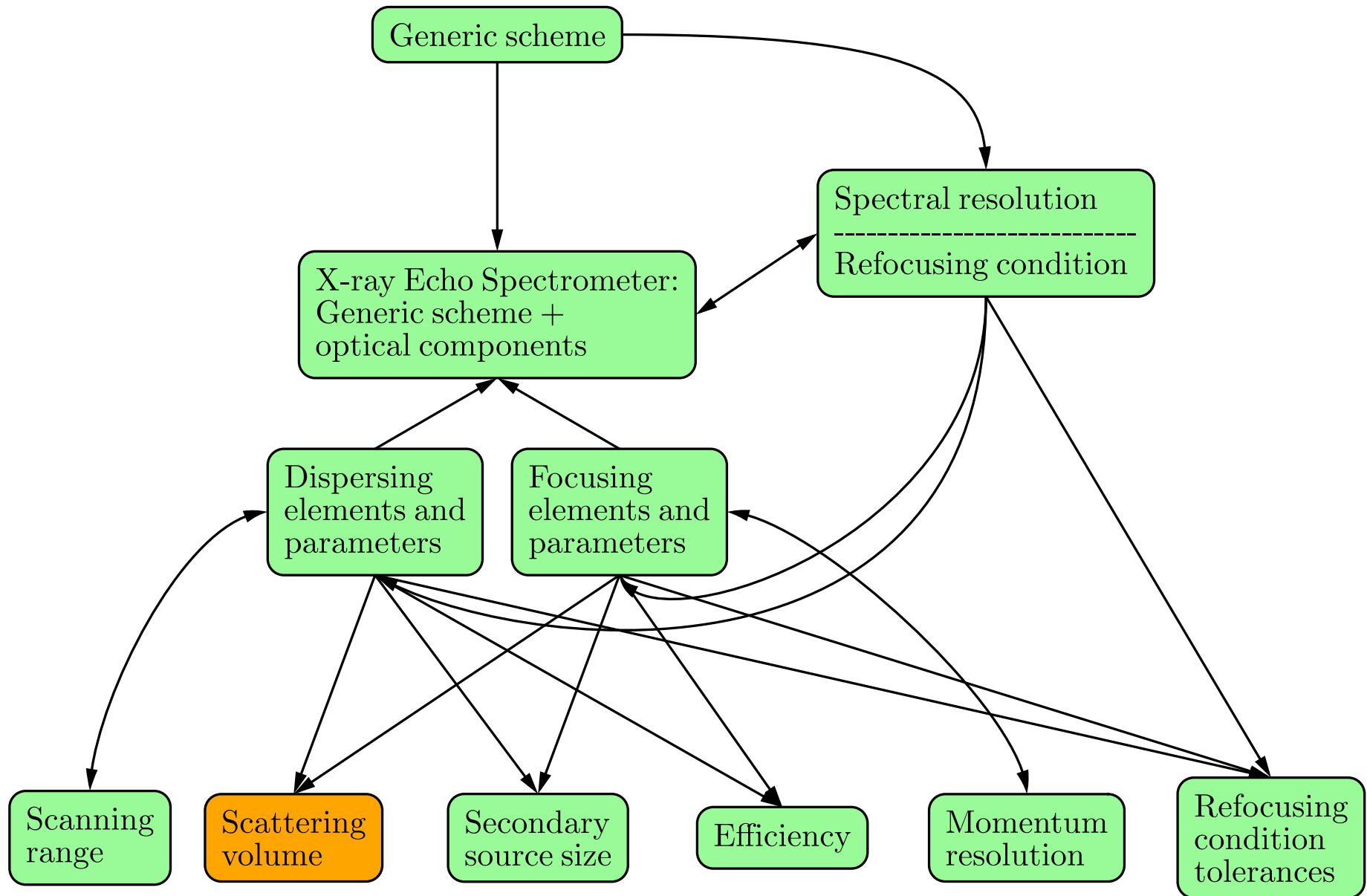
If $\Delta X_R / f_1 > \Delta \theta_{D_R}$,

the spot size and the spectral bandwidth accepted by the refocusing system is further reduced to: $\Delta X'_R \simeq f_1 \Delta \theta_{D_R}$

$\Delta \theta_{D_R} \simeq 250 \mu\text{rad}$ is the angular acceptance of D_R .
 $\Delta X'_R \simeq 50 \mu\text{m}$, for $f_1 = 0.2 \text{ m}$.



X-ray echo spectrometer design & performance



Scattering volume: absorption limited

Signal strength scales with the scattering volume and, therefore, with the absorption length, provided sample thickness is larger.

Sample	L_a^{XES}	L_a^{HERIX}	$L_a^{\text{HERIX}} / L_a^{\text{XES}}$
YBa ₂ Cu ₃ O ₇	10	300	30
HgBa ₂ Ca ₂ Cu ₃ O ₈	4	34	8.5
Bi ₂ Sr ₂ Ca ₂ Cu ₃ O ₁₀	7	31	4.5
SmFeAs	6	58	10
CeFeAs	8	70	9
NbSe ₂	16	32	2
VO ₂	18	260	14
Fe ₃ O ₄	8	140	18
SrTiO ₃	50	180	3.6
Sr ₃ CuIrO ₆	36	120	3.3
URu ₂ Si ₂	3	9	3
H ₂ O	1500	21000	14

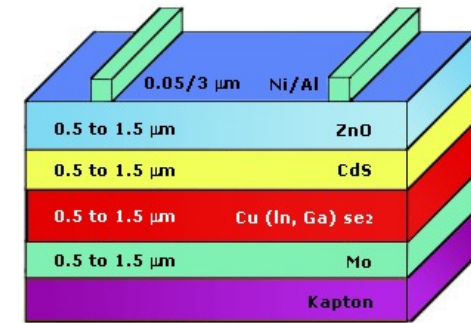
Table 3: Absorption/attenuation lengths L_a in selected high- T_c superconductors and other materials with diverse properties of fundamental and practical interest at the operating photon energies of the HERIX (23.74 keV) and XES (9.13 keV) spectrometers. Larger absorption length is advantageous for the IXS signal strength. Smaller absorption length is advantageous if the samples are inhomogeneous.

Scattering volume: sample thickness limited

Thin-film samples ($\lesssim 1 \mu\text{m}$)

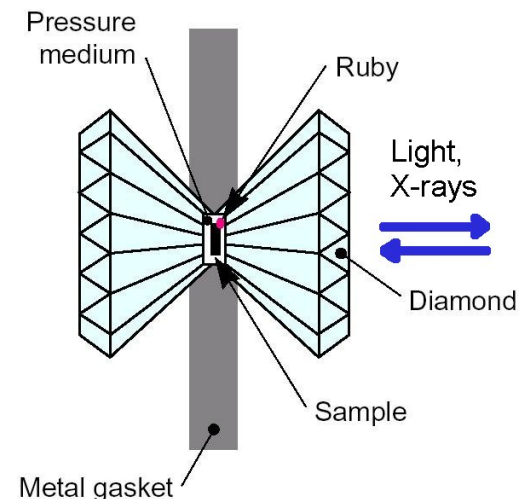
Same scattering volume for 9-keV (XES) and for 24-keV (HERIX) x-rays.

Expected signal strength enhancement $\simeq 10^3$ with a 1-meV-resolution x-ray echo spectrometer compared to HERIX.



Samples in diamond anvil pressure cells ($3 - 40 \mu\text{m}$)

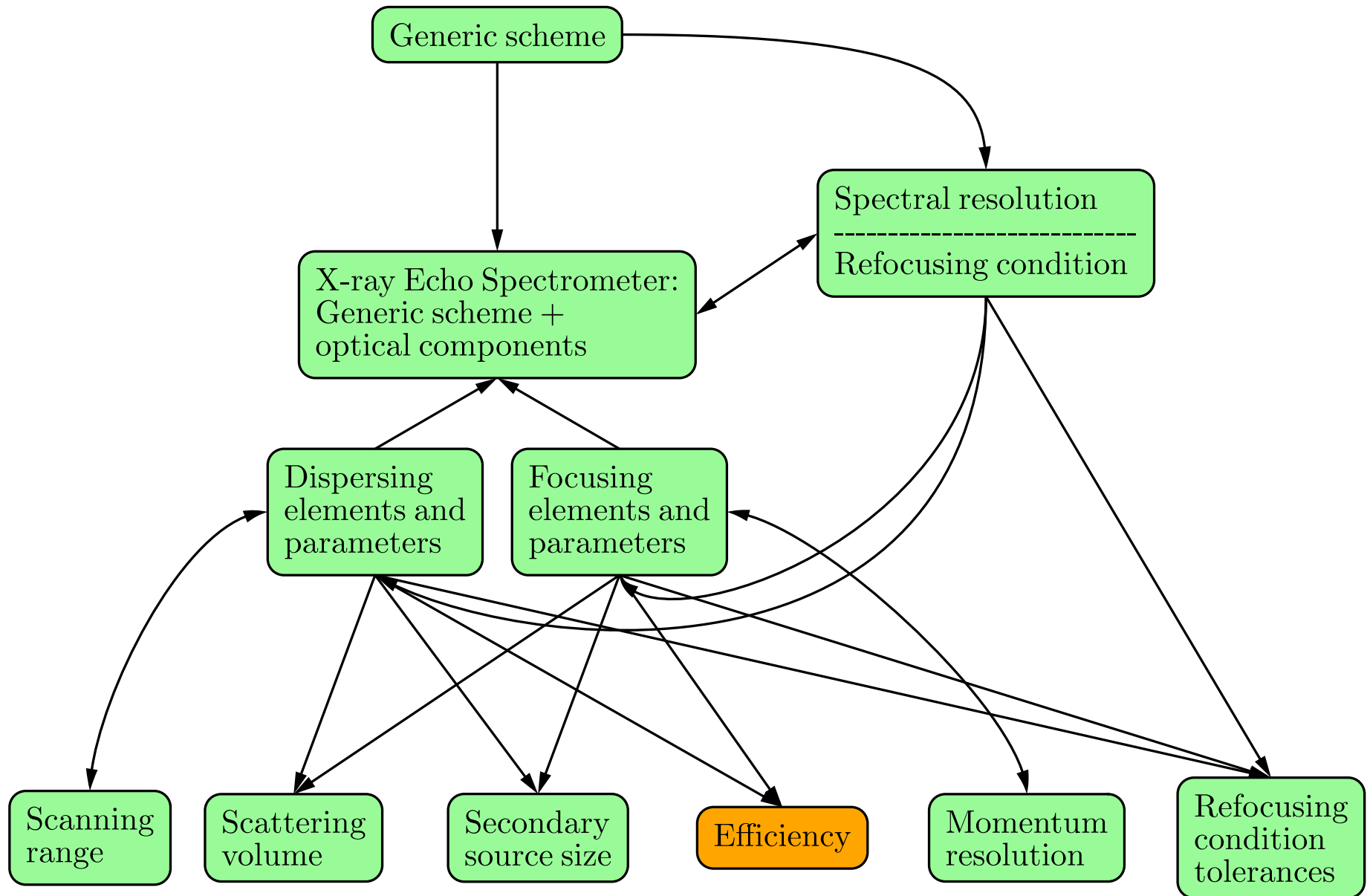
pressure GPa	sample diameter μm	sample thickness μm
30	100-200	20-40
60	60-100	10-15
100	50-70	<10
200	30-40	$\simeq 3$



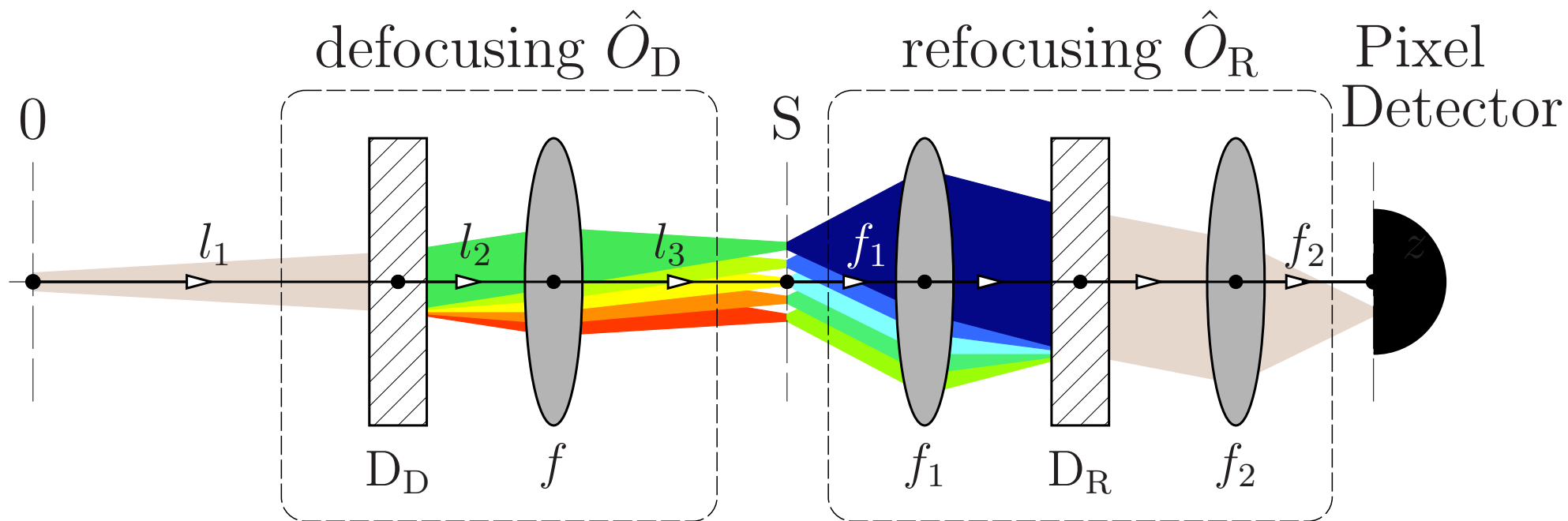
Sample size depends on pressure range. A few typical examples (Victor Struzhkin).

Same or similar scattering volume for 9 keV x-rays (XES) and 24 keV HERIX. Though, transmission of the 9-keV photons through a 2-2.4-mm thick diamond is 10-times smaller, the expected signal strength enhancement is still very high $\simeq 170 - 55$ with a 1-meV-resolution x-ray echo spectrometer compared to HERIX.

X-ray echo spectrometer design & performance



X-Ray Echo Spectrometer Efficiency



1-meV XES:	80%	50%	50%	50%	80%	Total=10%
0.1-meV XES:	50%	50%	50%	50%	80%	Total=7%



Content

- X-ray echo spectroscopy principles.
- X-ray echo spectrometer design & performance.
- **Comparison with HERIX.**
- Feasibility.
- Conclusions and outlook.

X-Ray Echo Spectrometers compared with HERIX

Parameter:	Spectrometer:	XES1	XES05	XES02	XES01	HERIX
Photon energy E [keV]		9.13	9.13	9.13	9.13	23.74
Photon momentum K [nm^{-1}]		46.2	46.2	46.2	46.2	120.3
Spectral resolution $\Delta\varepsilon$ [meV]		1	0.5	0.2	0.1	1.5
Spectrometer bandwidth ΔE_U [meV]		14.2	14.2	5.5	5.5	0.9
Momentum transfer resolution ΔQ [nm^{-1}]		0.4	0.2	0.12	0.02	1.2
Angular acceptance $\Omega_v \times \Omega_h$ [mrad ²]		10×10	5×5	2.5×10	0.43×5	10×10
Max. scattering angle Φ_M		154°	154°	154°	154°	35°
Max. momentum transfer Q_M [nm^{-1}]		90	90	90	90	70
Analyzer arm size [m]		2	3.5	3.0	3.5	9
Incident photon polarization		π	π	π	π	σ
Spotsize (V×H) on the sample [μm^2]		70×5	140×5	130×5	280×5	20×35
Required detector resolution [μm]		14	10	13.5	6.8	-
Spectral flux F @APSU [ph/meV/s] $\times 10^{10}$		30	30	30	30	4.2
Rel. signal strength $S^{\text{XES}}/S^{\text{HERIX}}$		$1767/\xi$	$442/\xi$	$66/\xi$	$5.8/\xi$	1

Table 1: Operation parameters and performance characteristics of the proposed echo spectrometers XES1, XES05, XES02, and XES01 compared with the parameters of the IXS spectrometer HERIX at 30ID@APS. The signal strength $S \propto \Delta E_U^2 \times \Omega_v \times \Omega_h \times F \times L_s$, where L_s is the scattering length. The relative signal strength values in the bottom row have to be corrected for each particular sample by the ratio $\xi = L_s^{\text{HERIX}}/L_s^{\text{XES}}$. The scattering length L_s is related either to the absorption length L_a , or to the sample thickness L . Typically $\xi \simeq 2 - 30$. A $5 \times 5 \mu\text{m}^2$ monochromatic focal spot size on the sample is assumed in all cases.

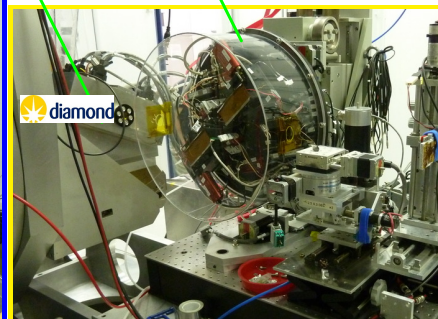
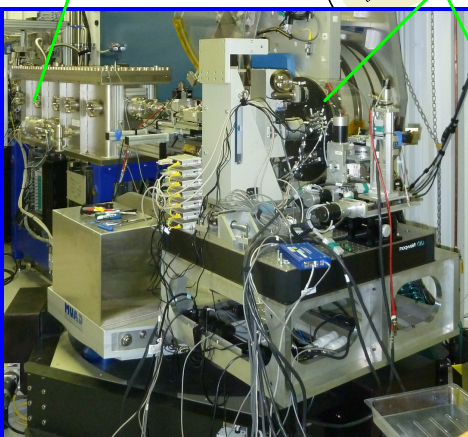
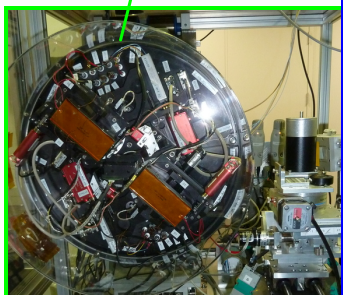
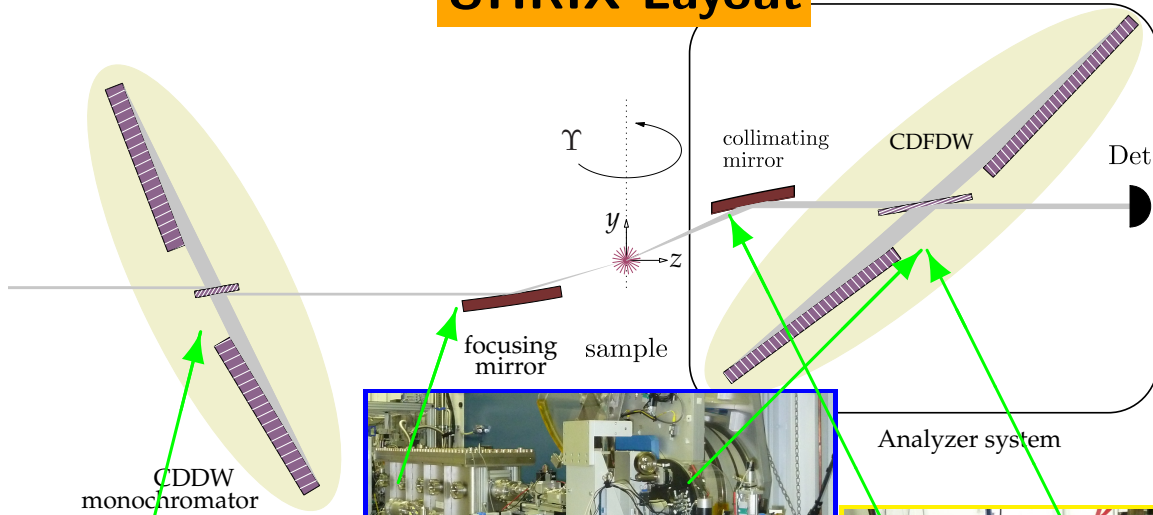
Content

- X-ray echo spectroscopy principles.
- X-ray echo spectrometer design & performance.
- Comparison with HERIX.
- **Feasibility.**
- Conclusions and outlook.

Ultra-high-resolution IXS spectrometer (UHRIX)

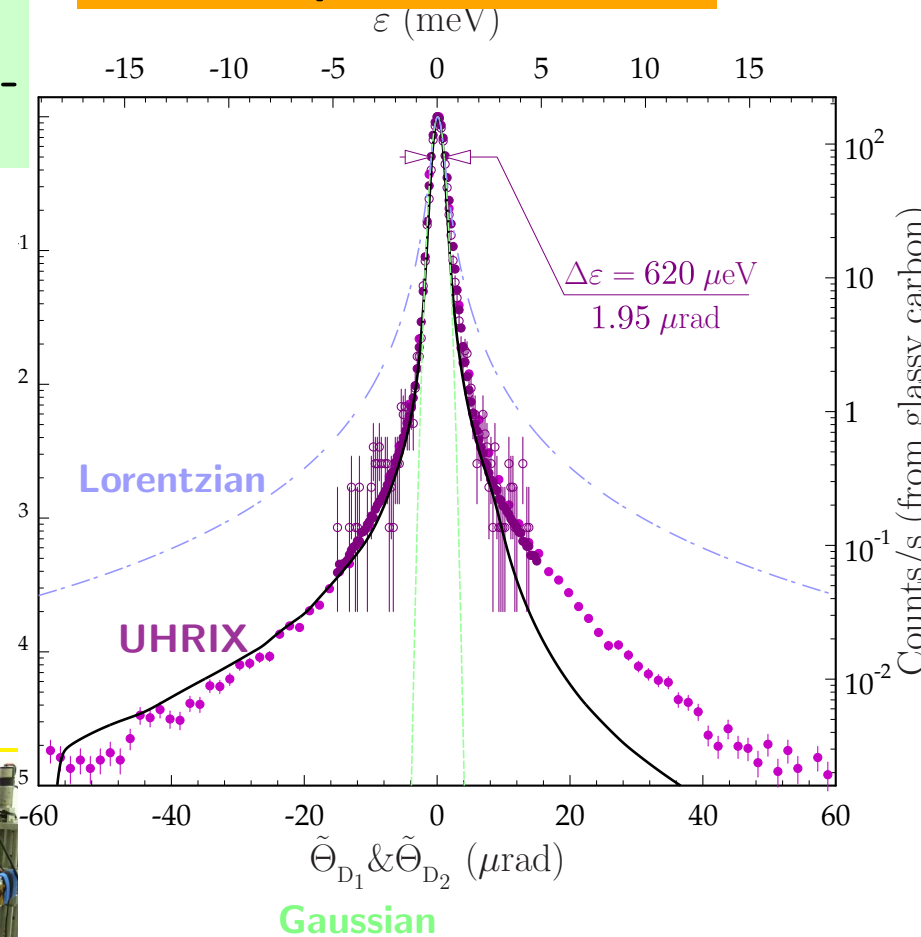
- UHRIX: demonstrated at the APS in 2013
- Features high-contrast spectral resolution function with a 0.6-meV bandwidth.
- Enables IXS with a sub-meV spectral and a 0.25-nm^{-1} momentum transfer resolution.

UHRIX Layout



Flux on the sample: 2.4×10^9 ph/s/0.25meV

UHRIX Spectral Function



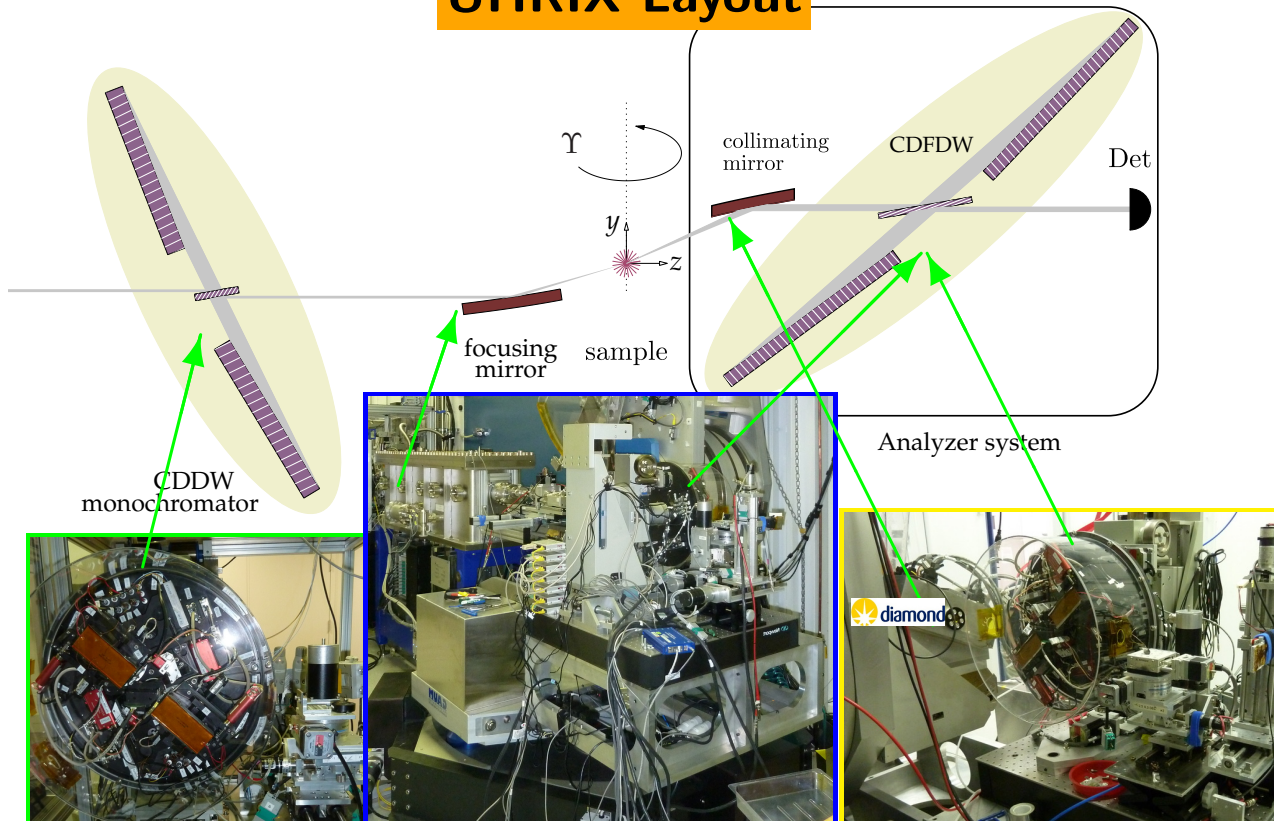
Sh., Stoupin, Shu, Collins, Mundboth, Sutter, Tolkienn *Nature Comm.* (2014)



Ultra-high-resolution IXS spectrometer (UHRIX)

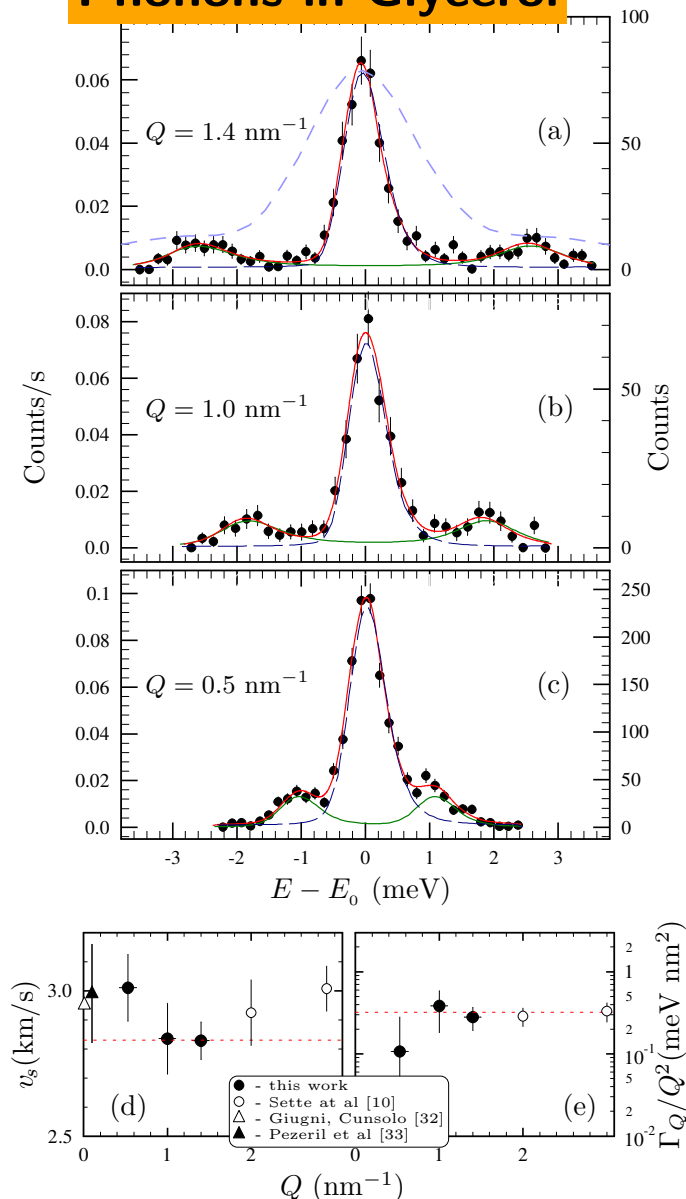
- UHRIX: demonstrated at the APS in 2013
- Features high-contrast spectral resolution function with a 0.6-meV bandwidth.
- Enables IXS with a sub-meV spectral and a 0.25-nm^{-1} momentum transfer resolution.

UHRIX Layout



Flux on the sample: 2.4×10^9 ph/s/0.25meV

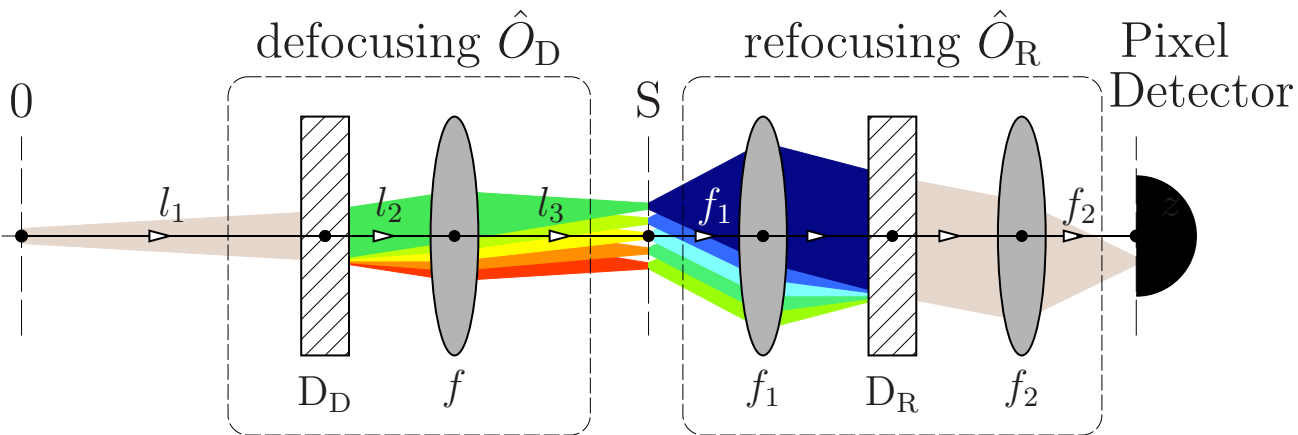
Phonons in Glycerol



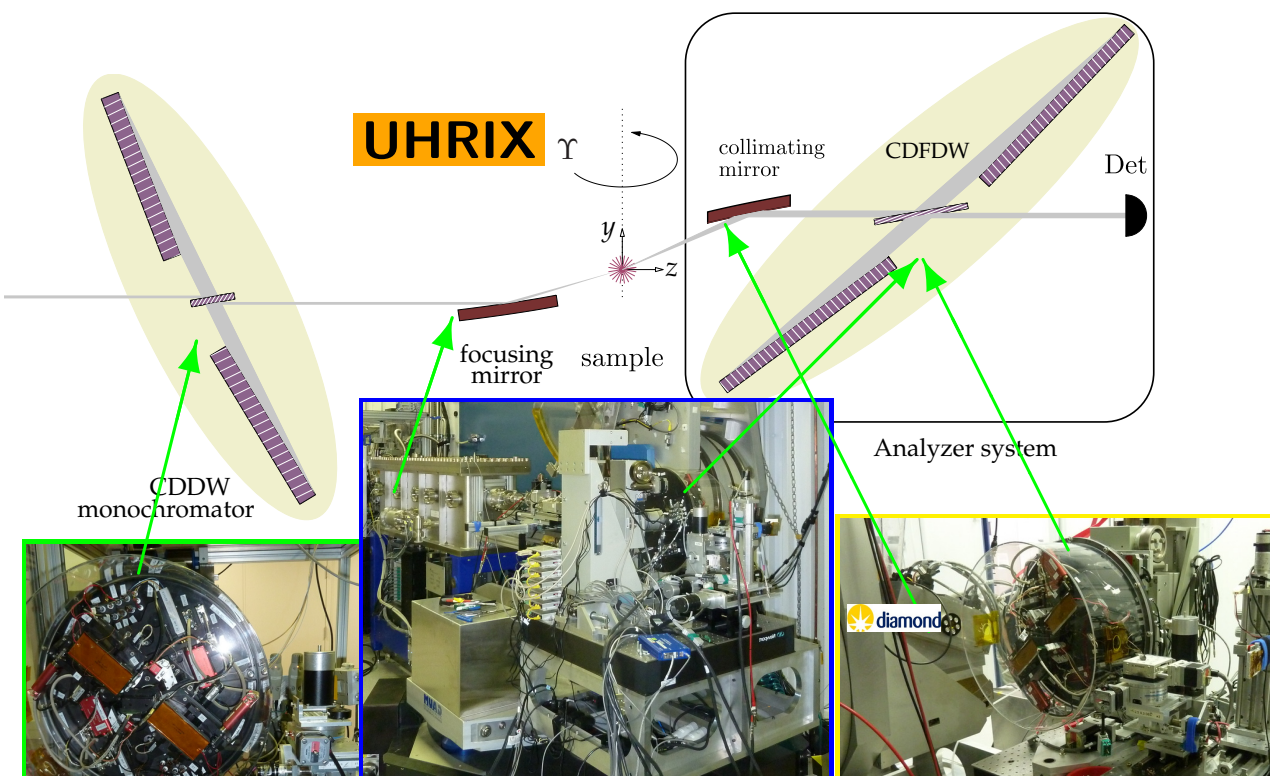
Sh., Stoupin, Shu, Collins, Mundboth, Sutter, Tolkienn *Nature Comm.* (2014)



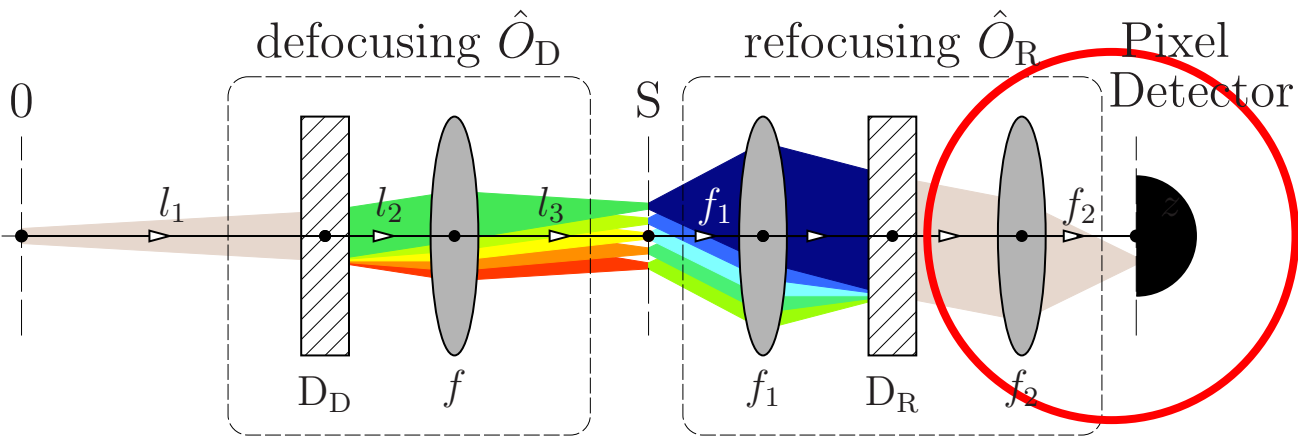
X-Ray Echo Spectrometers vs UHRIX



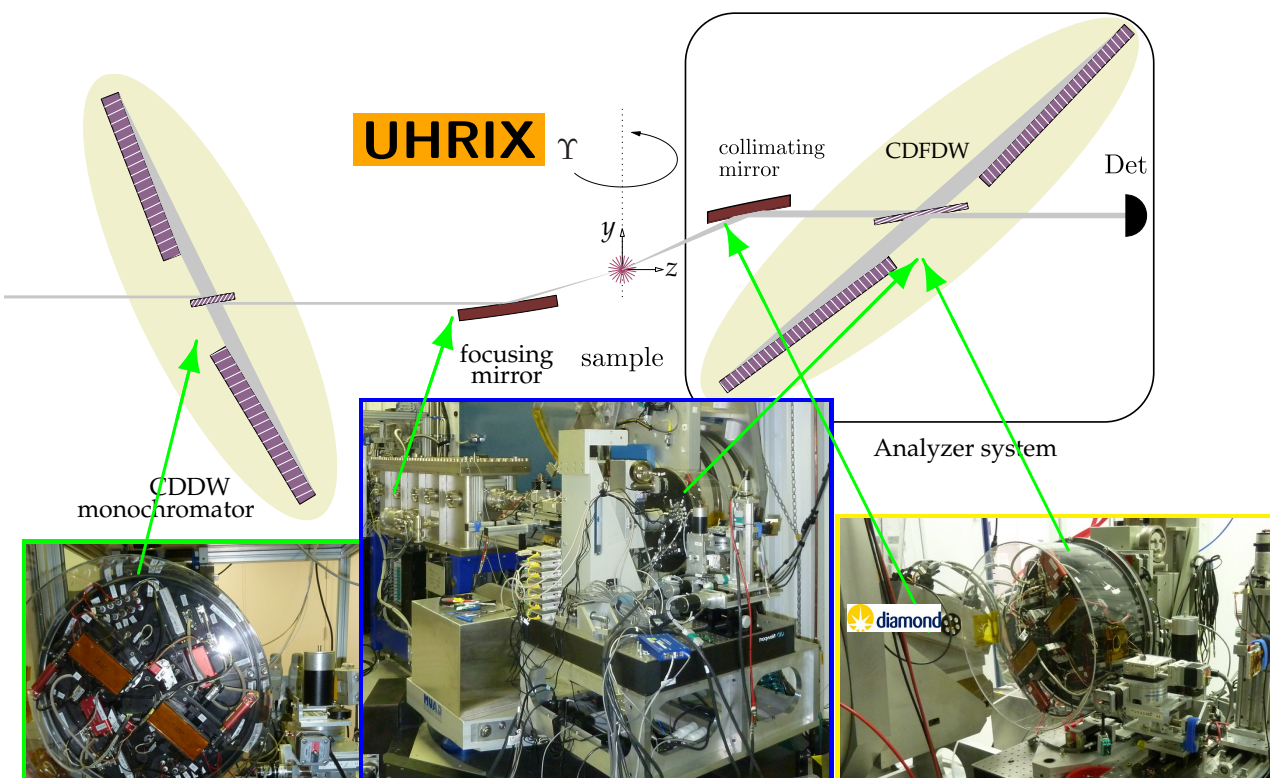
• X-ray echo spectrometers (XES) are conceptually new and different from all existing IXS spectrometers. However, technically XES are very similar to UHRIX.



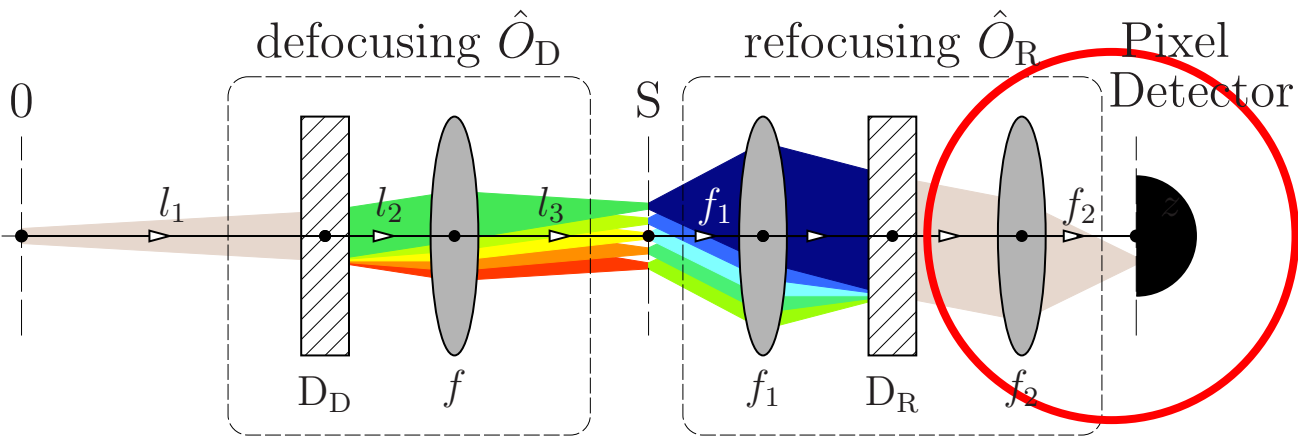
X-Ray Echo Spectrometers vs UHRIX



- X-ray echo spectrometers (XES) are conceptually new and different from all existing IXS spectrometers. However, technically XES are very similar to UHRIX.
- All the components of the XES except for the imaging mirror f_2 and the pixel detector have been used in the UHRIX spectrometer.



X-Ray Echo Spectrometers vs UHRIX



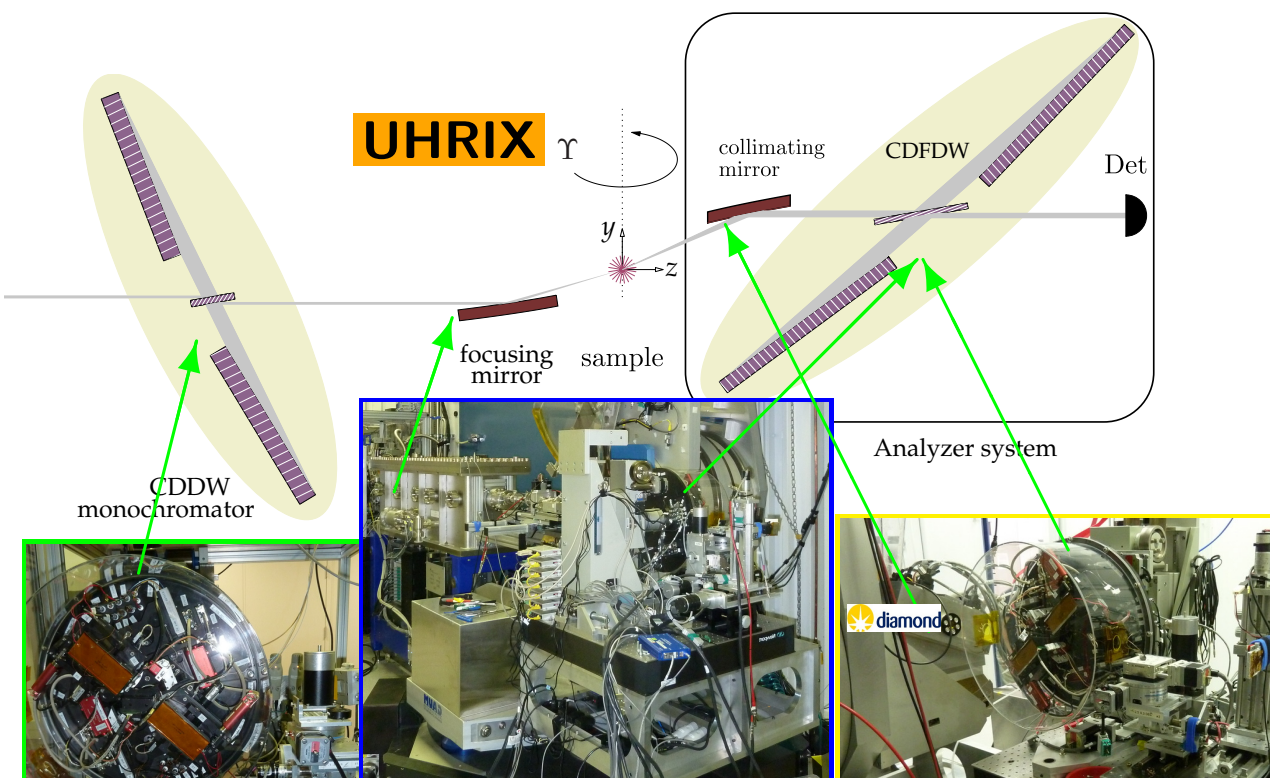
- X-ray echo spectrometers (XES) are conceptually new and different from all existing IXS spectrometers. However, technically XES are very similar to UHRIX.

- All the components of the XES except for the imaging mirror f_2 and the pixel detector have been used in the UHRIX spectrometer.

- The narrow-band angular dispersive multi-crystal CDDW monochromators and analyzers used in UHRIX, have to be converted into broadband CDDW dispersive elements.

- 2- μm -resolution charge integrating pixel detectors with single photon sensitivity are state of the art

A. Schubert et al, J. of Synchrotron Rad. 19 (2012) 359

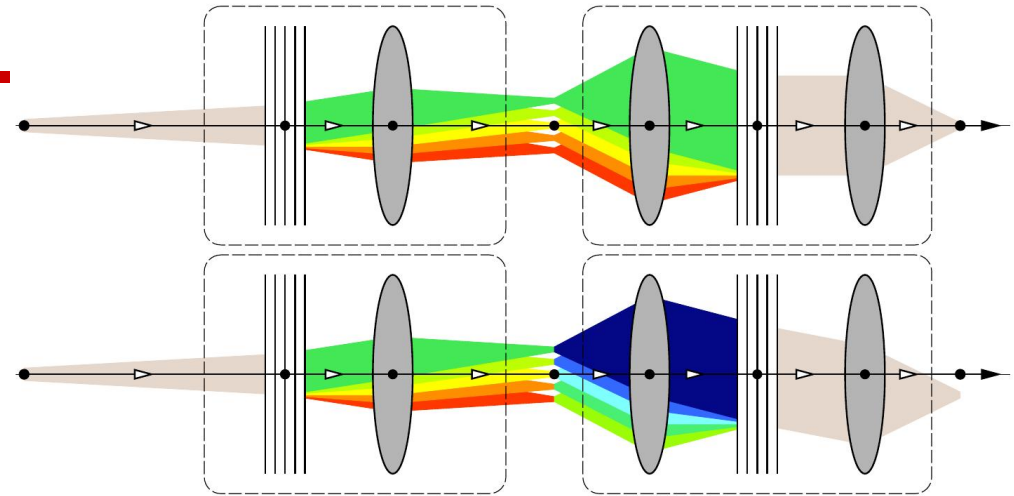


Content

- X-ray echo spectroscopy principles.
- X-ray echo spectrometer design & performance.
- Comparison with HERIX.
- Feasibility.
- **Conclusions and outlook.**

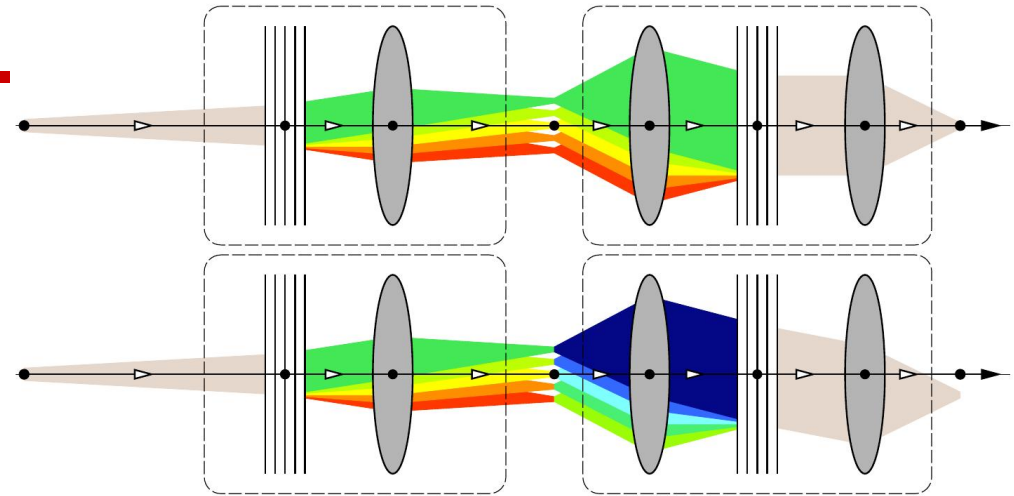
Conclusions & Outlook

- X-ray echo spectroscopy, a counterpart of neutron spin-echo, is being introduced to overcome limitations in spectral resolution and weak signals of the traditional inelastic x-ray scattering (IXS) probes.



Conclusions & Outlook

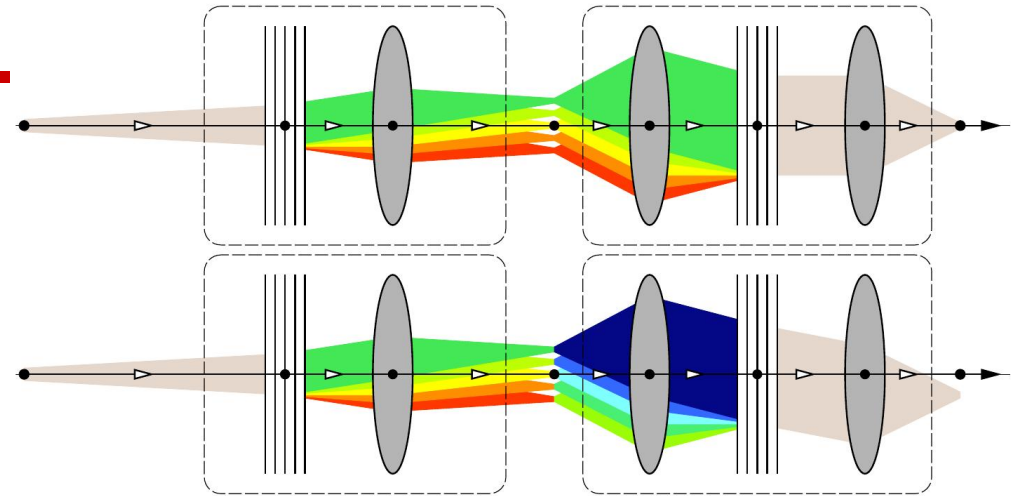
- X-ray echo spectroscopy, a counterpart of neutron spin-echo, is being introduced to overcome limitations in spectral resolution and weak signals of the traditional inelastic x-ray scattering (IXS) probes.



- The spectral resolution of the x-ray echo spectrometers does not rely on the monochromaticity of the x-rays, ensuring strong signals along with a very high spectral resolution.

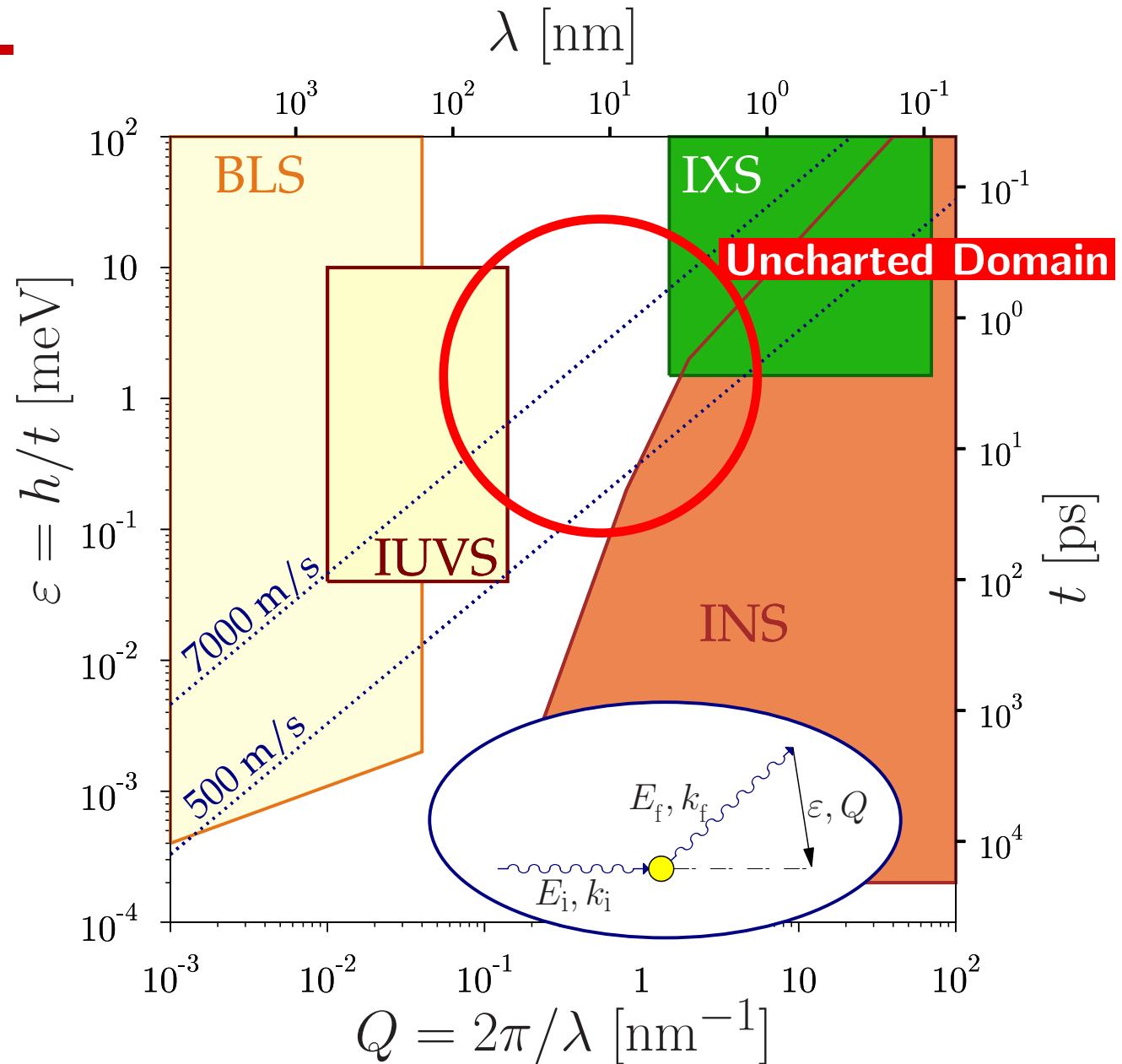
Conclusions & Outlook

- X-ray echo spectroscopy, a counterpart of neutron spin-echo, is being introduced to overcome limitations in spectral resolution and weak signals of the traditional inelastic x-ray scattering (IXS) probes.

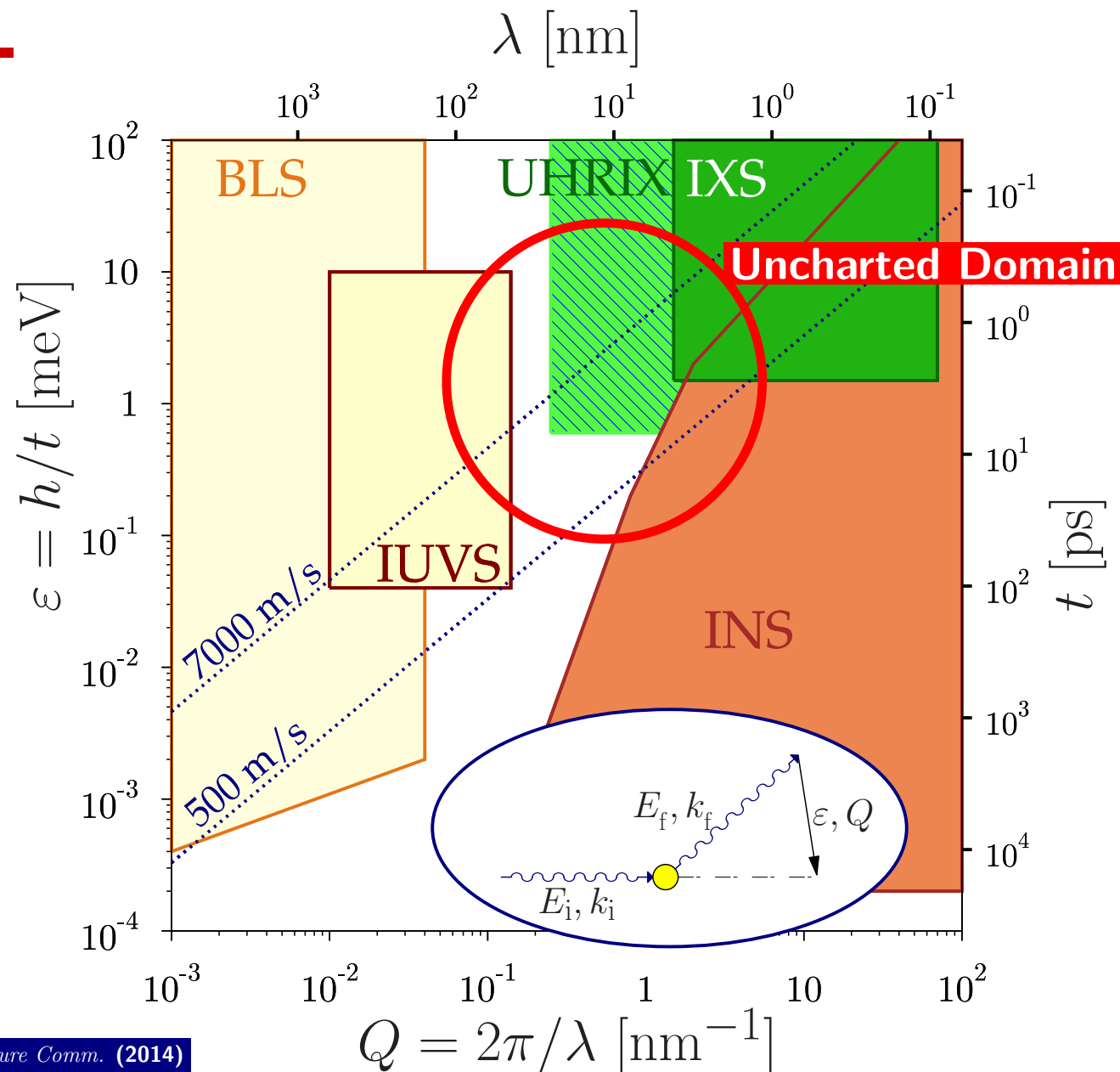


- The spectral resolution of the x-ray echo spectrometers does not rely on the monochromaticity of the x-rays, ensuring strong signals along with a very high spectral resolution.
- The x-ray echo spectrometers will allow, either, up to $\simeq 1000$ -fold reduction in measurement time for experiments at presently available $\simeq 1 \text{ meV}/1 \text{ nm}^{-1}$ resolution, or an unprecedented $\simeq 0.1 \text{ meV}/0.1 \text{ nm}^{-1}$ resolution with a up to $\simeq 10$ -fold improved signal strength.

Time-Length Space of Excitations & Scattering Probes



Time-Length Space of Excitations & Scattering Probes



Shvydko, Stoupin, Shu, Collins, Mundboth, Sutter, Tolkiehn *Nature Comm.* (2014)

Time-Length Space of Excitations & Scattering Probes

X-ray echo spectrometers featuring strong signals, $\Delta\varepsilon = 0.1\text{-meV}$ & $\Delta Q \simeq 0.1 \text{ nm}^{-1}$ instrument resolutions will allow us to bridge the gap between the high- and low-frequency probes

